REJUVENATION OF MILDLY DEGRADED REVERSE OSMOSIS
MEMBRANES

A THESIS SUBMITTED TO
THE BOARD OF GRADUATE PROGRAMS
OF
MIDDLE EAST TECHNICAL UNIVERSITY, NORTHERN CYPRUS CAMPUS

BY

BENDE MERVE KAYHAN

IN PARTIAL FULFILLMENT OF THE REQUIREMENTS
FOR
THE DEGREE OF MASTER OF SCIENCE
IN SUSTAINABLE ENVIRONMENT AND ENERGY SYSTEMS PROGRAM

SEPTEMBER 2021

Approval of the Board of Graduate Programs

_____
Prof. Dr. Cumali SABAH
Chairperson

I certify that this thesis satisfies all the requirements as a thesis for the degree of Master of Science

_____
Assoc. Prof. Dr. Ceren
İNCE DEROGAR
Program Coordinator

This is to certify that we have read this thesis and that in our opinion it is fully adequate, in scope and quality, as a thesis for the degree of Master of Science.

_____   _____
Asst. Prof. Dr. Aykut   Asst. Prof. Dr. Bengü
ARGÖNÜL   BOZKAYA SCHROTTER
Co-Supervisor   Supervisor

Examining Committee Members

Asst. Prof. Dr. Bertuğ AKINTUĞ   .
METU NCC Civil Engineering
                                                                    _____

Asst. Prof. Dr. Bengü BOZKAYA SCHROTTER .
METU NCC Chemical Engineering
                                                                    _____

Asst. Prof. Dr. Aykut ARGÖNÜL
METU NCC Chemical Engineering
                                                                    _____

Asst. Prof. Dr. Cemal ALBAYRAK
METU NCC Chemistry
                                                                    _____

Asst. Prof. Dr. İme AKANYETİ
CIU Faculty of Engineering
                                                                    _____

I hereby declare that all information in this document has been obtained and presented in accordance with academic rules and ethical conduct. I also declare that, as required by these rules and conduct, I have fully cited and referenced all material and results that are not original to this work.

Name, Last name: Bende Merve Kayhan

Signature :

ABSTRACT

**REJUVENATION OF MILDLY DEGRADED REVERSE OSMOSIS
MEMBRANES**

Kayhan, Bende Merve
Master of Science, Sustainable Environment and Energy Systems Program
Supervisor: Asst. Prof. Dr. Bengü Bozkaya
Co-Supervisor: Asst. Prof. Dr. Aykut Argönül

SEPTEMBER 2021, 112 pages

Depletion of freshwater resources is one of the inconvenient truths of the 21st century. Appropriately treated municipal wastewater can be utilized for industrial, agricultural, and potable purposes which is a sustainable option rather than discharging it into the environment. Today, one of the main technologies used in desalination of sea water and wastewater reuse is reverse osmosis (RO). The RO technology uses membranes to achieve the separation of water from contaminants, and it is very efficient in rejecting monovalent ions, bacteria and viruses. Especially, the use of thin-film composite polyamide (TFC PA) membranes has brought significant advantages in the water treatment industry since they offer high permeate flux and high salt rejection performance. However, the polyamide-based active layer of these membranes is prone to failure by chlorine attack used in disinfection and membrane cleaning operations. These operations are necessary for municipal wastewater treatment for reuse, but they cause decrease of the useful life of membranes. Thus, rejuvenation of membranes, which ensures salt rejection restoration, arises as a promising method to repair damaged membranes. This thesis investigates the performance of a commercial rejuvenation agent, which acts as a coating layer on the membrane surface. In this experimental study, the membranes were first degraded under various chlorine concentrations, contact time and pH

values and their performance was determined. Thereupon, damaged membranes were treated with the rejuvenation agent, and their performance after rejuvenation was recorded in terms of permeate flux and salt rejection. The change in the chemical structure of membranes was examined via FTIR-ATR method. The results showed that membranes were mildly degraded, and rejuvenation agent successfully restored the salt rejection of mildly degraded membranes.

Keywords: RO Membranes, Rejuvenation, Degradation, Wastewater reuse, Sustainability

ÖZ

HAFİF ZARAR GÖRMÜŞ TERS OZMOZ MEMBRANLARININ ONARIMI

Kayhan, Bende Merve
Yüksek Lisans,
Tez Yöneticisi: Asst. Prof. Dr. Bengü Bozkaya
Ortak Tez Yöneticisi: Asst. Prof. Dr. Aykut Argönül

EYLÜL 2021, 112 sayfa

Tatlı su kaynaklarının tükenmesi, 21. yüzyılın rahatsız edici gerçeklerinden biridir. Uygun şekilde arıtılmış belediye atıksuları, çevreye deşarj etmek yerine sürdürülebilir bir seçenek olan endüstriyel, tarımsal ve içme amaçlı kullanım için kullanılabilir. Günümüzde deniz suyunun tuzdan arındırılması ve atık suların yeniden kullanımında kullanılan ana teknolojilerden biri ters ozmozdur (RO). RO teknolojisi, suyun kirleticilerden ayrılmasını sağlamak için membranlar kullanır ve tek değerli iyonları, bakterileri ve virüsleri reddetmede çok etkilidir. Özellikle ince film kompozit poliamid membranların kullanımı, yüksek su akısı ve tuz giderim performansı sundukları için su arıtma endüstrisinde önemli avantajlar sağlamıştır. Bununla birlikte, bu membranların poliamid bazlı aktif tabakası, dezenfeksiyon ve membran temizleme işlemlerinde kullanılan klor nedeniyle zarar görmeye eğilimlidir. Bu işlemler, yeniden kullanım için belediye atıksu arıtımı için gereklidir fakat membranların kullanım ömrünün azalmasına neden olurlar. Bu nedenle tuz giderimi restorasyonunu sağlayan membranların gençleştirilmesi, hasarlı membranların onarımı için umut verici bir yöntem olarak ortaya çıkmaktadır. Bu tez, membran yüzeyinde bir kaplama tabakası görevi gören ticari bir gençleştirme ajanının performansını araştırmaktadır. Bu deneysel çalışmada, membranlar önce çeşitli klor konsantrasyonları, temas süresi ve pH değerleri altında indirgenmiş ve

performansları belirlenmiştir. Bunun üzerine hasarlı membranlar gençleştirme kimyasalı ile onarılmış ve gençleştirme sonrası performansları su akısı ve tuz giderimi açısından kaydedilmiştir. Membranların kimyasal yapısındaki değişim FTIR-ATR yöntemi ile incelenmiştir. Sonuçlar, gençleştirme maddesinin, hafif derecede bozulmuş membranların tuz reddini başarılı bir şekilde restore ettiğini göstermiştir.

Anahtar Kelimeler: Ters Ozmoz Membranları, Gençleştirme, Atıksu Gerikazanımı , Sürdürülebilirlik, Bozulma

Dedicated to The Great Founder of the Turkish Republic Mustafa Kemal Atatürk,

and My Parents; Talat and Ayşe

ACKNOWLEDGMENTS

TABLE OF CONTENTS

LIST OF TABLES

LIST OF FIGURES

xvii

LIST OF ABBREVIATIONS

ABBREVIATIONS

BOD	Biological oxygen demand
DPR	Direct potable reuse
EPA	Environmental protection agency
IP	Interfacial polymerization
IPR	Indirect potable reuse
LMH	Liter per square meter per hour
MCA	Monochloramine
MF	Microfiltration
MWWTP	Municipal wastewater treatment plant
NF	Nanofiltration
PVA	Polyvinyl alcohol
PVME	Polyvinyl methyl ether
PVP	Polyvinyl pyrrolidone
RO	Reverse osmosis
SD	Solution-diffusion
TA	Tannic acid
TDS	Total dissolved solids
TFC PA	Thin-film composite polyamide
UF	Ultrafiltration
WWTP	Wastewater treatment plant

LIST OF SYMBOLS

SYMBOLS

A	Water permeability coefficient for Solution-diffusion model	$\dfrac{m^3}{m^2 \cdot s \cdot bar}$
A_m	Membrane area	m^2
A_s	Solute permeability coefficient	m/s
a	Activity	-
c_{avg}	The logarithmic mean of solute concentration	kg/m^3
c_w	Water membrane distribution coefficient	-
C_{fi}	Feed conductivity	μS
C_{pi}	Permeate conductivity	μS
ΔC_s	Concentration difference	kg/m^3
D_s	Solute diffusion coefficient	m^2/s
D_w	Water diffusion coefficient	m^2/s
EC	Electrical conductivity	$\mu S/cm$
K_s	Solute membrane partition coefficient	-
l_p	Water permeability coefficient for the phenomenological model	$g/s \cdot bar \cdot m^2$
J_s	Solute flux	m/s
J_w	Water flux	m/s
R	Salt rejection	-
V_w	Partial molar volume of water	$m^3/mole$
w	Solute permeability for phenomenological model	m/s
x	Mole fraction	-
Δx	Membrane thickness	nm
μ	Chemical potential	J/kg
π	Osmotic pressure	Pa
σ	Reflection coefficient	-

CHAPTER 1

INTRODUCTION

Despite the fact that the two thirds of earth's surface is covered with water, only three percent of it is freshwater and 30 % of available freshwater is trapped in icecaps and glaciers (Lui et al. 2011). Rapid increase in human population, industrialization, and climate change increased the stress on available water resources. Estimations point out that 700 million people might move due to water scarcity by 2030 which was influenced by two folds increase of global water use (UN, 2019). Water is a valuable source to be used once and treated municipal wastewater might supply water for agricultural, industrial, and potable reuse (IWA, 2018). Nearly 48 % of wastewater is released into the environment without adequate treatment (Jones et al., 2021).

Municipal wastewater needs to be treated with advanced methods to be used as a potable resource as either indirect or direct. Former, added to environmental buffer; either to a surface reservoir or groundwater reservoir, and latter is treated directly by adding to water treatment plant's influent or connected directly to an irrigation line (Warsinger et al., 2018). The remarkable increase in the usage of membrane technologies in direct and indirect potable projects proves polymeric membranes' effectiveness in water treatment. It was reported that reused water has reached 32 million^3/day worldwide (Lautze et al., 2014; Warsinger et al., 2018). There are four main steps of conventional wastewater treatment; preliminary, primary, secondary and tertiary treatment. Generally, the quality of the effluent coming out of the secondary treatment is good enough for environmental discharge; however, higher-level purification is a must for potable reuse. For instance, in the USA, various water treatment plants use membrane treatment prior to the discharge of an environmental buffer (Gerrity et al., 2013).

Polyamide membranes are vital constituents of reverse osmosis (RO) units since their discovery (M Wilf, 2010; Z. Yang et al., 2019). These membranes promise a stable performance in handling variable feed water quality, and most importantly, they are highly selective to pathogens and organic contaminants present in wastewater effluents (Warsinger et al., 2018). The organic and biological wastewater content requires unique methods to mitigate fouling, such as pre-treatment and cleaning (Nguyen et al., 2012). Regardless of the preventive

practices, performance decline or even membrane failure results from this dynamic process (A. Antony & Leslie, 2011a; García & Díaz, 2011). Hence, alkaline and acidic cleaning sequence are essential for removing biofilm (García & Díaz, 2011). Even though there are certain guidelines to follow, operational incidents lead to shortening of lifespan or even replacement of the membranes. Vast amounts of studies were carried out to understand the influence of chlorination on polyamide structure since this is the soft spot of polyamide membranes by using accelerated aging experiments (Cran et al., 2011; Kwon & Leckie, 2006b; Verbeke et al., 2017). Accelerated aging experiments is the investigation of membrane degradation under increased oxidant (chlorine) concentrations and decreased duration to mimic the exposure of chlorine on a shorter time.

It has been reported that over 14,000 tonnes of end-of-life membranes were sent to landfills in 2015 (Landaburu-Aguirre et al., 2016). Considering the fact that reverse osmosis market growth was estimated as 10.9 % between 2016-2021, the waste will tend to keep increasing if it is not dealt with (Senán-Salinas et al., 2019). In the current literature, numerous researchers Several scientists studied the valorization of end-of-life membranes through oxidation to lower grade membranes. Their research on efficiency and salt removal capability showed that it is possible to use the oxidized membranes in water treatment plants (Lawler et al., 2012; Paula et al., 2017; Rodríguez et al., 2002); however, these require energy and chemicals. Besides the environmental impact of wastes due to discarded membranes, membrane replacement leads to an additional approximately 10-15 % of the operational costs (Paula et al., 2017; Senán-Salinas et al., 2019).

Rejuvenation is a mildly degraded membrane treatment that overcomes the drawbacks of membrane cleaning and disinfection which causes membrane degradation due to chlorine by restoring the salt rejection capability. According to the literature, researchers apply different coatings on the membrane surface, and they found out that tannic acid-containing rejuvenation agents effectively adhere to the membrane surface. Due to their abundant phenolic structure, they may enhance the passage of water molecules. Bartl (2014) states that waste prevention and reuse should be prioritized in sustainable membrane operation because it prevents recycling the membranes by utilizing cleaning and surface modification (Bartl, 2014).

1.1   Objectives

While researchers proved that rejuvenating agents that contain polyphenols can restore the salt rejection of degraded membranes, no studies were carried out which investigated the role of a commercial rejuvenation agent; on commercial BW30XFR PA TFC membranes which were degraded by hypochlorite. Initially, this thesis focused on understanding the role of pH on membrane degradation by active degradation, several experiments were conducted in a cross-flow system with two different pH values. The degraded membranes were then treated with the rejuvenating agent and evaluated in terms of their performance; water permeability, brackish water permeability (2000 ppm NaCl), and chemical characteristics change by FTIR-ATR. The detailed objectives were:

1. To determine the performance of virgin membranes by performance tests, water permeability and brackish water permeability to determine the transport parameters for further comparison.
2. To investigate the exposure concept and clarify the suitable experimental conditions for bench-scale filtration experiments.
3. To investigate and understand the degradation of membranes by considering pH effect under active degradation.
4. To verify the effectiveness of Rejuvenating agent, on commercial membranes by considering the transport parameters after the treatment.
5. To assess the chemical change of membrane structure after degradation and rejuvenation.

1.2   Approach

The commercial membrane: BW30XFR, used in experiments is TFC PA membrane used in brackish water treatment plants. These membrane's water flux and salt rejection is well documented by the manufacturer and in other research (Donose et al., 2013; Jang et al., 2019). NaOCl exposure, and pH was investigated for degradation experiments, former was applied by considering concentration and duration. NaOCl concentration was 1000 ppm, and 250 ppm; duration was six, four and eight hours. The pH of the solution was four (active chlorine species; hypochlorous acid) and nine (active chlorine species; hypochlorite). Rejuvenating agent, which contains 95 % tannic acid, was used to restore the salt rejection performance.

Performance tests with deionized and brackish water was conducted at four different pressures by bench-scale filtration set-up. The results obtained from these experiments used in calculation of transport parameters according to solution diffusion theory.

FTIR-ATR spectroscopy was used to inspect changes or shifts of specific peaks related to membrane degradation and rejuvenation. Consequently, the change in the chemical structure due to rejuvenation was evaluated with FTIR-ATR knowledge. The rejuvenation studies in the literature depict a preliminary understanding of interactions between rejection-enhancing agents and the degraded membrane surface.

1.3   Scope and Outline

This thesis comprises five chapters and five appendices. The first two chapters;1-2 contain the introduction and background information, respectively. Chapter 3 includes experimental procedures, set-up, chemicals and materials, and instruments used in this experimental work. Chapter 4 is divided into two parts i.e., performance tests results and chemical structure change. First part gives the results of performance tests of the virgin, degraded, rejuvenated, re-rejuvenated and directly rejuvenated membranes, respectively. The second part evaluates the FTIR-ATR scans of the virgin, degraded, rejuvenated, re-rejuvenated, and directly rejuvenated membranes, respectively. Lastly, Chapter 5 concludes the main findings and suggests future work for this study.

CHAPTER 2

LITERATURE REVIEW

This chapter comprises the theoretical background and literature review of water reuse and municipal wastewater treatment plants (MWWTP). The technology used to produce potable water; reverse osmosis (RO) and thin-film composite polyamide (TFC PA) membranes.

2.1 Wastewater Reuse

The water industry aims to deliver clean water as potable water, protect environment by treating industrial or municipal wastewater for safe discharge or reuse. It was estimated that globally 359.4 $m^3.yr^{-1}$ municipal and industrial wastewater is produced which is equal to the volume of 143,760 olympic swimming pools (Jones et al., 2021). Only 11 % of produced wastewater is utilized for reuse, most of it being released to environment (Jones et al., 2021).The water reuse is the process of reclaiming the wastewater and treating it to reuse. There are different classifications of water reuse i.e., direct and indirect, and direct potable reuse (DPR) and indirect potable reuse (IPR) (Warsinger et al., 2018). Direct reuse is the transfer of either treated or untreated wastewater to the location of planned application. On the other hand indirect reuse is the usage of treated water after augmenting to a surface water reservoir or groundwater supply (Roccaro, 2018).

The importance of utilizing treated municipal wastewater for potable reuse is increasing worldwide due to increased water stress in many urban areas. Reuse of wastewater may enhance the water supply for agriculture and industry; it can play a crucial role as potable use in regions where climate change poses adverse effects on water resources (Warsinger et al., 2018). Potable water reuse requires treating wastewater for drinking water, which can be done either by DPR or IPR (EPA, 2017). In DPR, reclaimed wastewater is directly added into a municipal water supply system after ensuring that quality standards have been met (Roccaro, 2018). DPR can reduce the costs related to water transport since it can cut the distance that treated water would need to be pumped. IPR projects are preferred because there is a lack of real-time water quality control in DPR (Drewes & Khan, 2015; Leverenz et al., 2011). In IPR systems, reclaimed water

is provided to an environmental buffer (Warsinger et al., 2018). Roccaro (2018) states that the difference between IPR and DPR was the delay in delivering treated water. For about two decades, the installation of DPR and IPR were increased in certain countries (Warsinger et al., 2018). In the capital of Namibia, 50 % of the city's water demand was supplied by the DPR system, which was utilized in providing recycled water for domestic consumption (Van Rensburg, 2016). Figure 2.1. shows six different treatment trains after secondary treatment to obtain high quality reclaimed water quality in USA.
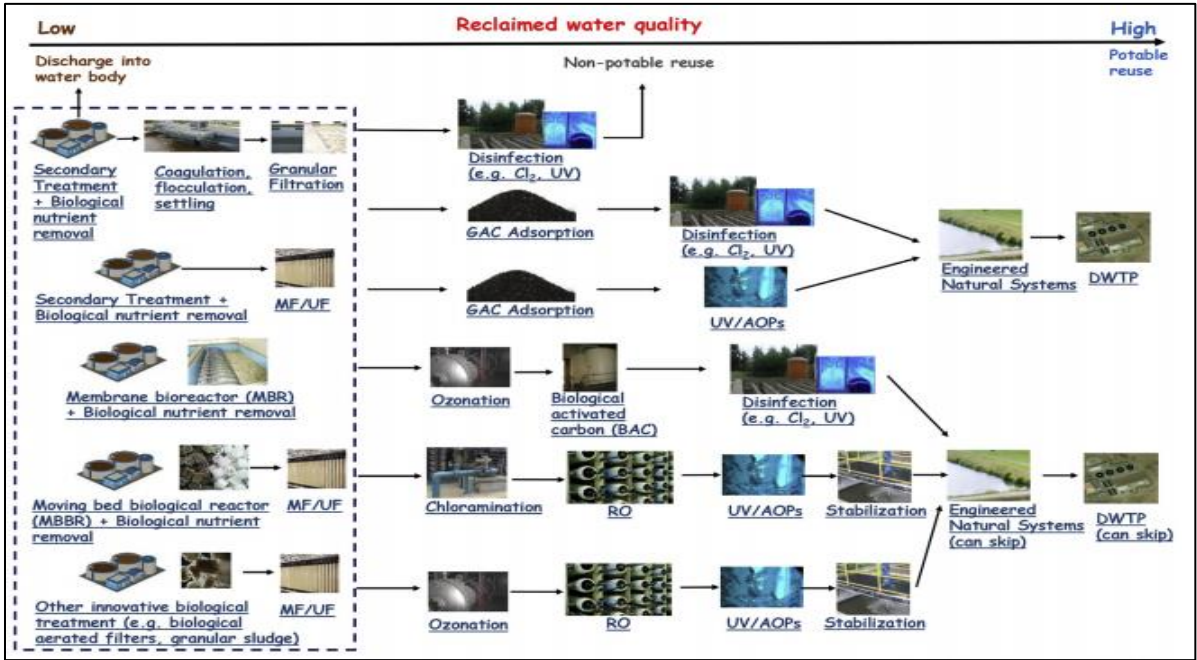
Figure 2.1. Wastewater treatment trains for different end-uses (Roccaro, 2018)

Municipal wastewater is comprised of biological, chemical, and physical pollutants. There are various constituents like suspended solids; organic matters such as proteins, carbohydrates, and fats; inorganic matters like calcium and heavy metals; fundamental nutrients like nitrogen and phosphorus; pathogens; trace elements and total dissolved solids (TDS) (Mohan et al., 2014). The wastewater from various sources is treated through treatment trains for various purposes according to rules and regulations on reuse, considering who is delivering the rule and where to be applied. WHO, FAO, World Bank, ISO, and EPA are several national and international organizations that published recommendations for reuse, mainly used as reference (Salgot & Folch, 2018). The regulations of EPA according to end-use are given in Table 2.1.

Table 2.1.End-use based wastewater reuse guidelines (Mohan et al., 2014)

Water reuse	Treatment goals	Examples of applications
Urban use		
Unrestricted	Secondary, filtration, disinfection BOD_5: ≤10 mg/L Turbidity: ≤2 NTU Fecal coliform: ND/100 mL Cl_2 residual: 1 mg/L; pH 6–9	Landscape irrigation (parks, playgrounds, schoolyards), fire protection, construction, ornamental fountains, recreational impoundments, in-building uses (toilets, air conditioning)
Restricted access	Secondary, and disinfection BOD_5: ≤30 mg/L TSS: ≤30 mg/L Fecal coliform: 200/100 mL Cl_2 residual: 1 mg/L; pH 6–9	Irrigation of areas where public access is infrequent and controlled (golf courses, cemeteries, residential, greenbelts)
Agricultural irrigation		
Food crops	Secondary, filtration, disinfection BOD_5 : ≤10 mg/L Turbidity: ≤2 NTU Fecal coliform: ND/100 mL Cl_2 residual: 1 mg/L; pH 6–9	Crops were grown for human consumption and consumed uncooked
Non-food crops and food crops consumed after processing	Secondary, and disinfection BOD_5: ≤30 mg/L TSS: ≤30 mg/L Fecal coliform: 200/100 mL Cl_2 residual: 1 mg/L; pH 6–9	Fodder, fiber, seed crops, pastures, commercial nurseries, sod farms, commercial aquaculture
Recreational use		
Unrestricted	Secondary, filtration, disinfection BOD_5: ≤10 mg/L Turbidity: ≤2 NTU Fecal coliform: ND/100 mL Cl_2 residual: 1 mg/L; pH 6–9	No limitations on body contact (lakes and ponds used for swimming, snowmaking)
Restricted	Secondary, and disinfection BOD_5: ≤30 mg/L TSS: ≤30 mg/L Fecal coliform: 200/100 mL Cl_2 residual: 1 mg/L; pH 6–9	Fishing, boating, and other noncontact recreational activities
Groundwater recharge	Site-specific	Groundwater replenishment, saltwater intrusion control, and subsidence control
Potable reuse	Meet requirements for safe drinking water; specific regulations do not exist, and specific goals remain unresolved	Blending with municipal water supply (surface water or groundwater)

One of the biggest challenges in front of water reuse is public acceptance (Ormerod & Scott 2013). Hartley (2006) claimed that the challenge posed by 'the people side' of water reuse is equal or greater than the technical side. In a recent study on public acceptance in Spain, researchers have found a public unwillingness to domestic usage of treated water in certain areas (López-ruiz et al., 2020). In Turkey, 10.5 million m^3 of wastewater was treated daily, and a significant portion of the treated water was used in the industry. People are hesitating consuming food irrigated with the treated water (Nas et al., 2020). On the contrary, some studies have shown a positive acceptance of recycled water in use, including Australia (Khan & Anderson, 2018), the United States (Hui & Cain, 2018), and China (Zhu et al., 2018).

2.2 Wastewater Treatment Technology

The aim of municipal wastewater treatment plants is to make water proper for environmental discharge or future use, i.e., potable, industrial, and agricultural (Shmeis, 2018). Water holds a great portion of wastewater; only 0.1 % of feedwater to WWTPs are comprised of contaminants such as organic and inorganic, suspended and dissolved solids, together with microorganisms (von Sperling, 2007). Even though contaminants are in a small portion, they must be treated according to the purpose of end-use. In the design and operation of WWTPs, physical, chemical, biological, and biochemical characteristics of wastewater are important (Metcalf & Eddy, 2003). The conventional WWTP with activated sludge process is shown in Figure 2.2.

Wastewater treatment starts with the physical removal of coarse solids such as pieces of wood, floating materials, and plastics that are removed which is called preliminary treatment (Lin & Lee, 2007). Screens comprised of parallel bars or stepped plates remove large debris from the influent (U.S. EPA, 2000). This step is essential since it protects piping and downstream equipment from blockage and/or damage (Lin & Lee, 2007; Metcalf & Eddy, 2007).

The removal of settleable solids and part of organic matter occurs through primary treatment (von Sperling, 2007). The initial separation occurs in settling tanks or clarifiers depending on the type or design of operation (Lin & Lee, 2007). At this stage, the wastewater flows down where suspended materials either float or settle down (Lin & Lee, 2007). The former skimmed from the surface, and the latter was sent to sludge treatment. Primary effluent removes 60 to 70 % of the suspended solids (SS), 25–50 % of BOD_5 (amount of oxygen needed to remove digest organic material in water over five days), and 35–40 % of coliforms (von Sperling, 2007)
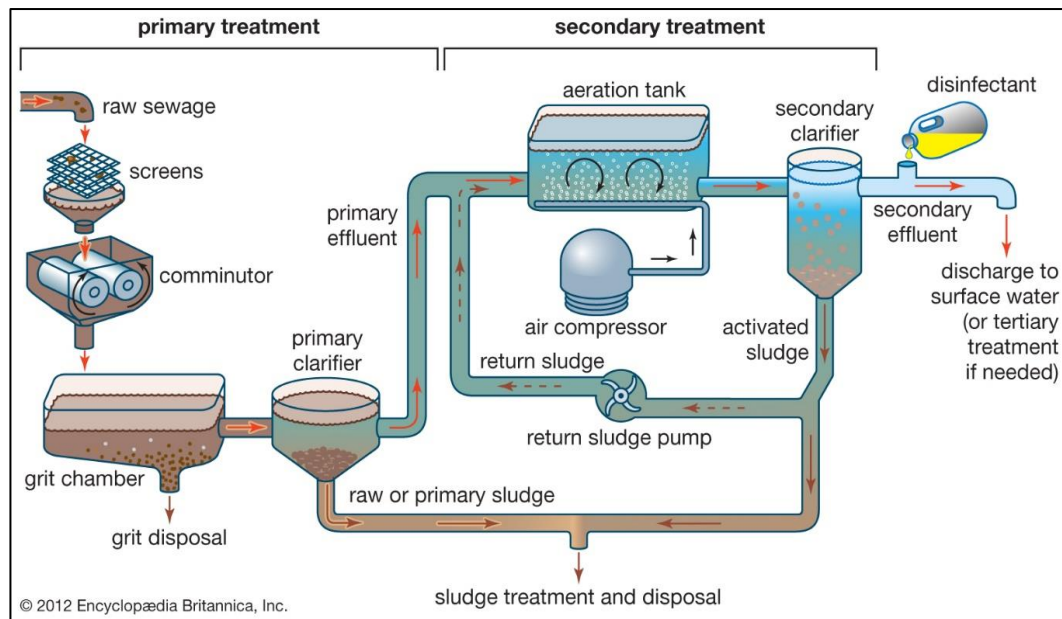
Figure 2.2. Primary and secondary treatment (Ambulkar, 2021)

The secondary treatment further treats primary effluent biologically. Primary effluent contains organic material of dissolved and finely suspended or colloidal solids. Large number of microorganisms used in biological treatment consume fine particulate and soluble BOD and, in some cases, nutrients and pathogens (Lin & Lee, 2007; von Sperling, 2007). Aerobic bacteria such as bacteria, fungi, and protozoa use the dissolved organic portion of the primary effluent as food and stabilize the material by converting them into carbon dioxide, water, sulfate, and nitrate compounds (von Sperling, 2007). The sludge produced during primary settling is led to digesters. With the help of anaerobic bacteria, the sludge's organic material is digested, carbon dioxide and methane gas are produced (Metcalf & Eddy, 2007). The secondary treatment removes SS, BOD_5, and coliforms of primary effluent by 65–95%, 60–99%, and 60-99%, respectively (von Sperling, 2007).

Tertiary treatment, sometimes called advanced treatment, is the last step before sending the effluent to the distribution system, reuse, or recycling. The composition of secondary effluent comprises organic matter, suspended solids, synthetic organic compounds, microorganisms, and ions. There are several technologies used in tertiary treatment, i.e., post-precipitation, sand filtration, dissolved air floatation, and

membrane technologies such as microfiltration (MF), ultrafiltration (UF), nanofiltration (NF), and RO. The selection of appropriate technology depends on secondary effluent quality, the purpose of the reuse, economic feasibility, etc.

Warsinger et al. (2018) claim that after tertiary treatment and disinfection, a treatment train including MF/UF that is followed by RO and advanced oxidation process (AOP) appeared as a standard in water reuse standard in the USA (Warsinger et al., 2018). Membrane processes might be a good selection because they can provide better effluent quality (Collivignarelli et al., 2018; Warsinger et al., 2018)

Disinfection primarily deactivates or kills pathogenic microorganisms that can be classified as conventional, advanced, and natural. (Collivignarelli et al., 2018; Lenntech, n.d.-b) Its implementation downstream of WWTPs is necessary because disinfection is efficient in prevent biofouling in RO membranes (Warsinger et al., 2018).

2.3   Membrane Technology

The urge for sustainable water resource management leads to applying pressure-driven membranes as an integral part of reuse facilities (J. Yang et al., 2020). Membranes play a crucial role in separation processes by controlling the permeation of the different solutes under a driving force i.e., applied pressure (Mulder, 2003). Because of applied pressure, solvent molecules and some portion of solute molecules permeated through the membrane, which is called permeate, but some molecules were rejected due to membrane structure called concentrate (Mulder, 2003).

The separation occurs via the transportation of solvent molecules, i.e., water, through the membrane, porous or dense, while partial rejection of particles and dissolved contents according to their size, charge, and shape (Bruggen et al., 2003). The pore size decrease of the membrane as microfiltration (MF), ultrafiltration (UF), nanofiltration (NF), and RO in descanting order. Figure 2.3 illustrates the removed solutes and particles by membrane processes considering their range of separation.

Membrane processes can be classified as low and high-pressure (J. Yang et al., 2020). The selection of the membrane process depends on the molecular size and chemical properties of solutes present in the water (Mulder, 2003).

MF and UF membranes are low-pressure membranes that separate the particles based on their sizes (Mulder, 2003; Siddiqui et al., 2016). MF membranes separate micro and macroparticles through (0.05─10 μm) large pores by sieving, and they work under an applied pressure of less than 2 bar. The other low-pressure membranes, UF, can be operated up to 10 bar and separate broader particle range to the smaller (1–100 nm) pore size (Mulder, 2003; Warsinger et al., 2018). Due to the better high molecule selectivity of UF membranes, there are preferred for municipal water treatment since removing viruses and bacteria is essential in this operation (Su, 2019).
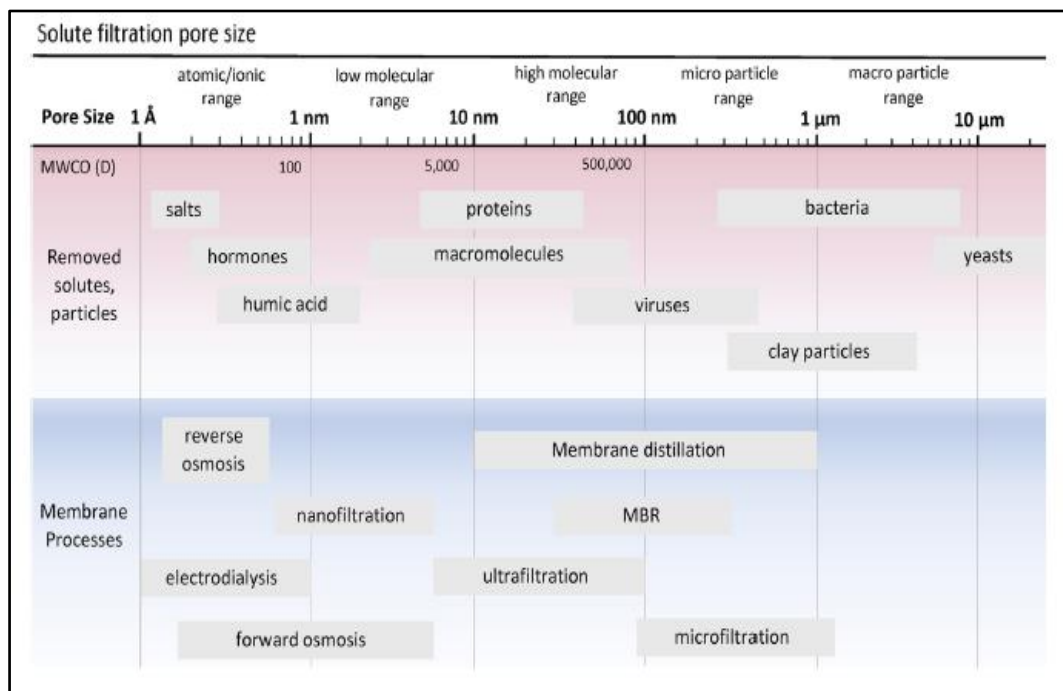
Figure 2.3. Range of separation through pore size (Warsinger et al., 2018)

High-pressure membranes are efficient in removing dissolved chemicals and salts. In theory, NF and RO membranes are similar in separation principle, solution diffusion. However, the former is not as effective as RO membranes in separating

monovalent ions such as Na$^+$ and Cl$^-$ (Mulder, 2003). The pore size of NF membranes is smaller than 2 nm, allowing them to retentate divalent ions, small organic molecules (Mulder, 2003; Su, 2019). NF membranes are advantageous when less concentrated feed water needs to be purified since it gives 2 to 5 times higher flux than RO membranes (Mulder, 2003; Su, 2019).

2.4 Reverse Osmosis

When two solutions having different concentrations, i.e., concentrated and diluted, are in contact through a semipermeable membrane, water molecules in the diluted side flow from less concentrated media to highly concentrate media, as shown in Figure 2.4. When the system reaches equilibrium, i.e., equal chemical of solvent molecules, a hydrodynamic pressure arises which is called osmotic pressure.
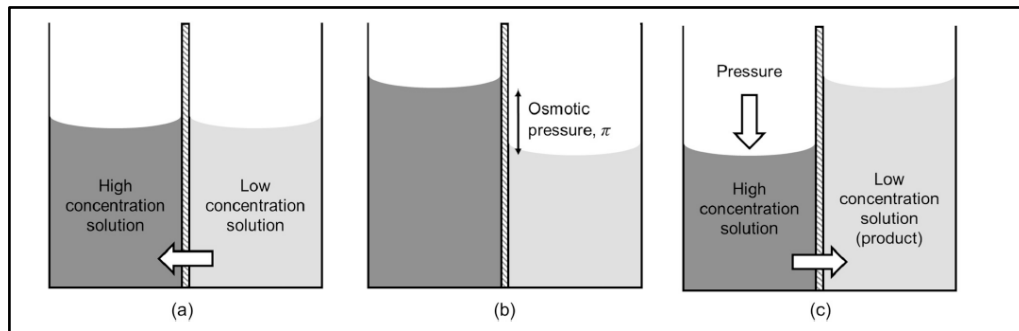
Figure 2.4. (a) osmosis (b) equilibrium (c) reverse osmosis (Qasim et al., 2019)

When external pressure is applied to overcome osmotic pressure, the water molecules in the concentrated side are forced to flow from the concentrated side to the diluted side through the semipermeable membrane.

The chemical potential of the solvent ($\mu_{i,1}$) in the concentrated side of component i, given in Equation 2.1. $\mu_{i,1}^{\circ}$ is chemical potential of pure substance at standard pressure and temperature. R is gas constant, T is temperature, $a_{i,1}$ is the activity and V_i is volume.

$$\mu_{i,1} = \mu_{i,1}^{\circ} + R \cdot T \cdot \ln(a_{i,1}) + V_i \cdot P_1 \qquad \text{Equation 2.1}$$

The chemical potential of the diluted side of component i is given in Equation 2.2.

$$\mu_{i,2} = \mu_{i,2}^{\circ} + R \cdot T \cdot \ln(a_{i,2}) + V_i \cdot P_2 \qquad \text{Equation 2.2}$$

When the system reaches equilibrium chemical potential of the concentrated and diluted side is equal ($\mu_{i,1} = \mu_{i,2}$), combining Equation 2.1 and Equation 2.2;

$$R \cdot T \cdot \left(\ln(a_{i,1}) - \ln(a_{i,2})\right) = (P_1 - P_2) \cdot V_i \qquad \text{Equation 2.3}$$

Osmotic pressure is the pressure difference between two media which is shown as $\Delta\pi$ (Pa) and when $a_{i,2} = 1$; the pure solvent is in the one side of semipermeable membrane Equation 2.3 can be written as Equation 2.4.

$$\pi = \frac{R \cdot T}{V_i} \ln(a_{i,1}) \qquad \text{Equation 2.4}$$

For dilute solutions $ln(a_i) = ln(x_i)$ where x_i is the mole fraction of component i, the mole fraction of solutes x_j which is equal to $1 - x_i$ and $x_j = (n_j/(n_i))$ where n_j and n_i are moles of solute and solvent, respectively. Using Equation 2.4 and $\frac{n_j}{V} = \frac{c_j}{M}$, then osmotic pressure can be written as Equation 2.5.

$$\pi = \frac{c_j \cdot R \cdot T}{M} \qquad \text{Equation 2.5}$$

The equation that relates osmotic pressure and solute concentration is called Van't Hoff equation which is given in Equation 2.5. Nevertheless, deviation from Van't Hoff equation occurs in RO due to high feed concentration.

In addition, for 100 ppm, total dissolved solids (TDS) in the feed water osmotic pressure ranges from 0.60 to 1.1 psi. Nevertheless, considering the membrane's resistance, applied pressure should be significantly higher than the osmotic pressure (Mulder, 2003).

2.4.1   Transport through the membranes

The separation of contaminants occurs via the transport through the membranes as a result of a driving force. Transmembrane pressure forces water molecules to pass through the membrane. In a cross-flow system, three streams, i.e., feed, permeate, and concentrate, are present. The feed that flows parallel to the membrane leaves the system as permeate and concentrate. Figure 2.5 illustrates the cross-flow mode of transport on membrane separation. Clean water exits the system as permeate and concentrated effluent collected as retentate.
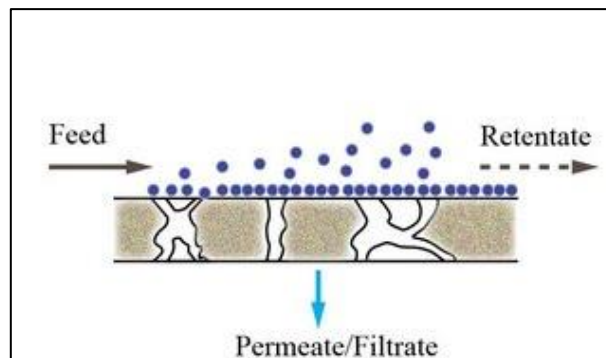
Figure 2.5. Cross-flow through the membrane (D. C. Hung et al., 2017)

Understanding the transport of solutes and water through membranes is vital to determine the performance of reverse osmosis membranes. Two models are used to describe the transport in membranes, i.e., phenomenological and mechanistic models (Qasim et al., 2019).

Phenomenological models assume that transport is independent of mechanism and membrane structure. This model was developed using irreversible thermodynamics by treating membranes as a black box, and the system is close to equilibrium (Gauwbergen & Baeyens, 1998; Mulder, 2003; Qasim et al., 2019).

Two well-known models, The Kedem-Katchalsky and Spiegler-Kedem, use irreversible thermodynamics to define the water (J_w) and solute flux (J_s) (Qasim et al., 2019). The former assumes that hydraulic net pressure controls the water and solute flux through the membranes as in Equation 2.6 and Equation 2.7. The

hydraulic and osmotic pressure difference through the membrane are ΔP and $\Delta \pi$, logarithmic mean of solute concentration is C_{avg} and l_p, w, and σ are phenomenological constants, i.e., water permeability, solute permeability, and reflection coefficient, respectively (Kedem & Katchalsky, 1958).

$$J_w = l_p \cdot (\Delta P - \sigma \cdot \Delta \pi) \qquad \text{Equation 2.6}$$

$$J_s = w \cdot \Delta \pi + (1 - \sigma) \cdot J_w \cdot c_{avg} \qquad \text{Equation 2.7}$$

When water and salt are considered as components on the diluted side, the reflection coefficient is the ratio of the flux of water under its chemical potential gradient to the contribution of the chemical gradient of salt to water flux (Mulder, 2003). When no solute transport across the membrane is assumed reflection coefficient equals 1. However, membranes are permeable to a small amount of solutes, making osmotic pressure term $\sigma \cdot \Delta \pi$; therefore, the reflection coefficient ranges from 0 to 1 (Mulder, 2003).

- $\sigma = 1$, no solute transport
- $\sigma < 1$, solute transport
- $\sigma = 0$, no selectivity

Mechanistic Models take into account the chemical and physical characteristics of membrane structure and solutes and proposes a transport mechanism (Qasim et al., 2019). One of the classifications in mechanistic models is non-porous models, where membranes are assumed to be homogeneous and non-porous. In this model, the common transport mechanism is the solution-diffusion model (SD) (Mulder, 2003; Wang et al., 2014). Diffusion occurs independently after the dissolution of species in the non-porous surface of the membrane.

Assuming that membranes are totally impermeable to low molecular solutes. In this case, flux is calculated from the following equation (Mulder, 2003).

$$J_w = A \cdot (\Delta P - \Delta \pi) \qquad \text{Equation 2.8}$$

Hence, water flux is directly proportional to the difference between the applied pressure and osmotic pressure difference. A is the water permeability coefficient, and it is specific to each membrane. Value of A is in the range of $3 \times 10^{-3} - 6 \times 10^{-5}$ $m^3 \cdot m^{-2} \cdot h^{-1} \cdot bar^{-1}$ for reverse osmosis (Mulder, 2003; Qasim et al., 2019).

$$A = \frac{D_w \cdot c_w \cdot V_w}{R \cdot T \cdot \Delta x} \qquad \text{Equation 2.9}$$

where D_w is the water diffusion coefficient, c_w is the water membrane distribution coefficient, V_w is the partial molar volume of water, R is gas constant, Δx is the thickness of the membrane (Mulder, 2003).

Solute flux, on the other hand, is directly proportional to the difference in the solute concentration across the membrane and it is independent of applied pressure (Mulder, 2003; Wang et al., 2014). It is calculated from

$$J_s = B \cdot \Delta c_s \qquad \text{Equation 2.10}$$

B is the solute permeability coefficient that is the function of diffusivity and distribution coefficient. Its value is in the range of $5 \times 10^{-3} - 10^{-4}$ $m \cdot h^{-1}$ where NaCl is considered as solute (Mulder, 2003; Wang et al., 2014).

$$B = \frac{D_s \cdot K_s}{\Delta x} \qquad \text{Equation 2.11}$$

where D_s is solute diffusion coefficient, and K_s is solute membrane partition coefficient (Mulder, 2003; Wang et al., 2014).

Above mentioned equations are useful for the determination of performance parameters such as water flux and solute rejection. Retention or rejection coefficient R is a measure of membrane selectivity (Mulder, 2003; Wang et al., 2014). It is expressed as

$$R = \frac{c_f - c_p}{c_f} \qquad \text{Equation 2.12}$$

where c_f is feed concentration, and c_p is the permeate concentration. Combining water flux, solute flux, and rejection coefficient R can be defined as:

$$R = \frac{J_w}{J_w + B} = \frac{A \cdot (\Delta P - \Delta \pi)}{A \cdot (\Delta P - \Delta \pi) + B}$$

Equation 2.13

SD model is applicable to RO considering the non-porous behavior of membranes and diffusion as a transport mechanism but with the limitation of solute rejection approximately unity (Qasim et al., 2019).

2.4.2   Thin-film composite reverse osmosis membranes

TFC PA RO membranes that are produced by interfacial polymerization have a three-layer structure, (i) dense top layer and (ii) porous supporting, and (iii) backing layer (Lau et al., 2012) as shown in Figure 2.6. The interfacial polymerization (IP) method enables the production of the ultrathin active layer, which is an important factor of flux (Cadotte et al., 1975). The thickness of the membranes is inversely proportional to flux. The ultrathin layer, also called the dense top layer, is either integral asymmetrical or composite (Mulder, 1997). It is cast on a porous substrate, a non-woven fabric, as a supportive layer with a thin active layer (Li et al., 2016).
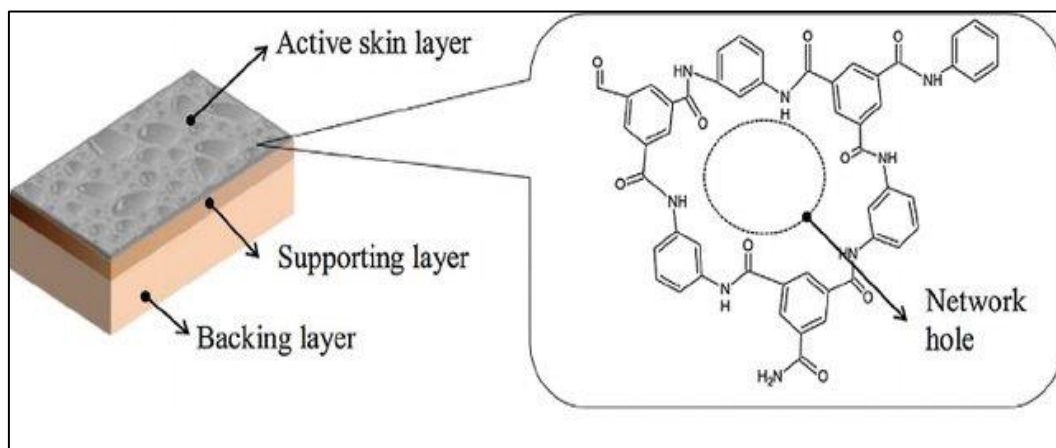
Figure 2.6. Three-layer layout of typical TFC PA membranes (Warsinger et al., 2018)

The copolymerization of two monomers produces the barrier layer of a TFC membrane at the immiscible interface (Morgan, 2011; Raaijmakers & Benes, 2016). Hence, building the interfaces and distributing the monomer between two phases are the main aspects of this reaction (Song et al., 2017). In their review, Song et al. (2017) classified the interphases into three categories: Liquid-solid interphase, liquid-liquid interphase, and liquid in liquid emulsion. They further state that liquid-solid IP is used for RO membrane fabrication. The precursors of IP synthesis are polyfunctional amine monomer and polyacyl chloride (acidic chloride) monomer in liquid phases (Lau, 2016), which are given in Figure 2.7. The difference between the liquid phases' chemical potential is the driving force behind monomer diffusion to the interface (Song et al., 2017). The monomers used in the synthesis vary, influencing the dense barrier layer's characteristics (Lau et al., 2012).
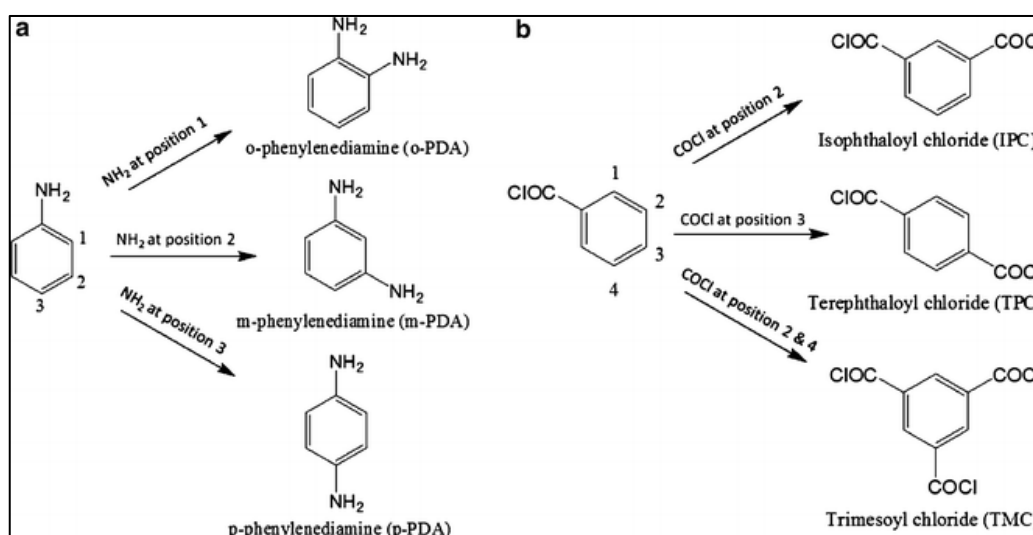
Figure 2.7. PA synthesis monomers (a) polyfunctional amine monomer and (b) polyacyl chloride monomer (Lau, 2016)

The first layer of composite membranes, PA, presents high salt and silica rejections. Selectivity and flux of the membranes are vital parameters for their properties. This method results in a highly crosslinked and thinner dense barrier layer, leading to higher flux and salt rejection (Liu et al., 2019). According to membrane suppliers, PA TFC membranes operate under pH 2-10 and show up to 45 °C thermal stability. However, the rough ridge-and-alley surface of PA TFC membranes is prone to

fouling and highly reactive towards oxidants which are used to clean fouled surfaces during the operation (A. Antony & Leslie, 2011a; Kucera, 2010; Verbeke et al., 2017).

The RO membrane's barrier layer is fabricated by immersion of the supportive layer in reactive primary monomer, m-phenylenediamine, in most cases 2 wt % (Fathizadeh et al., 2012; Z. Zhang et al., 2020). This step allows the primary monomer to diffuse through pores, which is then immersed in a second bath containing the secondary monomer, trimesoyl chloride, preferably at low around 0.1 wt % to 0.15 wt % (Fathizadeh et al., 2012; Wong et al., 2016; Y. Zhang et al., 2020; Z. Zhang et al., 2020). The porous sublayer and porous support resist high-pressure compaction and mechanical resistance (Liu et al., 2019).
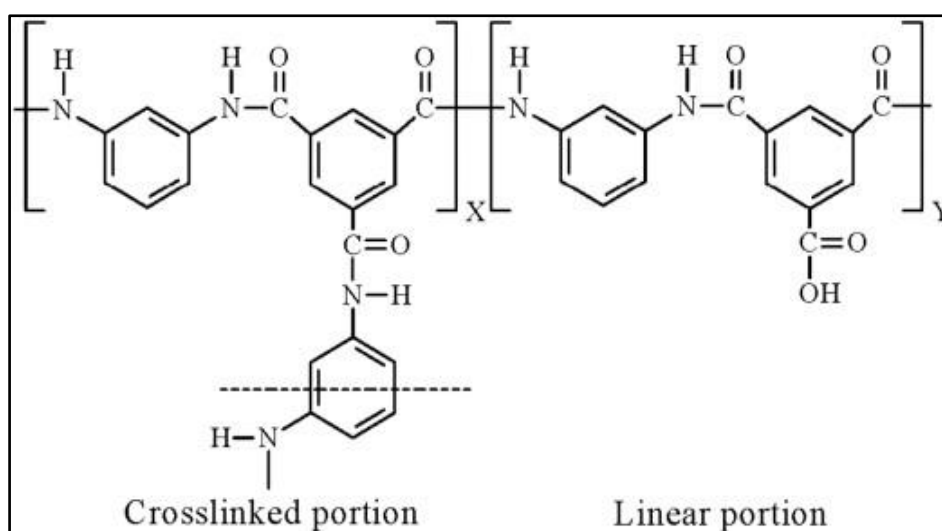
Figure 2.8. Cross linked polyamide membrane (Xu et al., 2013)

2.5   Membrane Degradation

Membrane integrity is an important area in RO treatment processes. It is highly possible that operational parameters and maintenance cause membrane failure during the water treatment process. The loss in the membrane performance affects effluent water quality and quantity (A. Antony & Leslie, 2011a). As mentioned in 2.4.2, PA layer is prone to fouling due to its surface structure that needs periodical cleaning

with oxidants. Oxidants such as hypochlorite, chloramines, and hydrogen peroxide depreciate the polymeric membrane performance in operation (da Silva et al., 2006).

Additionally, membranes are exposed to chlorine species which are used as disinfectants and bactericides. Although influent dechlorinated before the membrane process, small exposures gradually degrade the membranes throughout the operation (Verbeke et al., 2017). Therefore, it has been studied by several researchers to investigate the performance failure due to membrane degradation (Ambrosi & Tessaro, 2013; A. Antony & Leslie, 2011a; Cran et al., 2011; da Silva et al., 2006; Gabelich et al., 2005; Gohil & Suresh, 2017; Kwon & Leckie, 2006a, 2006b; Tessaro et al., 2005; Xu et al., 2013).

2.5.1   Disinfection process in municipal wastewater treatment plants

Pre-treatment of feed water to RO units is essential in operation due to membranes' morphology, as mentioned in section 2.4.2. Fouling adversely affects membrane performance by causing flux decline and transmembrane pressure rise, thus results in poor permeate throughput or higher energy consumption. There are four main foulants responsible for this functional impairment: particulate, organic, inorganic, and biofoulants (Alsawaftah et al., 2021; Mulder, 2003). Due to the hydrophobicity of the dense top layer of the membrane, they are more prone to organic and biofouling (Alsawaftah et al., 2021).

Disinfection of water with conventional methods such as chlorine, chlorine dioxide, ozone, peracidic acid and ultraviolet radiation (UV) (Collivignarelli et al., 2018). Chlorine in the form of chloramines, hypochlorite, and chlorine gas is common disinfection practice in the water industry, especially hypochlorite is used since it is easy to handle and cheap (Collivignarelli et al., 2018; da Silva et al., 2006; Kobylinski & Bhandari, 2010; Verbeke et al., 2017). However, Wasinger et al. (2018) state that chloramine is used instead of stronger biocide before RO to minimize the biofouling since chloramine tolerance is higher in PA membranes

(Gabelich et al., 2005; Warsinger et al., 2018). Additionally, studies proved that hypochlorite is exceedingly aggressive on membranes (da Silva et al., 2006).

Pure chlorine (Cl_2), available as NaOCl in liquid form, has pH-dependent dissociation kinetics. When hypochlorite is added to water, it dissociates to give hypochlorite ion (OCl^-) and hypochlorous acid (HOCl) as given in Equation 2.14 and Equation 2.15. HOCl is a dominant oxidizer in drinking water disinfection (Veatch & Black, 2009a). Due to its pH-dependent nature, different species such as hypochlorous acid, hypochlorite ion, and chlorine gas are present in aqueous form (Y. C. Hung et al., 2017).

$$NaOCl \leftrightarrow Na^+ + OCl^- \qquad \text{Equation 2.14}$$

$$OCl^- + H^+ \leftrightarrow HOCl \qquad \text{Equation 2.15}$$

Figure 2.9 gives the chlorine species in water as a function of solution pH. When NaOCl is dissolved in water, OCl^- ions react with H^+ ions and forms hypochlorous acid. At pH 5, HOCl is the main chlorine species; moving towards the left, chlorine gas starts forming, and through the right, to alkaline conditions OCl^- dominates the other species. At neutral pH, the concentration of HOCl is higher than OCl^-.
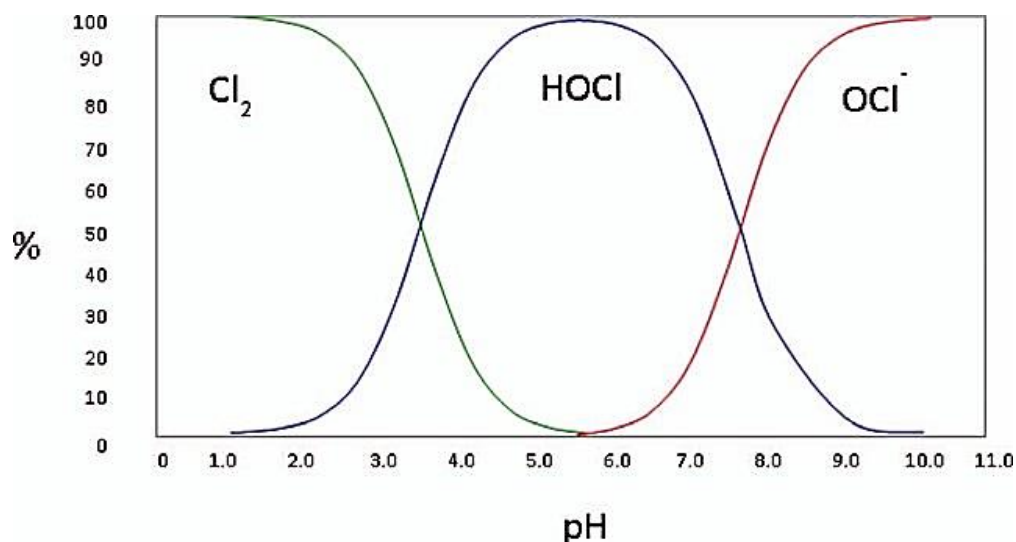
Figure 2.9. The abundance of chlorine species in different pH ranges (Gombas et al., 2017)

2.5.2   Oxidation with hypochlorite

Verbeke et al. review the PA- chlorine interaction on the membrane surface by comparing a number of studies and questioning the effectiveness of accelerated aging experiments (Verbeke et al., 2017). Antony and Leslie report the main issues with polymeric membrane degradation in wastewater treatment by giving details on the chemical mechanism for several types of membranes (A. Antony & Leslie, 2011b).

In order to understand degradation mechanisms, accelerated degradation experiments have been conducted for extensive studies (Alice Antony et al., 2010; da Silva et al., 2006; Kang et al., 2007; Kwon & Leckie, 2006a; Tessaro et al., 2005). Since maximum allowable chlorine concentration is low as membranes are prone to chlorine attack (<1000 ppm·hr with 1 ppm chlorine concentration), they are subjected to forceful conditions. Hypochlorite and monochloramine (MCA) are oxidizing agents mainly used in degradation studies. Oxidation of PA membranes by chlorine attack is a complex process that is described in two mechanisms: electrophilic aromatic substitution, which is followed by ring chlorination and N-chlorination, which is followed by ring chlorination (Alice Antony et al., 2010; Kang et al., 2007; Kawaguchi & Tamura, 1984; Soice et al., 2003).
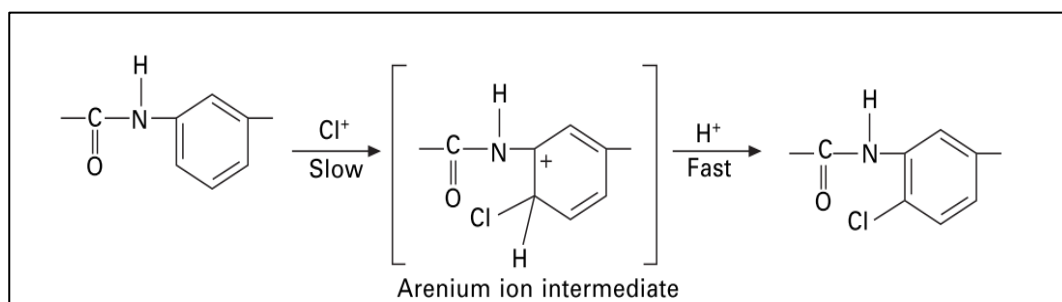
Figure 2.10. Electrophilic aromatic substitution to form ring-chlorinated products (A. Antony & Leslie, 2011a).

In the first mechanism, the chlorination reaction of aromatic rings requires an electron acceptor, $Cl^{+1,}$ from HOCl, which acts as a lewis acid (A. Antony & Leslie, 2011a). An arenium ion intermediate forms because of chlorine attack on polyamide,

which further rearranged to ring-chlorinated products which are given in Figure 2.10 (Gabelich et al., 2005). The formation of intermediate was considered as the rate-determining step.

The second mechanism of degradation is the formation of N-chlorinated intermediates due to the electron-withdrawing effects of the carbonyl group, presented in Figure 2.11.
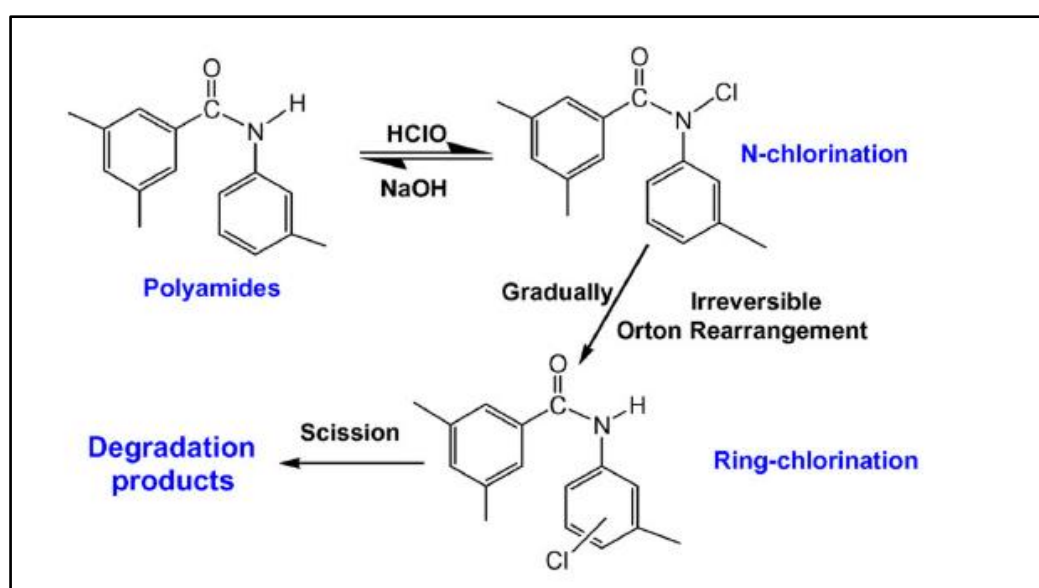
Figure 2.11. Chlorine degradation mechanism (Kang et al., 2007)

The reversible initial step chlorine is substituted to amide nitrogen, followed by irreversible ring chlorination via Orton rearrangement. These ring-chlorinated products are considered responsible for the salt rejection decrease (Alice Antony et al., 2010). Also, depending on the solution's pH, direct chlorination is possible in harsh environments (Soice et al., 2003). The degradation process was influenced by oxidizing agent type, chlorine concentration, exposure time, and process parameters. For example, n-chlorinated intermediate is favored by high pressures.

Various methods are used in order to assess membrane degradation from atomic to macroscopic levels. Antony and Leslie (2011) classified into five different groups as filtration, surface, chemical, morphological, and mechanical/thermal characteristics

(A. Antony & Leslie, 2011a). In this scope of this thesis, filtration and chemical characteristics determination will be explained in sections 2.5.4.1 and 2.5.4.2.

2.5.3 Oxidation with monochloramines

A group of researchers compared the ability of oxidants to degrade the PA membranes under similar operating conditions. They concluded that MCA degrades PA membranes to a certain extent; however, it is not as aggressive as chlorine (da Silva et al., 2006). Studies examining chloramines' effect on membranes use the characterization methods shown in Figure 2.12, proving that they are reliable for characterization assessments, likewise in hypochlorite studies.
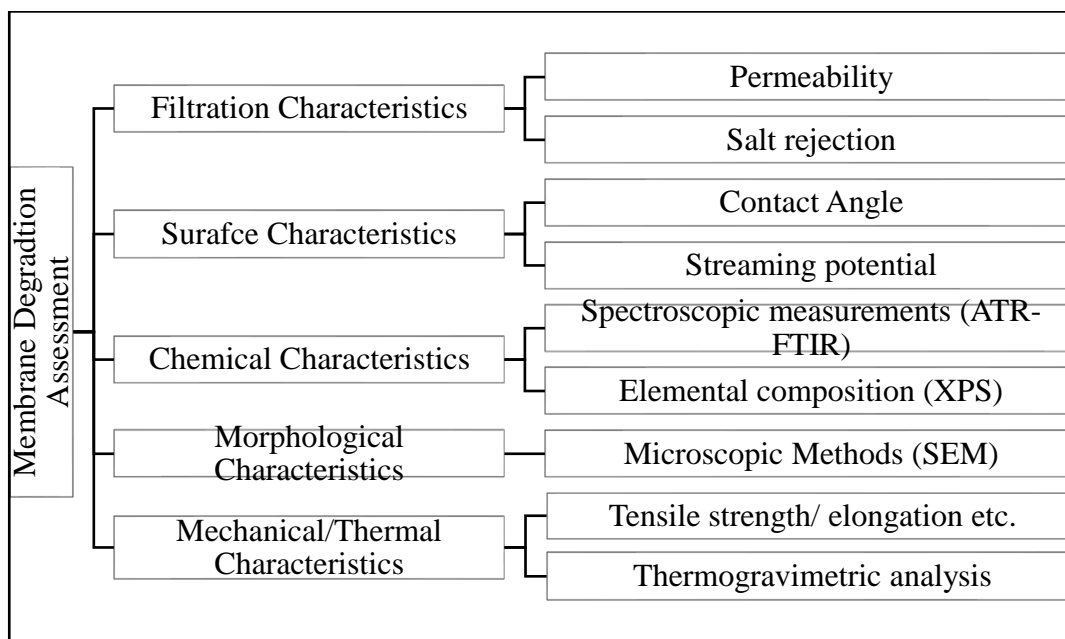
Figure 2.12 Membrane degradation assessment(A. Antony & Leslie, 2011a)

Cran et al. (2011) quantitively investigated the PA membrane degradation by subjecting them to MCA and various metal ions. The experiments were conducted via passive degradation using BW30 membranes manufactured by DOW.

They started their experiments by conditioning the membranes and performance testing through GE Osmonics. 2000 ppm NaCl standard solution was used for those aims, and flux is measured between 16 bar to 36 bar by increasing equal increments.

Membrane degradation experiments were conducted at room temperature at pH 8.3 by immersing the conditioned membranes into various solutions with and without metal ions. Degradation assessments were conducted following the experiments: filtration tests, SEM, ATR-FTIR
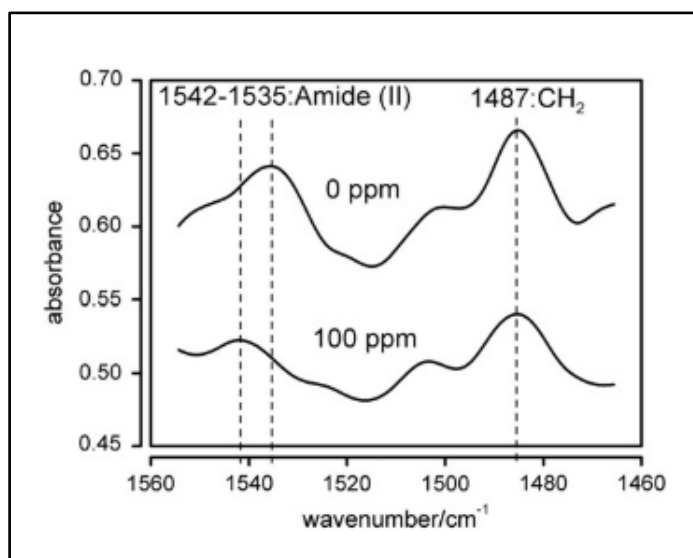
Figure 2.13. Infrared spectrum: (I) 0 ppm and (II) 100 ppm

They reported that according to filtration tests, flux increased after 1800 ppm·hr chloramine exposure; however, conductivity, which is the test for salt rejection, decreased up to 50%. Chemical characterization of the membranes was assigned by FTIR. There are two critical characteristic peaks for PA membranes. The peaks at 1540 cm^{-1} and 1487 cm^{-1} belong to the C-N stretch of amide (II) and CH_2 stretch of polysulfone, respectively. The results presented in Figure 2.13 reveals that after 400 ppm·hr exposure, the peak at 1540 cm^{-1} loses its intensity, and a slight hypochromic shift is observed.

One of the first active degradation methods used in chloramine degradation was the study of M.K. da Silva et al. (2006). They studied the degradation of commercial PA membranes from two suppliers with high MCA concentrations.

The membranes were tested before experimentation for comparison. Permeate flux was calculated by dividing volume measurement to time and membrane-active area. Active degradation was conducted at a constant temperature under 8 kg·cm^{-2} TMP and 4 L per min feed flow rate. A high and a low chloramine concentration were used at 70 ppm and 500 ppm, respectively (da Silva et al., 2006).

Their findings from degradation experiments were consistent with the literature in terms of salt rejection and permeate flux. They concluded that there is a threshold of exposure for salt rejection decrease, which means up 3000 ppm·hr chloramine exposure; salt rejection increases, but partial deformation due to amide cleavage causes a decrease after passing this threshold in salt rejection (da Silva et al., 2006).

2.5.4   Determination of membrane degradation

2.5.4.1   Filtration characteristics

Kwon et al. (2006) conducted membrane degradation experiments on a commercial PA membrane with 1000 ppm·hr chlorine tolerance. Membranes were degraded by using the passive method. Passive degradation is soaking tests conducted to investigate the chlorine concentration effect and pH effect on degradation; thus, two sets of conditions was conducted by keeping either concentrate or pH constant and varying the other parameter. The chemical and morphological characteristics after degradation were analyzed, and it was concluded that chlorine changed surface chemistry by attacking hydrogen bonding. The increase in chlorine concentration and decrease in pH levels increased the membrane degradation. Additionally, the roughness of the membrane remained unchanged (Kwon & Leckie, 2006a). In their complementary study, they focused on the change in the hydrogen bonding by using

passive degradation again. They determined the flux retardation by performance tests and commented on the chemical structure by using FT-IR ATR (Kwon & Leckie, 2006b).

Another passive degradation study with hypochlorite was conducted by Kang et al. was on the interfacial polymerized membranes. They investigated both filtration and chemical characteristics therewith proposed a degradation mechanism. The filtration tests upon hypochlorite exposure revealed that low pH and high concentration cause a greater decline in flux and salt rejection. The damage of PA rigid structure explains the decrease in salt rejection. The transformation to an amorphous state was triggered by n-chlorination and ring chlorination reactions (Kwon & Leckie, 2006b). Furthermore, polymer chain failure and an increase in the hydrophobic surface structure were the causes of the decrease in flux (Kang et al., 2007).

A passive degradation was performed by Donose et al. (2012) to investigate the effect of solution pH on the degradation process with three different commercial membranes. They chose acidic, neutral, and basic regions to inspect the effect of different chlorine species. They contacted only the active layer of the membrane with chlorine solution and evaluated the process through performance testing and other analytical methods.

Active degradation method was performed in various studies (Alice Antony et al., 2010; Da Silva et al., 2012; Tessaro et al., 2005). Antony et al. (2010) compared passive and active degradation methods and revealed that the decrease in the salt rejection was higher in the active method when compared to passive. They observed a linear relationship between the salt rejection and exposure; calculated the average decrease of 1.3 % in the salt rejection when the exposure is 1000 ppm·hr. In another study, Tessaro et al. (2005) showed that after 3000 ppm·hr NaOCl exposure at pH 10.8 salt rejection decreased by 1 %.

2.5.4.2   FTIR-ATR

An organic molecule is in constant motion; thus, bonds stretch and bend. Those movements create vibration and, when irritated with electromagnetic radiation, shows characteristic peaks at different wavelengths if the frequency of the radiation corresponds to the frequency of the vibration (McMurry, 2012). Between wavelengths of 4000–2000 cm^{-1} peaks expected are broad bands. Especially, between 3370 and 3270 cm^{-1}, hydrogen-bonded N–H stretching of trans- form of secondary amide band is observed (Socrates, 2001). In the case of polyamide, the peak around 3330 cm^{-1} is associated with hydrogen-bonded N–H stretching or –OH vibrations which do not present as broad as expected due to the cross-linked structure of PA membranes (Kang et al., 2007). Two consecutive peaks between 3000 – 2500 cm^{-1} were assigned to aromatic =C–H and aliphatic C–H stretching (Kang et al., 2007). The region between wavelengths of 1500- 500 cm^{-1} is called the fingerprint region, and a large number of peaks are represented. Secondary amides absorb at 1680-1630 cm^{-1} which is due to C=O stretching vibration and contributed by C–N vibration and C–C–N deformation (Socrates, 2001).

The amide II band is mainly due to the N-H in-plane bending motion, which has a strong absorption at 1570–1515 cm^{-1} (Socrates, 2001). Amide II band is also contributed by N–C stretching vibration of a –CO–NH– group of amide II band (Socrates, 2001). Peak assignments were have been reported in the literature for nearly each degradation research (Donose et al., 2013; Kwon & Leckie, 2006b; Xu et al., 2013). Table 2.2. gives peak assignments from research that investigated the hypochlorite degradation of crosslinked PA membranes (Kwon & Leckie, 2006b).

Kwon & Leckie, (2006) showed that the FT-IR spectrum of PA membranes gives the peaks assigned to both PA thin layer and polysulfone active layer (Kwon & Leckie, 2006b). According to their study, the peaks around 1663, 1609, 1541, and 1444 cm^{-1} are specific to the PA layer, and the shifts should be inspected for chlorination (Kwon & Leckie, 2006b).

Table 2.2 Peak assignment of FTIR-ATR scans

Peaks	Explanation
1663 cm^{-1}	Amide I band
1609 cm^{-1}	N–H deformation vibration / C=O ring stretching vibration aromatic amide
1541 cm^{-1}	Amide II band
1416 cm^{-1}	Aromatic C–H bending
3330 cm^{-1}	N–H and O–H stretching
3100 – 3000 cm^{-1}	Aromatic =C–H stretching

The Figure 2.14. shows the spectra of tannic acid where it shows a strong unsymmetrical transmittance around 3700 and 3000 cm^{-1}, which are assigned to the hydroxyl groups (–OH) stretching vibrations and due to hydrogen bonding. The small shoulder around 2920 cm^{-1} belongs to aromatic CH_2–OH sp^2 bonding, and 1720 cm^{-1} to carboxylic C=O vibrations; the peaks around 1370 and 1050 cm^{-1} assigned to C–O stretch of esters, and 1240 cm^{-1} to phenolic O–H stretch (Hegab et al., 2016; Joong et al., 2016; Pantoja-Castro & González-Rodríguez, 2012).
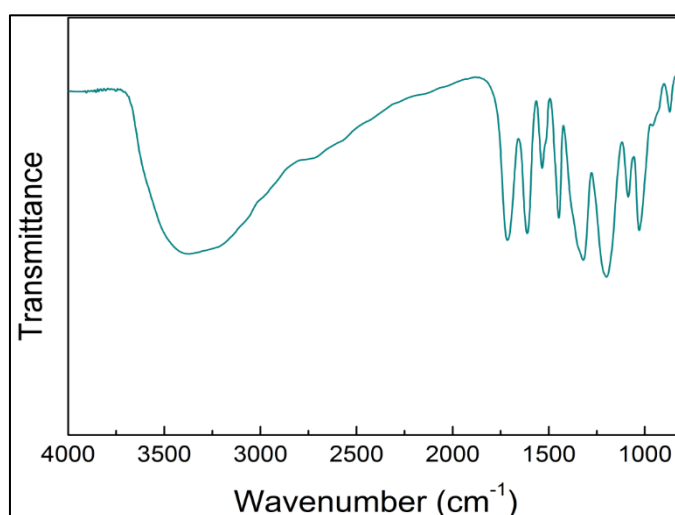
Figure 2.14. FTIR-ATR spectra of tannic acid (Joong et al., 2016)

2.6   Membrane Rejuvenation

The rejuvenation of membranes is defined as salt rejection restoration either by surface coating or hole plugging when RO membranes are affected from cleaning treatments or disinfection because of surface defects, abrasion damage, chemical attacks, and hydrolysis (Scott, 1995).

2.6.1   Tannic acid

Tannic acid, which is a specific tannin, is a water-soluble polyphenol. It contains a simple glucose core (A) which is conjugated by digalloyl groups (B), as shown in Figure 2.15. Ten equivalents phenylpropanoid-derived gallic acid forms ester bonds with a monosaccharide. Due to saccharide core, stereo centers are available (El Gharras, 2009). The dihydroxyphenyl (C) and trihydroxyphenyl (D) groups bring surface adhesive properties; thus, they have been used to build new surfaces and modify the surface properties (Cheng et al., 2020).
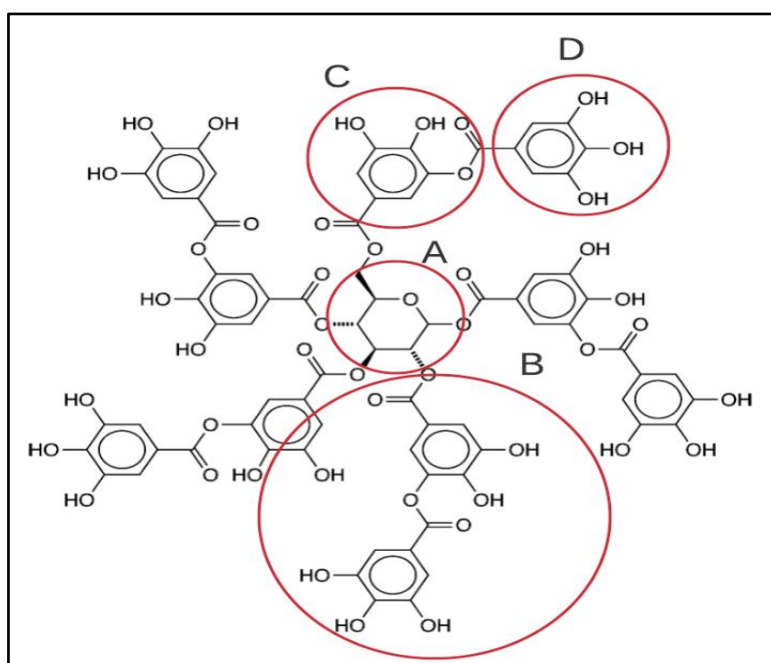
Figure 2.15. Tannic acid molecular representation (Yan et al., 2016)

Tannic acid is negatively charged when it is in a high pH solution which might be rejected by the negatively charged membrane surface (Da Silva et al., 2012). Digalloyl groups contain hydroxyl groups which allow tannic acid to form strong ionic bonds. Due to its –OH-rich chemistry, when applied on a surface, they are able to increase the hydrophilic character (Joong et al., 2016).

The reactivity of phenolic groups is given in Figure 2.16. Phenolate ions and phenoxenium cation can form ionic interactions with electrophiles and nucleophiles, respectively (Yan et al., 2016).
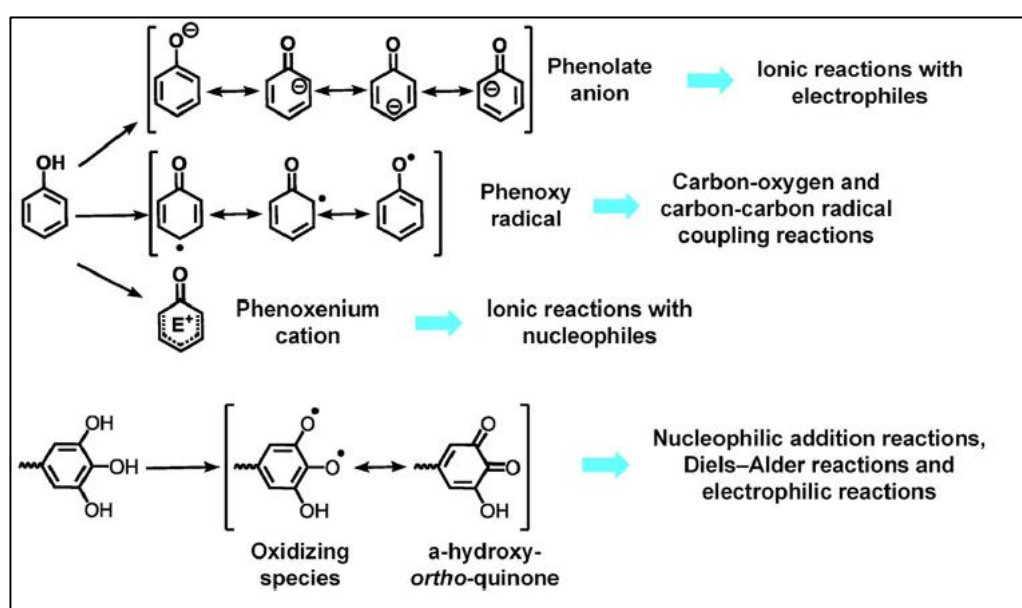
Figure 2.16. Phenolic group reactivity (Yan et al., 2020)

2.6.2 Performance restoration by using tannic acid

One of the earliest applications of tannic acid as a rejection-enhancing agent dates back to more than 35 years ago. The rejuvenation experiments were conducted under field operating conditions on commercial membranes operating between 0.5–5 years. Tannic acid was injected into the RO system, and an increase in salt rejection was observed (Mark Wilf & Glueckstern, 1985).

After 20 years from Wilf & Glueckstern's study, a group of researchers again focused on enhancing the membrane performance by applying "rejection enhancing agents" such as polyvinyl methyl ether (PVME), polyvinyl pyrrolidone (PVP), and polyvinyl alcohol (PVA), followed by tannic acid treatment on the virgin membrane and three years old membrane. They initiated the in-situ coating application on virgin membranes under nearly 14 bar by treating with TA only. In the following experiments, they concluded that PVME coupled application showed better performance. The initial results from the experiments led them to determine experimental conditions of cross-flow filtration with three years old membrane. They concluded that with the drawback of flux decrease (5–11.4 %), it was possible to increase the salt rejection(2.3–7.5 %) (Mitrouli et al., 2010).

One year after Mitrouli et al. (2010), a new study was published which investigates performance parameters such as pressure, pH of the rejuvenating solution, and TA concentration. The TFC PA membranes were obtained from two companies and received alkaline and acidic cleaning to simulate the membrane degradation. The degradation was followed by rejuvenation with TA, and they concluded that pH of the solution has more effect on the membrane's performance enhancement compared to pressure and TA concentration. In addition, 5 years operated BW30 membrane module treated with optimum conditions which were obtained from the first step of the study and they observed that salt rejection increased after rejuvenation; however, treatment caused decrease in the permeate flux. (Da Silva et al., 2012).

CHAPTER 3

MATERIALS AND METHODOLOGY

This chapter focuses on the experimental methodology that was used in this thesis. The experimental set-up, materials, and chemicals used, experimental procedure, equations used in the analysis, and chemical change determination method were explained in the following sections.

3.1 Description of the experiments

Throughout experiments, the virgin membranes were treated with five main steps. Each membrane was pre-treated initially according to treatment I to remove the preservation coating. Treatment II is testing of pre-treated membranes with two performance tests: deionized water permeability and brackish water permeability. Treatment I and II was applied for every virgin membrane. Treatment III comprises four different conditions to investigate the degradation of membranes and to decide degradation conditions prior to rejuvenation; treatment IV. The rejuvenation experiments performed on degraded membranes at pH 4 and pH 9, initially by applying single-step rejuvenation with 100 ppm Rejuvenating agent for one hour at pH 4. Treatment V applied on rejuvenated membranes after degrading them by 2000 ppm·hr NaOCl at pH 4. Finally, a direct rejuvenation was performed on pre-treated and performance tested virgin membranes. Treatments applied on for each set of experiments were summarized in Table 3.1.

Experiment set one was conducted to determine the initial performance of untreated membranes. After performing pre-treatment (I) and performance tests (II); water permeability and NaCl permeability, the membrane was placed in a desiccator for FTIR analysis.

Table 3.1. Summary of treatment conditions

Treatment #		*Explanation*
I	Pre-treatment	NaOH pre-treatment for 1 hr above pH 12
II	Performance test	Deionized water permeability test
		Brackish water permeability test with 2000 ppm NaCl
III	Degradation	6000 ppm·hr NaOCl degradation at pH 4
		2000 ppm·hr NaOCl degradation at pH 4
		1000 ppm·hr NaOCl degradation at pH 4
		2000 ppm·hr NaOCl degradation at pH 9
IV	Rejuvenation	100 ppm Rejuvenating agent treatment at pH 4 after degradation
		100 ppm direct Rejuvenating agent treatment at pH 4
V	Re-rejuvenation	100 ppm·hr rejuvenating agent treatment at pH 4 after degradation on rejuvenated membranes

Experiment set two, as presented in Figure 3.1, was performed to investigate the exposure (ppm·hr) and pH concept. In the first trial, membranes were subjected to harsh aging conditions to accelerate the degradation process. The change in their chemical structure was analyzed by FTIR-ATR. In the second and third trials, hypochlorite concentration was kept constant to observe the effect of treatment time on degradation. After determining the performance of degraded membranes through treatment II, the trials were proceeded with rejuvenation treatment and completed by FTIR scanning. After trial experiments, chemical and performance changes were investigated when membranes were subjected to hypochlorite solutions at two

different pH since active chlorine species is different in those two regions as explained before. Steps of experiment set three is given in Figure 3.1, the membranes were degraded with chlorine solutions at different pH levels by keeping the exposure constant. This set was terminated when performance tests and FTIR of degraded membranes were collected.
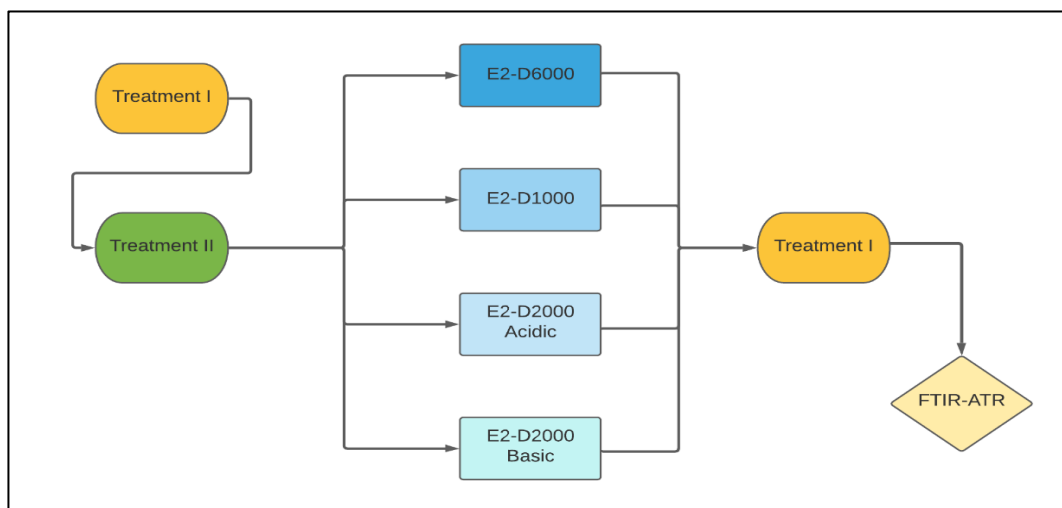
Figure 3.1. Flow chart of experiment set two

The flow of experiments for experiment set three and set four, which is given in Figure 3.2, was same except the degradation conditions. The membranes after treatment I, degraded with NaOCl solutions at pH 4 and 9. The performance tests were conducted to determine the membrane's filtration performance; then they were rejuvenated with 100 ppm Rejuvenating agent at pH 4 for one hour.
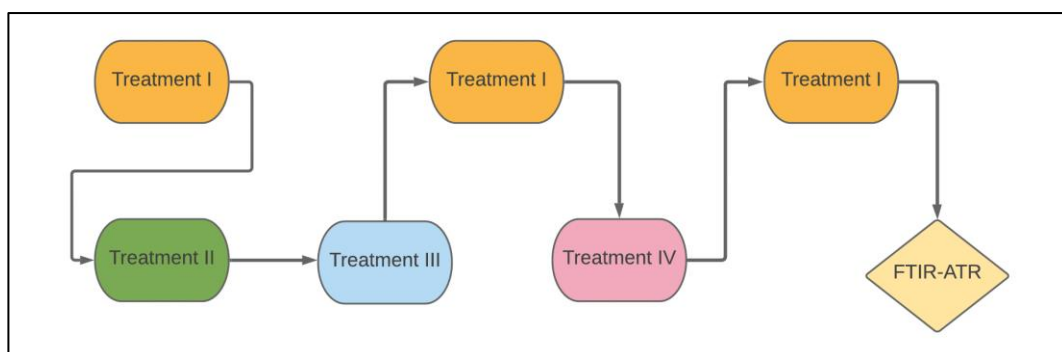
Figure 3.2. Flow chart of experiment set three and four

Re-rejuvenation experiments were performed to investigate the Rejuvenating agent's ability to restore salt rejection if rejuvenated membranes degrade again. Therefore, experiment set five was conducted by applying treatment I-II for virgin membranes followed by degradation with 2000 ppm·hr NaOCl at pH 4 and applying treatment IV. Rejuvenated membranes were then degraded again with same treatment conditions as in the first degradation and re-rejuvenated. Performance tests were conducted after second degradation and re-rejuvenation and membranes were dried for FTIR-ATR scanning.
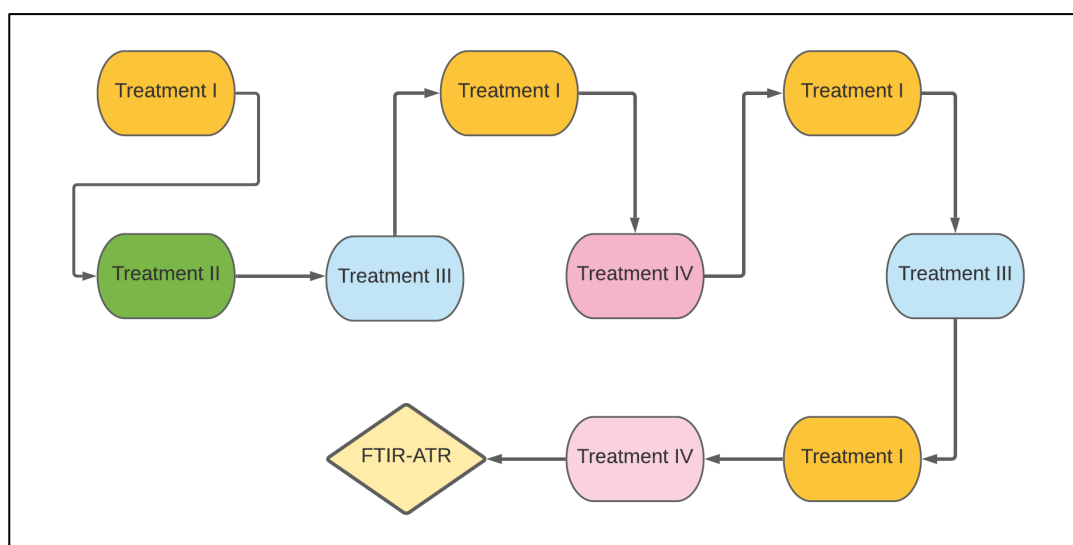
Figure 3.3. Flow chart of experiment set five

Last set of experiment; six, was direct rejuvenation of pre-treated virgin membranes by applying 100 mg/L Rejuvenating agent at pH 4. Performance tests were conducted after direct treatment as mentioned previously and membranes were dried 24 hr for FTIR-ATR analysis.
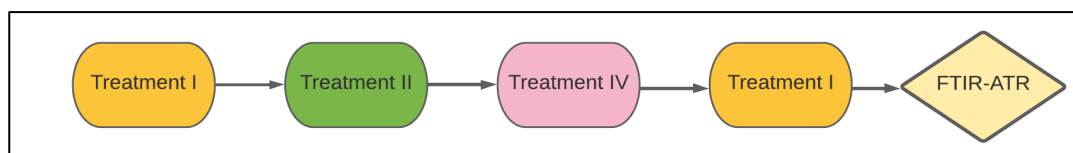
Figure 3.4. Flow chart of experiment set six

3.2   Membrane Filtration Set-up

Figure 3.5. SEPA Cell

This study was carried out by performing bench-scale experiments with SEPA CF II™, a cross-flow membrane cell system by General Electrics. The stainless-steel cell shown in Figure 3.5 holds membrane coupons that was purchased by the Sterlitech company. In order to mimic the hydrodynamic operation of membrane modules system is loaded by shim, medium foulant permeate spacer, RO membranes and permeate carrier, respectively, as in Figure 3.6. The water was fed to the system from a 2 L polypropylene beaker via Hydra-Cell, a high-pressure positive displacement pump. The feedwater passes through 4.7 mm diameter channels through the lower part of the cell holder and permeate was collected from the openings placed on the upper part of the cell holder. A hand pump was used to pressurize the cell holder to prevent any leakage during the operation. The pump power was adjusted from ABB controller, and a globe valve at the concentrate outlet was used to adjust the transmembrane pressure.
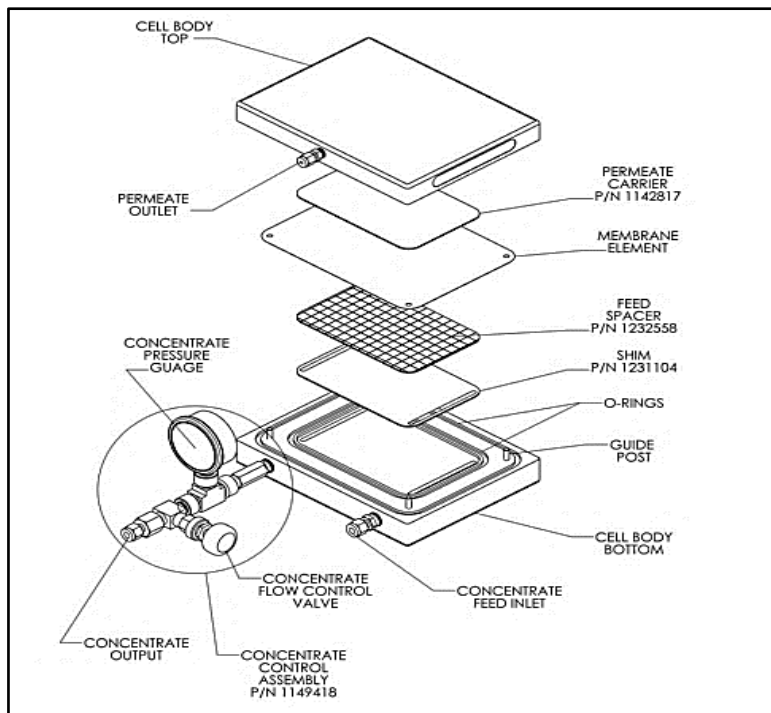
Figure 3.6 Cell Holder Assembly (Sterlitech, 2017b)

SEPA CF II is a membrane filtration unit that operates a maximum of 69 bar. The membrane cell system is comprised of: (i) a feed tank, (ii) a pump Hydra-Cell by Wanner Engineering with ABB controller, (iii) a flat plate cell with an effective membrane area of 140 cm^2.
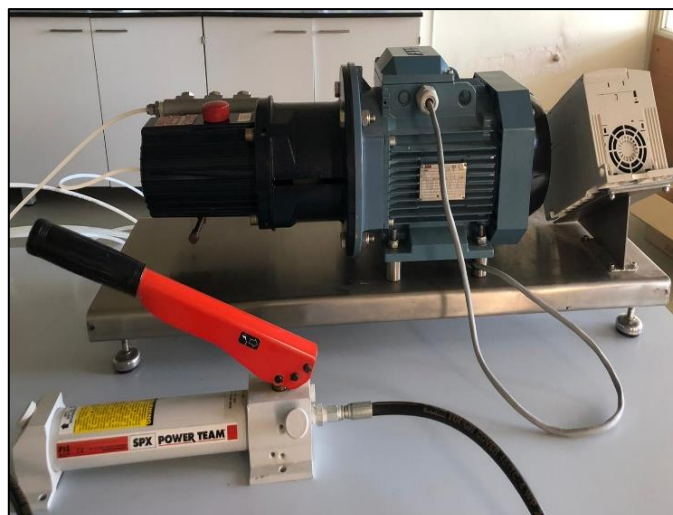
Figure 3.7 Hydra-Cell

3.3   Polyamide Membranes

Figure 3.8. DOW brackish water membrane specifications

The specification of thin-film composite polyamide BW30 XFR membranes from DOW are given below. All tested RO membranes were PA thin-film composite construction with a polysulfone support layer and had a chlorine exposure tolerance of less than 1,000 ppm·hr or a continuous free chlorine exposure of less than 0.1 mg··L^{-1}.

Table 3.2. DOW brackish water membrane specifications (Sterlitech, 2017a)

Series	BW30XFR
Feed	Brackish Water
Type	Fouling Resistant, Extra-Low Energy
pH Range (25°C)	2–12
Flux (gfd)/psi	28–33/225
Rejection	99.7%
Pore size/ MWCO	~100 Da

3.4 Chemical Characterization of Membranes

The first step of each experiment was Fourier transform infrared spectroscopy (FTIR) scanning of virgin membranes. Five points scanned through the Perkin Elmer Spectrum II, which is shown in Figure 3.9.

Figure 3.9 Perkin Elmer Spectrum II

Figure 3.10. Scan points of degraded membrane

Figure 3.10 represents the scanned points on the membrane. The spectrum of the membranes was scanned over the range of 450- 4000 cm$^{-1,}$ and corresponding peaks were evaluated for virgin, degraded, rejuvenated, re-rejuvenated and directly rejuvenated membranes. Infrared spectra were recorded on a Perkin-Elmer spectrometer (Spectrum II) using a universal attenuated total reflection (UATR) accessory. The UATR accessory contained a LiTaO3 with a diamond crystal at a nominal incident angle of 45°. Each spectrum presented is the result of 8 accumulations obtained with a resolution of 4 cm^{-1}. Each sample were analyzed with 30 N gauge pressure to obtain stable contact between ATR crystal and sample surface.

3.5   Deionized Water

The deionized water is obtained from a benchtop RO filtration system which was purchased from Zetaş.

Figure 3.11. Deionized water system

The tap water passes through two filters first to remove sediments and particles from the water. The activated carbon filter improves the taste, odor and appearance of the water and then it is sent to reverse osmosis membranes. The deionized water collected freshly daily for all the experiments. The system is given in Figure 3.11.

3.6   Membrane Pre-treatment Protocol

The virgin membranes require pre-treatment before any application. Pre-treatment solution was prepared from NaOH pellets (>99 %) which was purchased from Merck. After loading the FTIR scanned membranes into the SEPA CF II system, they were rinsed with NaOH solution of pH 12. The pump power was adjusted to 5 Hz manually from the controller, and the system was operated under total recirculation mode for 1 hr at 12 bar. The system was rinsed with deionized water for half an hour before the performance tests.

3.7   Performance tests

Before membrane degradation and rejuvenation experiments, virgin membranes were subjected to two types of performance tests. To evaluate the membrane's transport parameters and assess the operation results due to degradation and rejuvenation, as explained below, two filtration steps were followed for membrane performance validity.

3.7.1   Water permeability tests

Water permeability tests were performed with deionized water. Initial pressure was set to 4 bar, and pressure was increased by 4 bar to the final pressure of 16 bar. Permeate flow was measured by A&D company analytical balance over 5 minutes and recorded in terms of grams per minute. After every increment, the system was

running for 15 minutes to reach a steady state. The concentrate flow rate was collected for 10 seconds and recorded in grams per minute.

The following equation was used to calculate the flux of the membrane.

$$J_w = \frac{Q_p}{A_m} = \frac{\text{Volumetric Flow Rate of Permeate}}{\text{Membrane Area}} \qquad \text{Equation 3.1}$$

Due to the temperature dependency of permeate flux, a temperature correction is needed while calculating the permeate flux. The following equation is used when permeate concentration is higher than 25 °C.

$$TCF = EXP\left(2640 \times \left(\frac{1}{298} - \frac{1}{273 + T}\right)\right) \qquad \text{Equation 3.2}$$

Normalized flux calculated from Equation 3.3.

$$J_{w,n} = \frac{J_{w,rej}}{J_{w,vir.}} \qquad \text{Equation 3.3}$$

3.7.2   NaCl Permeability tests

Salt rejection tests was performed using 2000 ppm NaCl solution, rejection capacity of monovalent ions and charged species was evaluated. To prepare feedwater with a concentration equal to brackish water, sodium chloride (99.0 %) was purchased from Sigma-Aldrich and dissolved in deionized water. The method to perform the rejection capacity was the same as the permeability test. The concentration of dissolved solids was determined via conductivity measurements. WinLab data line conductivity meter was used, and conductivity was recorded in µS/cm. The conversion factor given in Equation 3.5 was used to convert conductivity to TDS where EC is electrical conductivity (Lenntech, n.d.). Normalized salt rejection calculated from Equation 3.8.

$$R_i = \left(1 - \frac{C_{pi}}{C_{fi}}\right) = \left(1 - \frac{\text{Conductivity of permeate}}{\text{Conductivity of feed}}\right) \qquad \text{Equation 3.4}$$

$$TDS\left(\frac{mg}{L}\right) = 640 \times EC\left(\frac{ds}{m} \text{ or } \frac{mmho}{cm}\right) \qquad \text{Equation 3.5}$$

$$SR\,(\%)_n = \left(1 - \frac{SR(\%)_{w,rej}}{SR(\%)_{w,vir}}\right) \qquad \text{Equation 3.6}$$

3.8 Membrane Degradation Protocol

The sodium hypochlorite (6–14 % active chlorine W/W) was purchased from Merck to perform membrane degradation by chlorine attack. The free chlorine concentration was determined by iodometric titration. Additionally, Cl_2 in concentrate was tested with a chlorine test kit which was purchased from Merck. In residual chlorination, pH is an important parameter because the proportion of HOCl decreases with the increasing pH. Generally, researchers worked pH under 5 because of active HOCl species, and it was adjusted by the addition of concentrated HCl and NaOH (>99 %). (Alice Antony et al., 2010; da Silva et al., 2006; Donose et al., 2013; Kwon & Leckie, 2006a).

Pre-treated membranes subjected to various exposure and pH conditions were explained above. The system was operated at 12 bar, and pump speed was adjusted to 5.0 Hz. Since the chlorine concentration is affected by environmental conditions, DPD method was used to verify the feed concentration by diluting 1:100 ratio.

3.8.1 DPD colorimetric method

The diethyl-p-phenylenediamine method effectively determines the free and total chlorine concentrations (Veatch & Black, 2009b). The operating range of this method is 0–4 mg/L Cl_2. In degradation experiments, 200 ppm hypochlorite solution

was used, which is higher than the operating range of DPD. For this region, 1 mL feed water containing chlorine was diluted by a 1:100 ratio. Since HOCl dissociates in the presence of light, it was essential to monitor the chlorine concentration regularly.
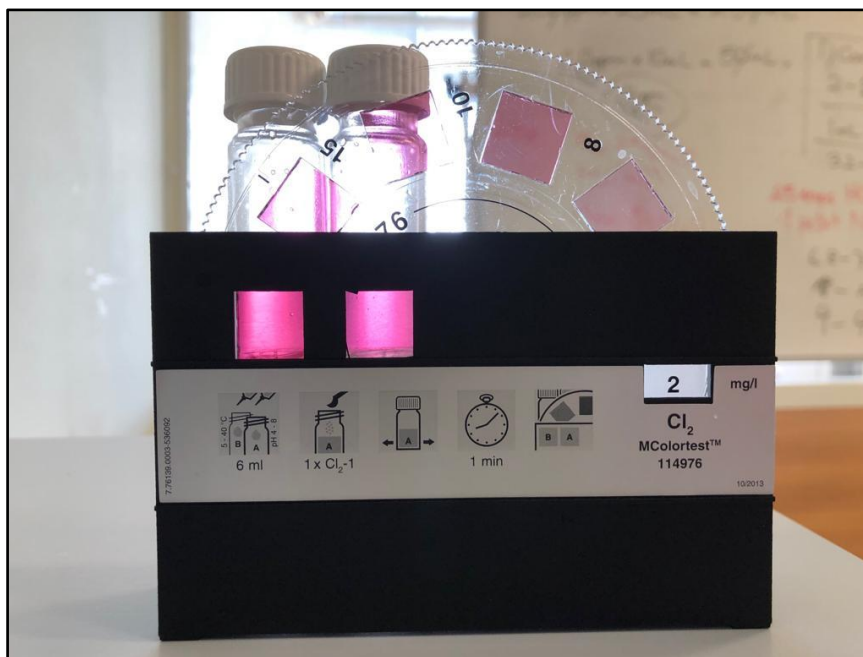
Figure 3.12. DPD test of diluted feed water

3.8.2   Determination of total chlorine concentration

The analyte concentration is determined by the redox reaction between the analyte and titrant. The starch indicator was used to determine the end point

3.8.2.1   Standardization of sodium thiosulfate

The chemicals used for this procedure were sodium thiosulfate anhydrous (> 98%) and sulfuric acid from Sigma- Aldrich, potassium iodate (99.7 – 100.4 %) from Riedel-de Haen, potassium iodide (> 99%) from Emboy, and soluble starch from Merck. The thiosulfate solution was prepared by dissolving 12.5 g of $Na_2S_2O_3$ in freshly boiled distilled water. In order to hinder bacterial formation, nearly one gram

of Na_2CO_3 was added. This solution was kept in a dark place until the standardization with potassium iodate.

$$KIO_3 + 5KI + 3\ H_2SO_4 \rightarrow 3I_2 + 3H_2O + 3\ K_2SO_4 \qquad \text{Equation 3.7}$$

$$6\ Na_2S_2O_3 + 3I_2 \rightarrow 6\ Na_2S_4O_6 + 6\ NaI \qquad \text{Equation 3.8}$$
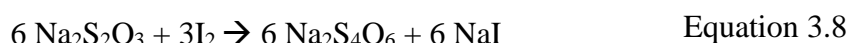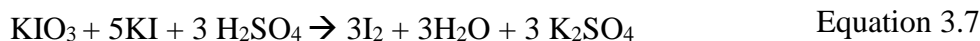
The primary standard KIO_3 was dried in a pre-heated oven for at least 1 hour at 103℃. $0.136 - 0.144$ g of KIO_3 was dissolved in 75 mL distilled water, and nearly 2g of KI was added. After adding 0.5 M H_2SO_4, thiosulfate was immediately titrated until the dark brown solution turned pale yellow. A starch indicator was added to determine the endpoint. This changed the color of the solution from yellow to dark blue.

$$HOCl + 2I^{-1} \rightarrow Cl^{-1} + I_2 + OH^- \text{ or}$$
$$Cl_2 + 2I^{-1} \rightarrow 2Cl^{-1} + I_2 \qquad \text{Equation 3.9}$$

$$I_2 + 2S_2O_3{}^{2-} \rightarrow S_4O_6{}^{2-} + 2I^- \qquad \text{Equation 3.10}$$
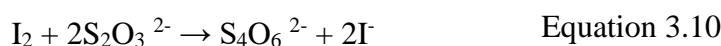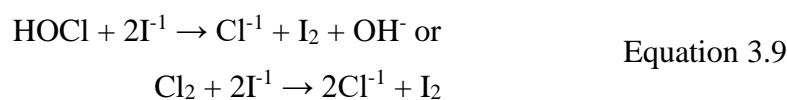
Following the determination of sodium thiosulfate concentration, total chlorine concentration of NaOCl was performed following the procedure. The stock solution was diluted by a 1:10 ratio with distilled water. 25 mL of diluted analyte was transferred to Erlenmeyer flask, and KIO_3 and KI were added. Once the addition of acid, the analyte was titrated with thiosulfate solution until the first endpoint.

3.9   Membrane Rejuvenation Protocol

The rejuvenating agent, which is a light brown powder that contains min. 90 % active substance (Tannic Acid), the rest is kept as trade secret. It promises to increase the salt rejection of mildly oxidized membranes; however, flux restoration is not guaranteed.

The solution was prepared by dissolving 0.1 g of product in 1 L deionized water, and it was recirculated in the system for 1 hour. Rejuvenating agent by Ochemate was slightly acidic; therefore, pH correction was required. The treatment solution was used at pH 4, and 1 w/v % citric acid solution was used for pH correction. The pH correction solution was prepared from citric acid powder (>99 %) which was purchased from Merck. The operational temperature was kept below 35 °C. Although the temperature was recorded manually and accepted as a nuisance factor in this study, it never went above the suggested temperature. Operation conditions were like degradation i.e., 12 bar pressure, and pump speed of 5.0 Hz.

CHAPTER 4

RESULTS & DISCUSSION

This chapter comprises of performance tests results, including chemical characterization via FTIR ATR of the following: virgin, degraded, rejuvenated, re-rejuvenated and rejuvenated virgin. Table 4.1. shows the identification of experiment sets, each set named as shown below Table 4.1.

Table 4.1. Experiment identification

Experiment ID	Explanation
E1	Performance test of virgin membranes
E2-D6000	Degradation with 6000 ppm·hr NaOCl at pH 4
E2-D2000- (pH 4)	Degradation with 2000 ppm·hr NaOCl at pH 4
E2-D2000- (pH 9)	Degradation with 2000 ppm·hr NaOCl at pH 9
E3-R2000	Rejuvenation with 1 hour 100 ppm rejuvenating agent after 2000 ppm·hr exposure at pH 4
E4-R2000	Rejuvenation with 1 hour 100 ppm rejuvenating agent after 2000 ppm·hr exposure at pH 9
E4-RR2000	Re-rejuvenation with 1 hour 100 ppm rejuvenating agent after degradation with 2000 ppm·hr NaOCl after rejuvenation
E5-DR	Rejuvenation of pre-treated virgin membranes

4.1   Performance Test Results

4.1.1   Virgin membrane testing

Two methods have been used to evaluate the membrane performance: water flux and salt rejection. The performance tests have been carried out on virgin membranes before any application to determine the characteristic transport parameters of the membranes and evaluate the modifications that might arise due to physical or chemical changes. In order to determine the transport parameters of the BW30XFR membrane, deionized and brackish water (2000 ppm NaCl) tests were performed with a bench scale cross-flow system.
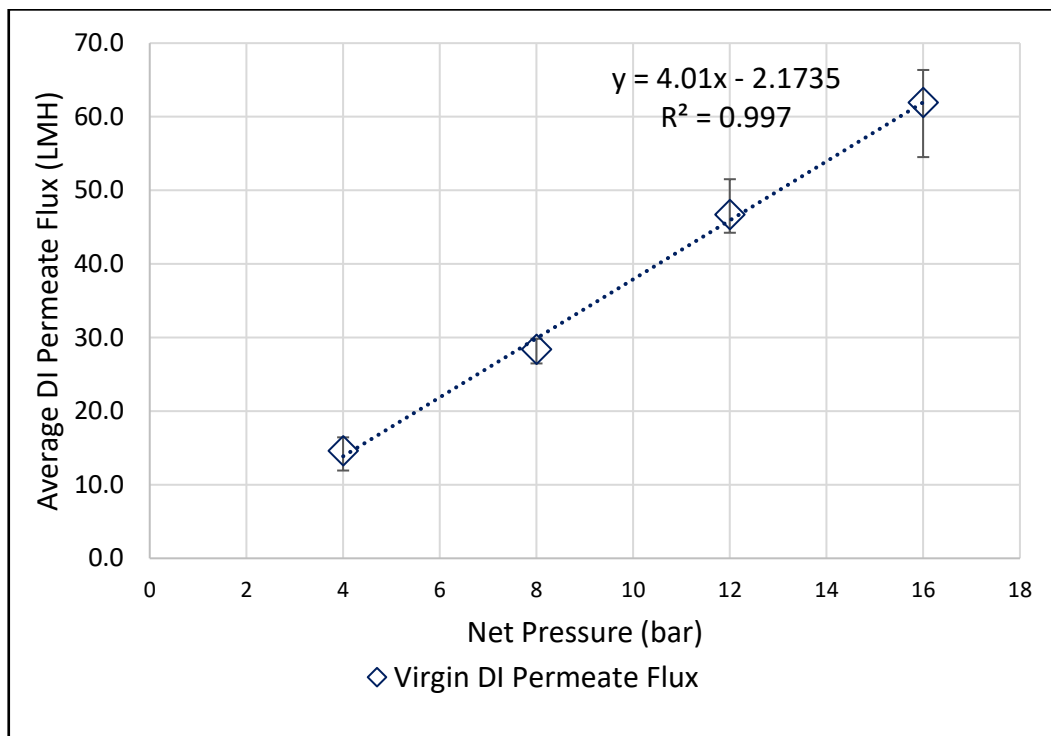
Figure 4.1. Virgin membrane: DI water permeate flux vs. pressure

Figure 4.1 presents the pressure dependence of average permeate flux for virgin membrane. The slope of the dotted line gives the intrinsic water permeability (**A**) coefficient of the virgin membrane. **A** is a constant, and it is specific to the membrane. Permeate flux versus pressure line is expected to be linear; in the

performed experiment, it is clear that these findings agree with the theory (Gauwbergen & Baeyens, 1998; Wijmans & Baker, 1995). The value of **A** has been calculated from the slope as $4.01 \times 10^{-3} \, m^3 \cdot m^{-2} \cdot h^{-1} \cdot bar^{-1}$ which is in the range of $3 \times 10^{-3} - 6 \times 10^{-5} \, m^3 \cdot m^{-2} \cdot h^{-1} \cdot bar^{-1}$ that was reported in the literature.

Unlike water permeability, the solute permeability coefficient **B** is the ratio of solute flux to feed and concentrate concentration difference. According to the solution diffusion model, solute flux is hardly affected by the applied pressure, and it is determined by the salt rejection (SR) (Wijmans & Baker, 1995). Thus, the plot of $1/SR$ versus $1/J_W$ should be linear. Figure 4.2 shows the linear relationship between mentioned terms; due to these findings, water flux was not corrected for concentration polarization. Additionally, Zhou and Song showed that concentration dependence of water flux is significant at a high salt concentration which causes deviation from linearity; however, this was not observed when the salt concentration is below 5000 ppm (Zhou & Song, 2005).
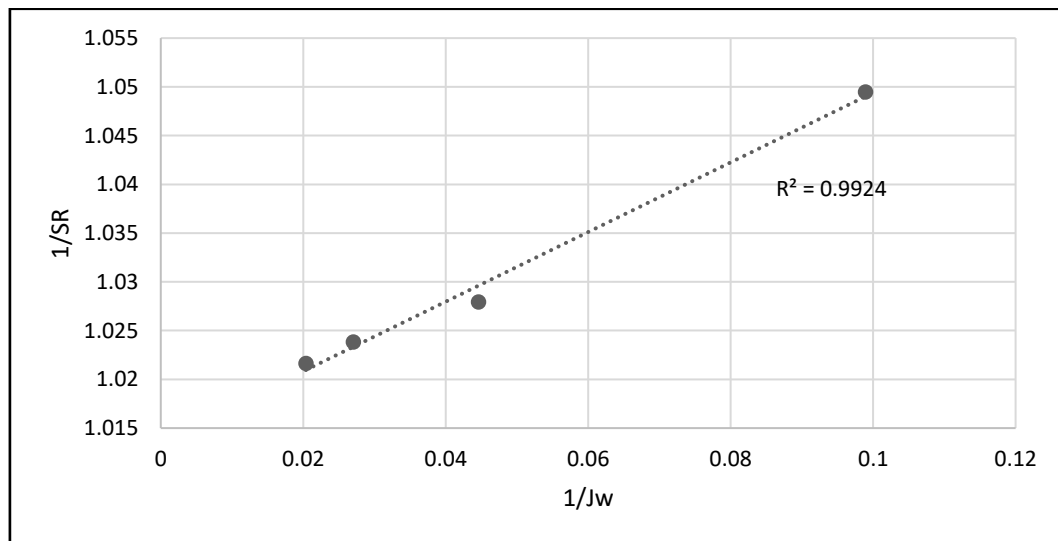
Figure 4.2. Virgin membrane solution-diffusion linearity plot

The results in terms of salt rejection for brackish water performance tests with cross-flow experiments of BW30XFR membranes were calculated using Equation 3.4 and presented in Figure 4.3. The brackish water test's permeate flux lies on the primary axis, while salt rejection is given on the secondary axis.
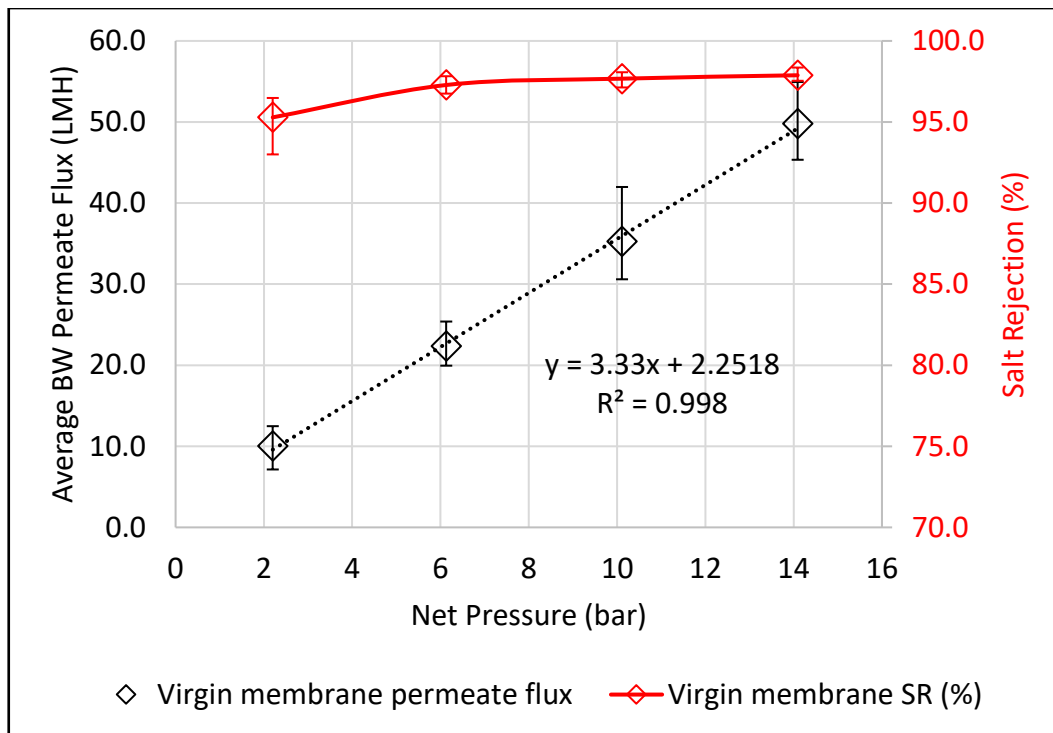
Figure 4.3. Virgin membrane: Average BW permeate flux & salt rejection vs. pressure

The salt rejection increase with pressure was an expected observation. Typically, salt rejection is the expression of membrane selectivity and increases with pressure in accordance with Equation 2.13. The increased pressures lead to increased water flux which decreases the salt concentration in the permeate. The salt rejection should increase up to a certain value and then reach a plateau of stabilization. The same trend was also observed by another study using BW30XFR membranes; however, the salt rejection values in this thesis were slightly lower than the reported salt rejections (Jang et al., 2019). Following these results presented in Figure 4.3, comparison of the salt rejection of degraded and rejuvenated membranes was done at 12 bar.

The primary axis of Figure 4.3 shows the linear pressure dependence of the permeate flux for brackish water performance tests as expected and A has been calculated as 3.36×10^{-3} $m^3 \cdot m^{-2} \cdot h^{-1} \cdot bar^{-1}$. This value is slightly lower than the one obtained for

deionized water performance tests which has also been reported in literature (Ettori et al., 2011)

4.1.2   Degradation experiments

4.1.2.1   Degradation exposure

Membrane ageing with chlorine species was studied extensively in the literature as explained previously. The discussion of the exposure concept arises while evaluating the performance of degraded membranes because membranes are subjected to a lower concentration of chlorine agents during regular operation. However, during aging studies, high chlorine concentrations are used for a short duration.

In this thesis, exposure trials were performed to optimize experimental parameters to obtain mildly oxidized membranes. It was targeted to decrease salt rejection performance of these membranes by 5 %.

Figure 4.4. 6000 ppm·hr degraded membrane

Initially, active degradation of BW30XFR membranes with 1000 ppm NaOCl solution at pH 4 was conducted for six hours under 12 bar. This provided 6000

ppm·hr exposure. The first trial aimed to subject membranes to very harsh conditions and monitor the response. There was no permeate; thus, applying a performance test was impossible. When membrane was taken out of the system, rust deposits were observed on the membranes, as shown in Figure 4.4. This is believed to be due to corrosion of metal parts of experimental set-up caused by high chlorine concentration. Deposits blocked permeate collection holes and caused a layer on the active side of the membranes. Therefore, experimental conditions were changed, and milder conditions were selected for further experiments.

Another critical concept in membrane degradation is the pH of the chlorine solution. After 2000 ppm·hr exposure was selected for the experimental procedure, pH 4 and 9 degradation experiments were performed, and results are presented below.

4.1.2.2   Membrane degradation with chlorine with pH 4 and pH 9

Experiments were carried out to study the impact of degradation with solutions at different pH levels to investigate the role of different active chlorine species i.e., HOCl and OCl$^-$.

E2-D2000-(pH 4) involved eight hours degradation of virgin membranes with 250 ppm NaOCl at pH 4 under 12 bar pressure. The performance test results showed that intrinsic water permeability constant, **A**, i.e., 1.06×10^{-3} m^3·m^{-2}·h^{-1}·bar^{-1} decreased significantly after degradation compared to the virgin membrane's **A**, i.e., 4.01×10^{-3} m^3·m^{-2}·h^{-1}·bar^{-1}.

In E2-D2000-(pH 9) the pH of the solution was adjusted to 9 and all other parameters were kept constant. The **A** of the membrane degraded under alkaline conditions slightly was higher than the virgin membranes i.e., 4.06×10^{-3} m^3·m^{-2}·h^{-1}·bar^{-1}. The reason behind this is the reactivity of end amine groups at alkaline pH conditions towards ClO$^-$. When the carboxylic group is ionized to R─COO$^-$, the membrane surface becomes more hydrophilic, making the passage of water molecules easier (Xu et al., 2013). The literature reports that pH 4 degradation causes a decrease in

the permeate flux of membranes, whereas pH 9 results in a slight permeate flux increase (Donose et al., 2013; Jang et al., 2019; Xu et al., 2013). This trend is explained by the hydrogen bonding loss, which causes rearrangement of flexible polymer chains or local polymer collapse at pH 4 under pressure (Kwon & Leckie, 2006b; Verbeke et al., 2017). Additionally, as seen in Figure 4.5, **A** was approximately three times higher than the membrane treated under acidic conditions which was expected according to the literature (Donose et al., 2013).
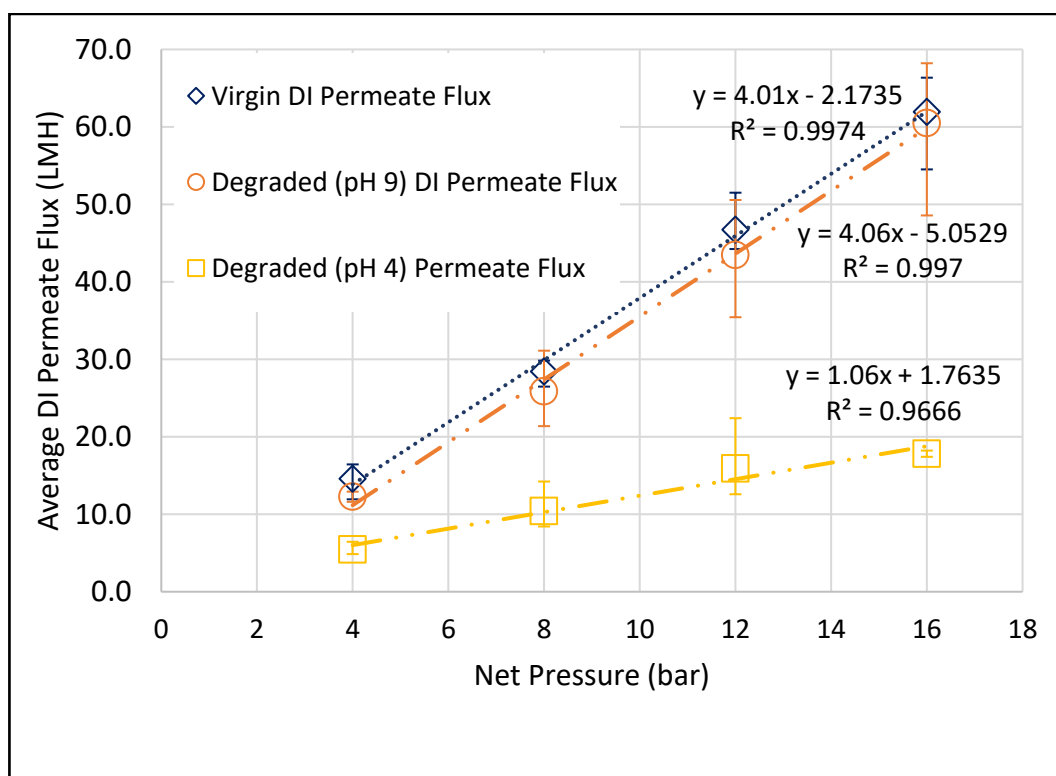
Figure 4.5. Degraded membrane: DI water average permeate flux vs. pressure (pH 4 & pH 9)

Figure 4.6 shows the average salt rejection value for degradation at pH 4. Up to 12 bar it was possible to observe the salt rejection increase with increasing pressure for each trial. However, due to pressure fluctuation at 16 bar, the results were inconclusive for this pressure. The salt rejection of the membranes degraded at pH 4 decreased from 97.7 % to 95.3 % as seen in Table 4.2. The dotted dash line represents the permeate flux for the brackish water performance test, the value of **A** i.e.,

55

1.76×10^{-3} m$^3 \cdot$m$^{-2} \cdot$h$^{-1} \cdot$bar^{-1}, was lower than the value obtained for deionized water performance testing.
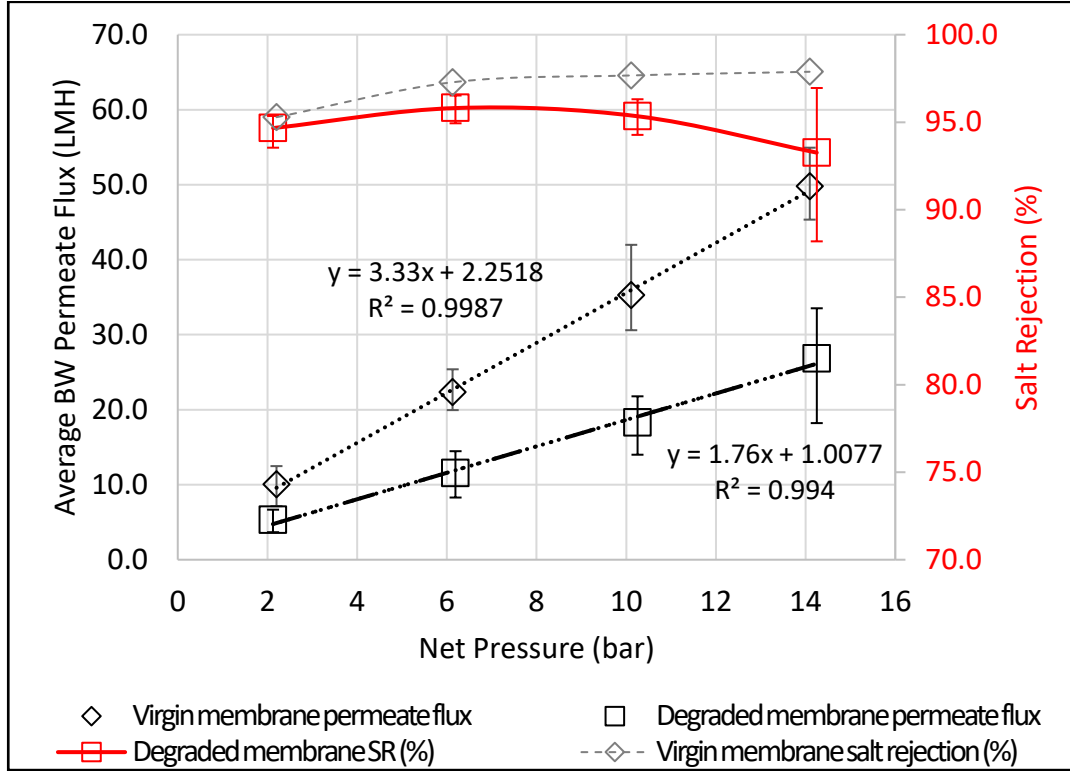
Figure 4.6. Degraded membrane (pH 4): Average BW permeate flux & salt rejection vs. pressure

Table 4.2. Degraded membrane transport parameters summary (pH 4 and pH 9)

Modification	A m^3.m^{-2}.h^{-1}.bar^{-1}	R (%)	B m.h^{-1}
Virgin	4.01	97.7	0.966
Degraded (pH 9)	4.06	85.2	7.24
Degraded (pH 4)	1.06	95.3	0.533

Numerous studies carried out degradation experiments for flux enhancement with the drawback of salt rejection decrease (Ambrosi & Tessaro, 2013; Lawler et al., 2013; Ould Mohamedou et al., 2010; Yip & Elimelech, 2011). The resulting

membrane was inspected in terms of intrinsic water permeability coefficient, **A**, and solute permeability coefficient, **B**. Due to the selectivity and permeability relation, high **A** and low **B** is needed as much as possible for effective separation. At 12 bar, it is possible to see the permeate flux decrease as shown in Table 4.3 due to acidic degradation. However, degradation in acidic media resulted in decreased intrinsic water permeability coefficient and solute permeability coefficient.

The salt rejection decreased from 97.7 % to 85.2 % when membranes degraded at pH 9. The average decrease of four trials was 12.5 %, but the second repetition, salt rejection dropped up to 78 % unexpectedly, which causes the large error range in pH 9 degradation experiments which is shown in Figure 4.7.
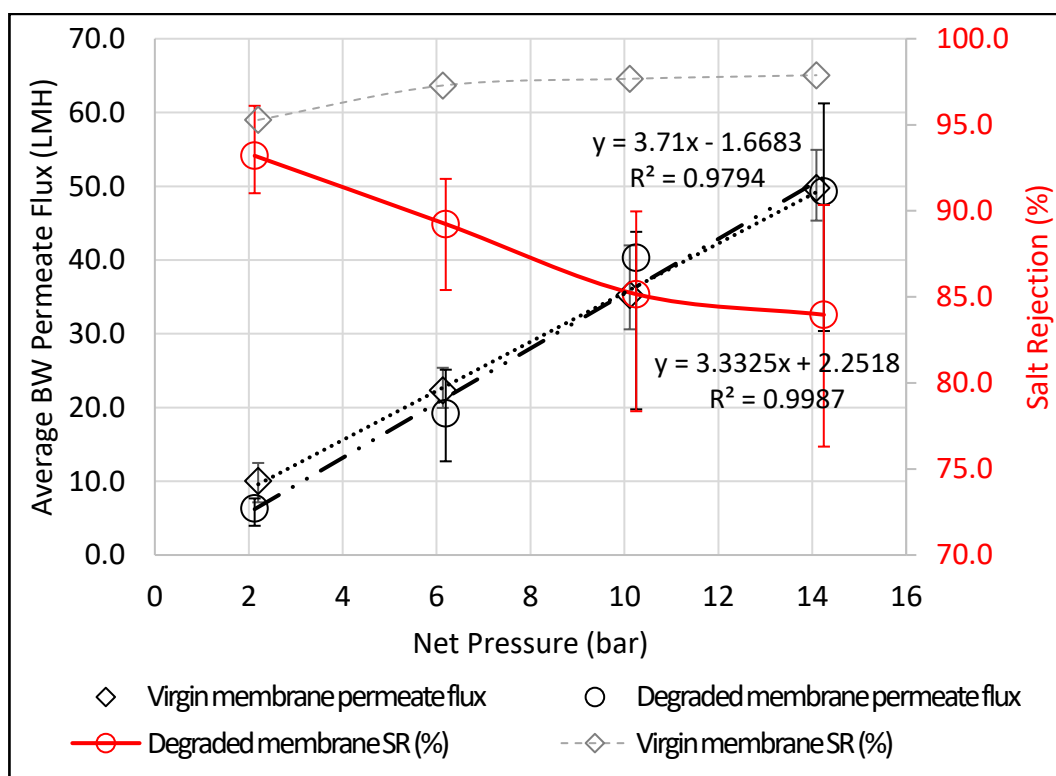
Figure 4.7. Degraded membrane (pH 9): Average BW permeate flux & salt rejection vs. pressure

According to the literature, OCl^- is a weaker oxidant than $HOCl$; therefore, the membrane in acidic solution was expected to degrade more than the membrane in the alkaline solution (da Silva et al., 2006; Kwon & Leckie, 2006b).Surprisingly, the

salt rejection of membrane treated with pH 9 was lower than that treated with pH 4. However, for each simultaneous trial, the salt rejection of membranes degraded with pH 9 solution showed a more significant salt rejection drop.

Table 4.3. Brackish water permeate flux (LMH)

Pressure (bar)	Virgin membrane	Degraded membrane (pH 9)	Degraded membrane (pH 4)
4	10.1	6.6	5.7
8	22.4	20.8	12.9
12	37.0	37.8	20.6
16	49.1	53.0	29.3

In the literature, the pH-degradation concept tested under passive degradation which was criticized in a review due to the severity of membrane degradation in the total immersion method (Donose et al., 2013; Kwon & Leckie, 2006b; Verbeke et al., 2017; Xu et al., 2013). Therefore, comparing our results to literature findings was not possible at this time.

4.1.3   Rejuvenated membranes

4.1.3.1   Rejuvenation after degradation at pH 4

In E3-R2000, the treatment of the membranes degraded at pH 4 (E2-D2000-(pH 4)) with rejuvenating agent was carried out for one hour.

The deionized water permeate flux after rejuvenation of these membranes is shown Figure 4.8, and **A** values are given in Table 4.4. It is meaningful to compare the water permeability constants of rejuvenated membranes with degraded membranes at this point. The decrease in permeate flux after degradation was observed and explained in the previous section. After rejuvenation, **A** value increased from $1.06 \times 10^{-3}\,\mathrm{m^3 \cdot m^-}$

$^{2}\cdot h^{-1}\cdot bar^{-1}$ to 1.99×10^{-3} $m^{3}\cdot m^{-2}\cdot h^{-1}\cdot bar^{-1}$. In the literature, studies applying tannic acid are available; however, membranes were degraded with OCl^{-} at alkaline region. Results including rejuvenation after acidic degradation are not available to the best of my knowledge.
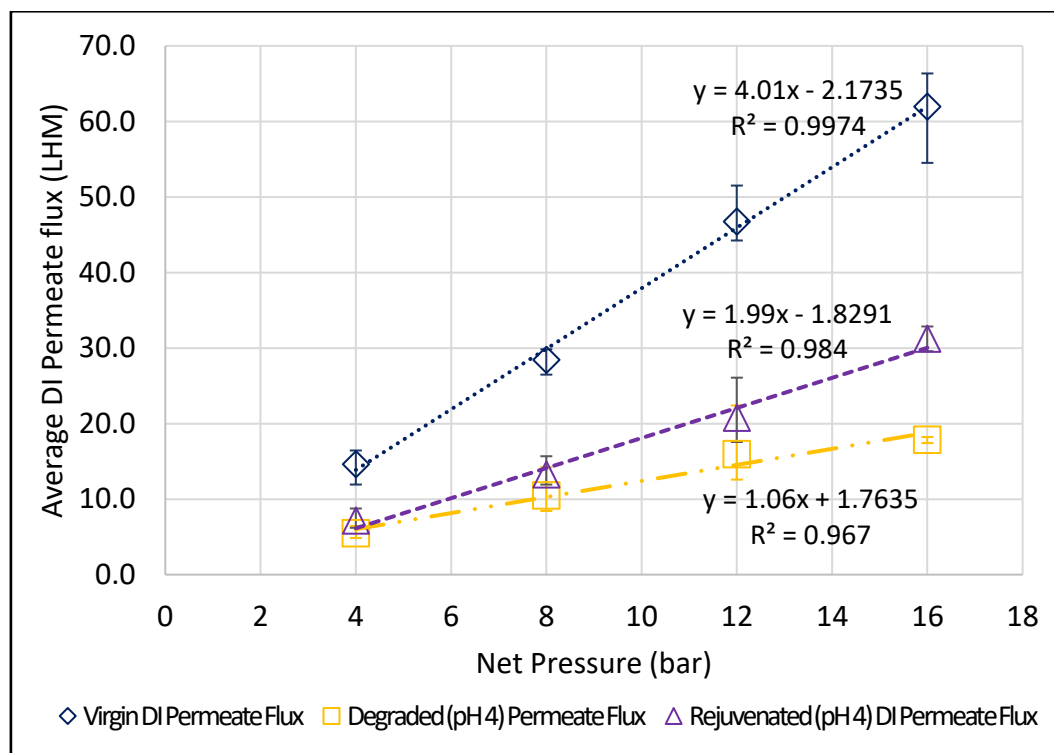
Figure 4.8. Rejuvenated membrane: DI water permeate flux vs. pressure (pH 4)

The rejuvenation of membranes degraded at pH 4 resulted in two times higher intrinsic water permeability and solute permeability constant **B**, was 0.9 times lower. The findings are given in Table 4.5.

Table 4.4. Rejuvenated membrane transport parameters summary (after pH 4 degradation)

Modification	$A\times10^{3}$ $m^{3}.m^{-2}.h^{-1}.bar^{-1}$	R $(\%)$	B $m.h^{-1}$
Virgin	4.01	97.7	0.966
Degraded (pH 4)	1.06	95.3	0.533
Rejuvenated (pH 4)	1.99	97.7	0.479

The main concern of rejuvenation treatment is restoring the salt rejection. After treatment, rejuvenating agent successfully increased salt rejection from 95.3 % to 97.7 % as shown in Figure 4.9.
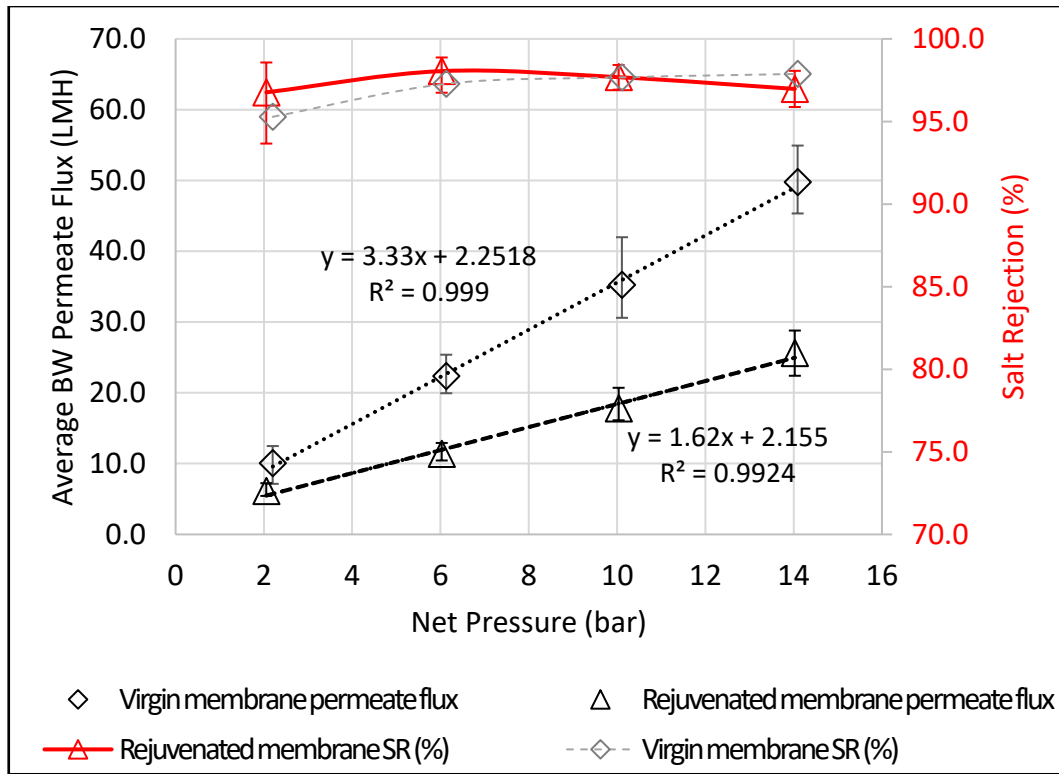
Figure 4.9. Rejuvenated membrane: Average BW permeate flux and salt rejection vs. pressure (pH 4)

4.1.3.2   Rejuvenation after pH 9 degradation

E4-R2000 was conducted for the rejuvenation of the membranes degraded at pH 9. The decrease of **A** can be observed from Figure 4.10, the **A** value decreased from 4.06×10^{-3} $m^3 \cdot m^{-2} \cdot h^{-1} \cdot bar^{-1}$ to 3.20×10^{-3} $m^3 \cdot m^{-2} \cdot h^{-1} \cdot bar^{-1}$ after rejuvenation treatment which is given in Table 4.5.

Considering the 60 % increase in solute permeability constant **B**, it is reasonable to observe the decrease in intrinsic water permeability decrease.

60
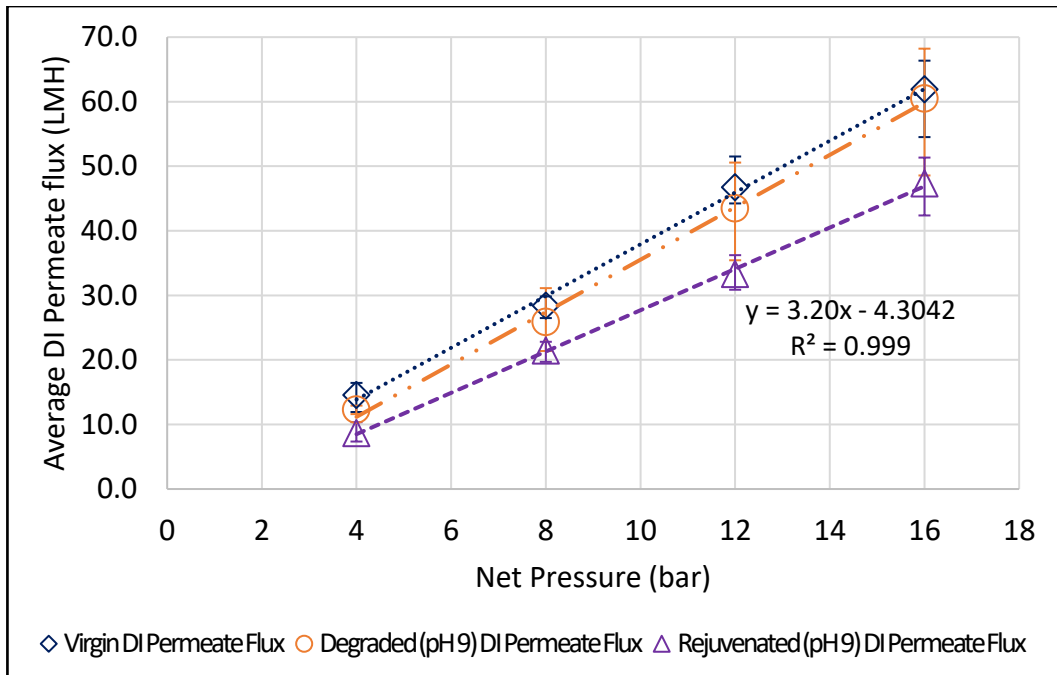
Figure 4.10. Rejuvenated membrane: DI water permeate flux vs. pressure (pH 9)

Table 4.5. Rejuvenated membrane transport parameters summary (after pH 4 and pH 9 degradation)

Modification	$A \times 10^3$ $m^3.m^{-2}.h^{-1}.bar^{-1}$	R (%)	B $m.h^{-1}$
Virgin	4.01	97.7	0.966
Degraded (pH 9)	4.06	85.2	7.24
Rejuvenated (pH 9)	3.20	91.7	2.98

After degradation experiments, it was observed that salt rejection decreased beyond mildly oxidization limits. Rejuvenating agent repaired the membrane by increasing the salt rejection after degradation with pH 9 from 85.2% to 91.7 %. However, the results were not as high as expected as shown in Figure 4.11. The safety data sheet of rejuvenating agent highlights that the rejuvenation efficiency is strongly dependent on the membranes' conditions.
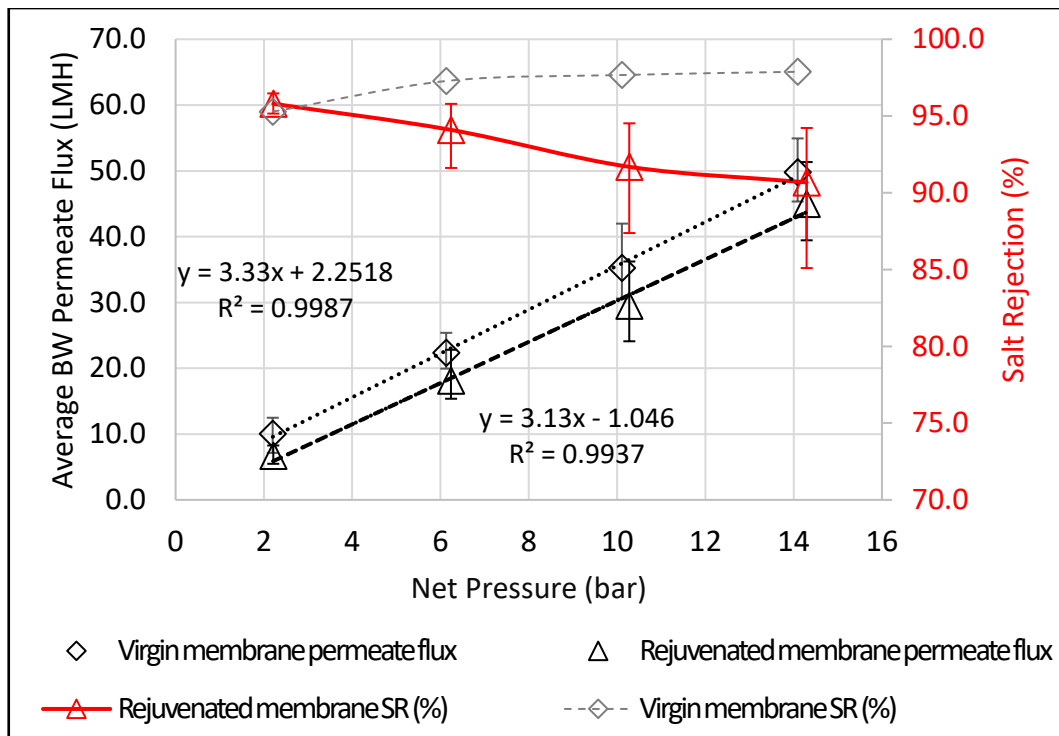
Figure 4.11. Rejuvenated membrane: Average BW permeate flux & salt rejection vs pressure

Figure 4.12 shows the normalized salt rejection after degradation at different pH levels. The salt rejection equals to 1 shows the virgin membranes' initial salt rejection. Salt rejection after degradation was normalized according to initial value. At 12 bar, salt rejection decrease was 12.8 and 2.4 % for pH 9 and pH 4, respectively. After rejuvenation, salt rejection was 7.6 % higher compared to degraded membrane at pH 9; however, it was 6.1 % lower compared to virgin membranes salt rejection. For the membranes degraded at pH 4, it is possible to see the complete salt rejection restoration.

The normalized permeate flux given in Figure 4.13, shows the virgin membrane's BW permeate flux as 1. After degradation at pH 9, the BW permeate flux increased when compared to virgin membrane's permeate flux. Rejuvenation treatment caused nearly 16 % decrease of permeate flux. The degradation at pH 4 caused significant decrease of virgin membranes BW permeate flux and rejuvenation treatment did not change the mentioned term.
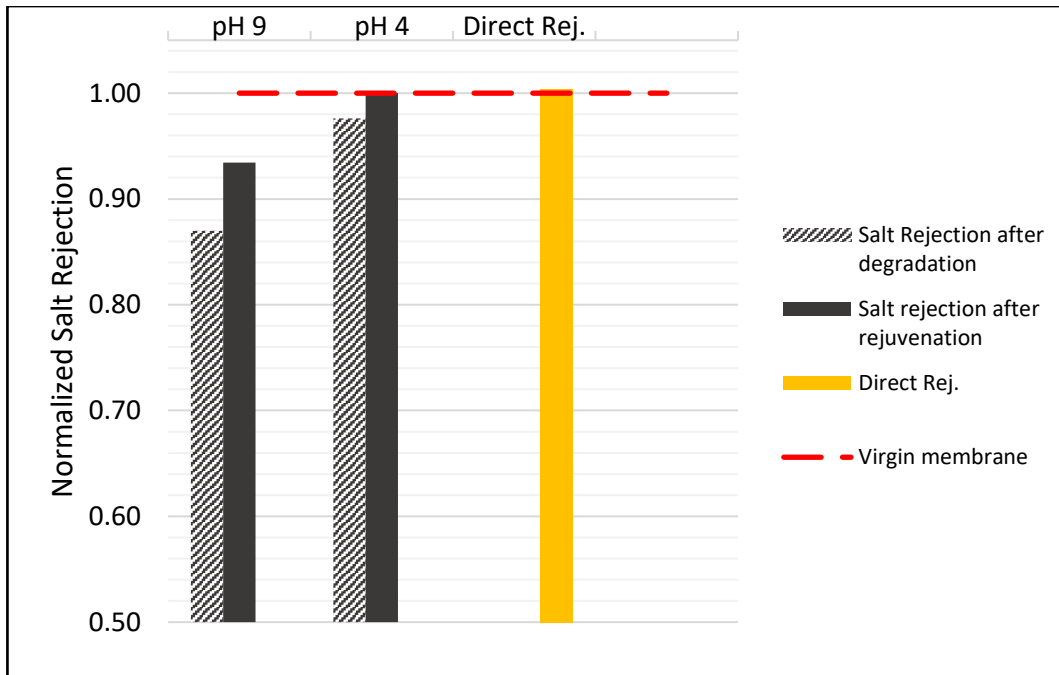
Figure 4.12. Normalized salt rejection after degradation and rejuvenation at 12 bar
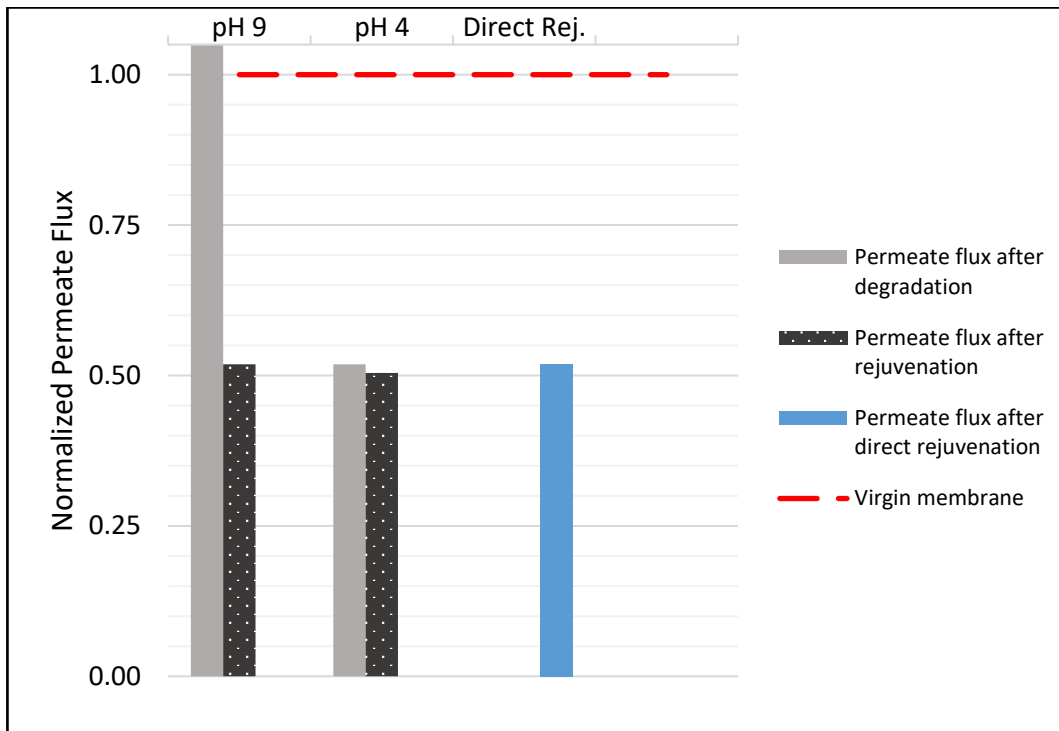
Figure 4.13. Normalized permeate flux after degradation and rejuvenation at 12 bar

Similar results obtained after direct rejuvenation of virgin membranes; the salt rejection increased slightly while permeate flux is increasing as shown in Figure 4.12 and Figure 4.13.

The color of rejuvenated membranes after degradation at pH 4 is presented in Figure 4.14.

Figure 4.14. Rejuvenated membranes after drying 24 h

4.1.4 Re-rejuvenated membranes

4.1.4.1 Degradation after rejuvenation

Re-rejuvenation experiments were conducted after rejuvenation of the membranes degraded at pH 4. Rejuvenated membranes were again subjected to 2000 ppm·hr degradation at pH 4 to mimic degradation again and also to observe if the rejuvenating agent treatment hinders chlorine attack on the membrane. Figure 4.15. below shows the results of the performance test before and after re-rejuvenation. The slopes of blue, green, and purple dotted lines give the intrinsic water permeability constant of rejuvenated, degraded, and re-rejuvenated membranes respectively. The comparison of intrinsic water permeabilities reveals that after the second

rejuvenation, the permeate flux increased further from 1.99×10^{-3} $m^3 \cdot m^{-2} \cdot h^{-1} \cdot bar^{-1}$ to 2.15×10^{-3} $m^3 \cdot m^{-2} \cdot h^{-1} \cdot bar^{-1}$ after the second degradation.
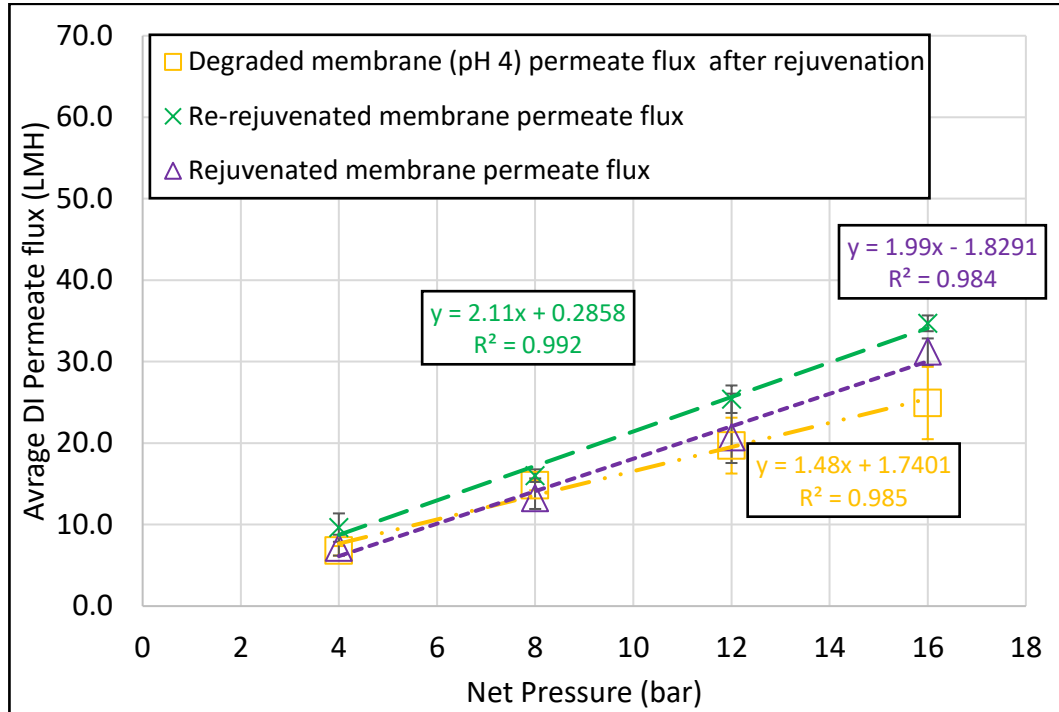
Figure 4.15. Re- rejuvenated membrane: Average DI water permeate flux vs. pressure

Table 4.6. BW30XFR membrane re-rejuvenation transport parameters summary

Modification	$A \times 10^3$ $m^3 \cdot m^{-2} \cdot h^{-1} \cdot bar^{-1}$	R (%)	B $m \cdot h^{-1}$
Virgin	4.01	97.7	0.966
Rejuvenated (pH 4)	1.99	97.7	0.479
Degraded after rejuvenation	1.48	95.4	1.07
Re-rejuvenated	2.15	94.1	1.42

The performance test results with brackish water after pH 4 degradation of rejuvenated membrane were illustrated in Figure 4.16. The brackish water permeate flux per applied pressure is higher than deionized water permeate flux which might

show that the membrane degraded inversely and the sharp decrease in salt rejection also supports this finding.

Considering the changes in intrinsic permeability constant and solute permeability constant, results were again unexpected. After the second degradation, the former decreased as the degradation of virgin membrane at pH 4 and B increased since less water molecules passed through the membrane. The salt rejection decreased from 97.7 % to 95.4 % the second degradation. This shows that rejuvenation treatment did not protect membrane from chlorine attack.
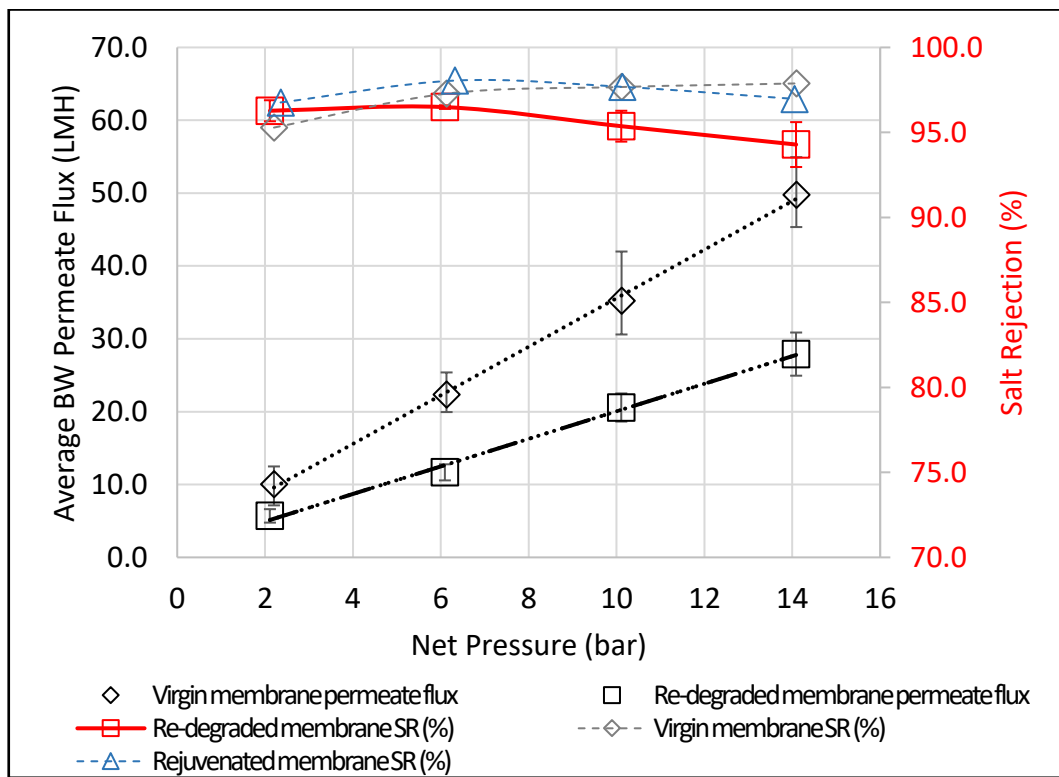
Figure 4.16. Re-degraded membrane: Average BW permeate flux & salt rejection vs. pressure

4.1.4.2   Re-rejuvenation of membranes

Rejuvenated membranes underwent further degradation at pH 4 and rejuvenated again for the second time. As mentioned before after re-rejuvenation, intrinsic water

permeability increased when compared to rejuvenated membranes as shown in Figure 4.15.

Figure 4.17. shows the result of brackish water performance test results after re-rejuvenation. Even though membrane was mildly oxidized, rejuvenating agent could not restore the salt rejection and further treatment caused increased salt passage compared to rejuvenated membranes. Hence, re-rejuvenated membranes might be used in lower pressure applications which will produce less amount of water.
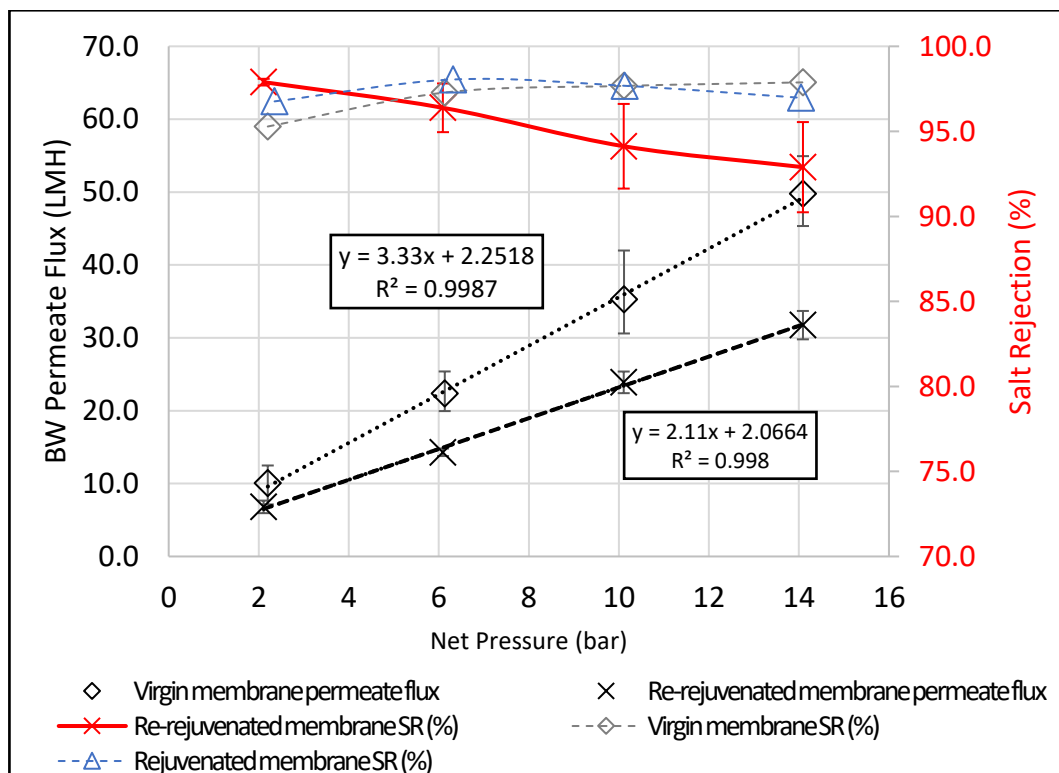
Figure 4.17. Re-rejuvenated membrane: Average BW permeate flux & salt rejection vs. pressure

4.1.5   Directly rejuvenated membranes

In E5, the impact of rejuvenation on virgin membranes was observed. Figure 4.18 compares the deionized water permeability for virgin and directly rejuvenated membranes. According to the slope of the lines, it is apparent that the rejuvenating

agent treatment decreases the membrane's intrinsic permeability constant when applied directly on the virgin membrane.
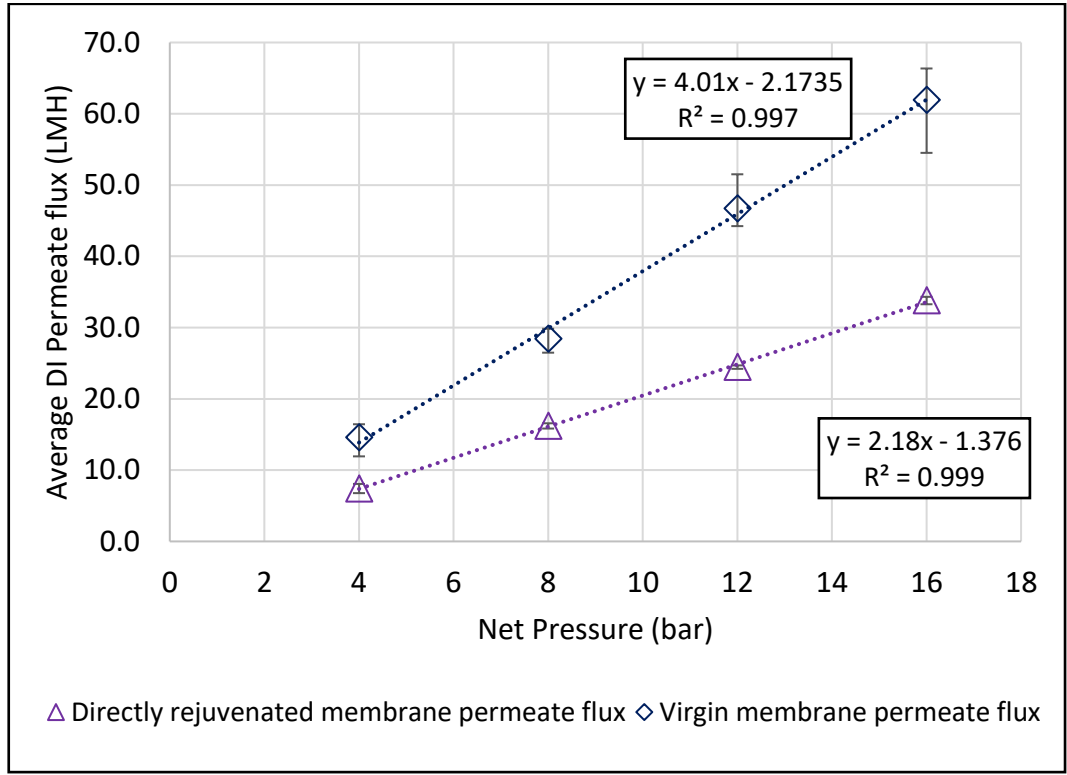
Figure 4.18. Directly rejuvenated membranes: DI water permeate flux vs. pressure

The solute permeability constant **B**, decreased with the drawback of decreaed water permeability **A**, constant as given in Table 4.7.

Table 4.7. BW30XFR membrane direct rejuvenation transport parameters summary

	$A \times 10^3$	R	B
Modification	$m^3.m^{-2}.h^{-1}.bar^{-1}$	(%)	$m.h^{-1}$
Virgin	4.01	97.7	0.966
Directly rejuvenated	2.18	98.1	0.369

The salt rejection of rejuvenated virgin membranes was improved after rejuvenation. It was possible to observe the increase of salt rejection from 97.7 % to 98.1 % after rejuvenating virgin membranes directly as shown in Figure 4.19.
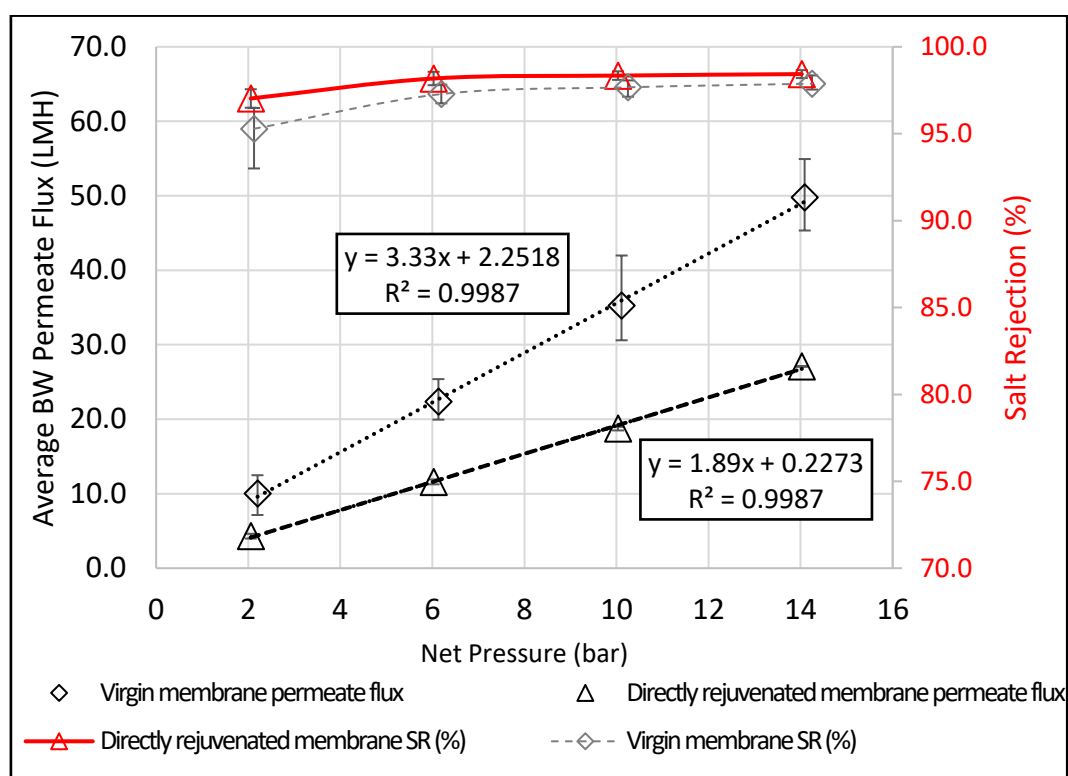
Figure 4.19. Directly rejuvenated membrane: Average BW permeate flux and salt rejection vs. pressure

4.2   FTIR Spectra Evaluation

4.2.1   Virgin membranes

The FTIR-ATR spectra of the polyamide membranes have various bands because of the amide group. The amide I band near the 1665 cm^{-1} represents the secondary amide groups' C=O stretching vibrations. Additionally, 1608 cm^{-1} is also linked with hydrogen bonded carbonyl of amide. The amide II band, which is at lower wavelength of 1544 cm^{-1} corresponds to N─H plane bending. The broad bands of

NH stretching of secondary amide group due to hydrogen bonding was observed near 3335 cm^{-1}. Aromatic C─H bending vibration was observed at 1442 cm^{-1}. Figure 4.20 shows the FTIR-ATR spectrum of untreated BW30XFR membrane and peaks observed agreed with the literature (Donose et al., 2013; Kwon & Leckie, 2006b; Xu et al., 2013).
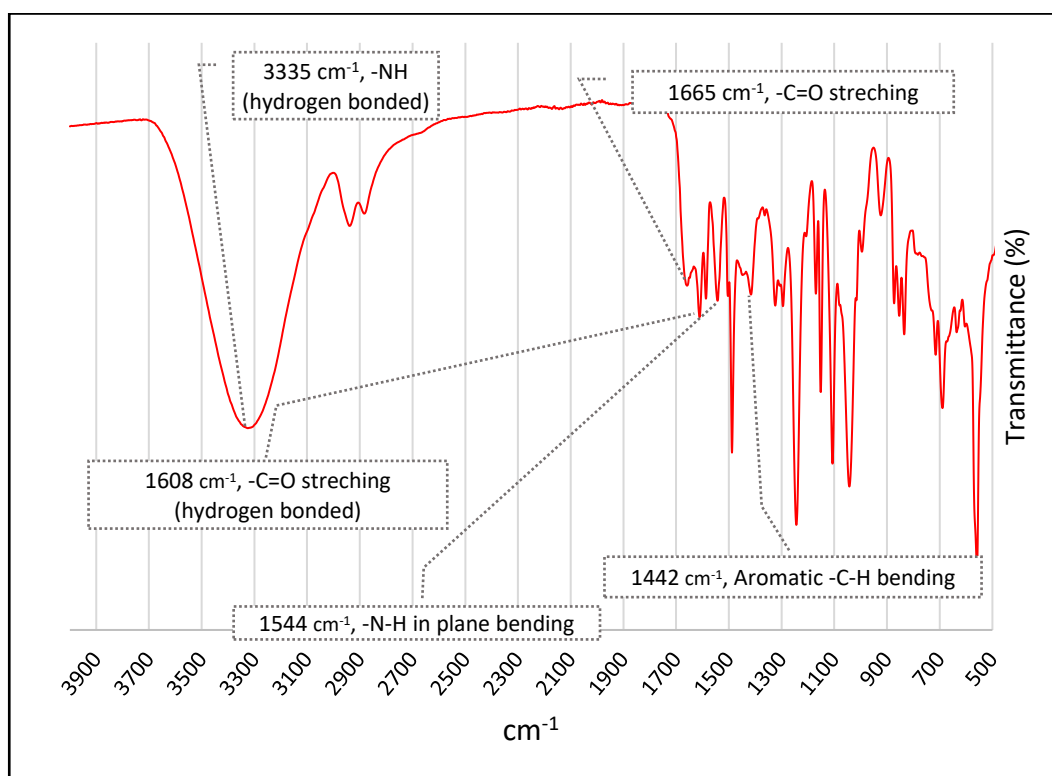
Figure 4.20. FTIR-ATR spectra of virgin membrane

In order to investigate degradation by N-chlorination and orthon rearrangement the shifts between 1600-1400 cm^{-1} and decrease in their intensity were the primary concerns.

4.2.2   Degraded membranes

After 2000 ppm·hr exposure to NaOCl at pH 4 where HOCl is the dominant specie, membranes' chemical characteristics changed significantly, presented in Figure 4.21. The amide I band at 1665 cm^{-1} shifted to 1678.5 cm^{-1} because of the breakage

of hydrogen bonding in the crosslink region. The doublet peak representing C=O stretching of hydrogen bonded carbonyl group, also shifted to lower frequency and band intensity decreased significantly. This indicates N-chlorinated species, since newly formed N─Cl does not form hydrogen bonding with the neighboring C=O. Additionally, amide II band at 1544 cm^{-1} shifted to lower wavelength which is also related to the gradual transformation of N─H species to N─Cl.
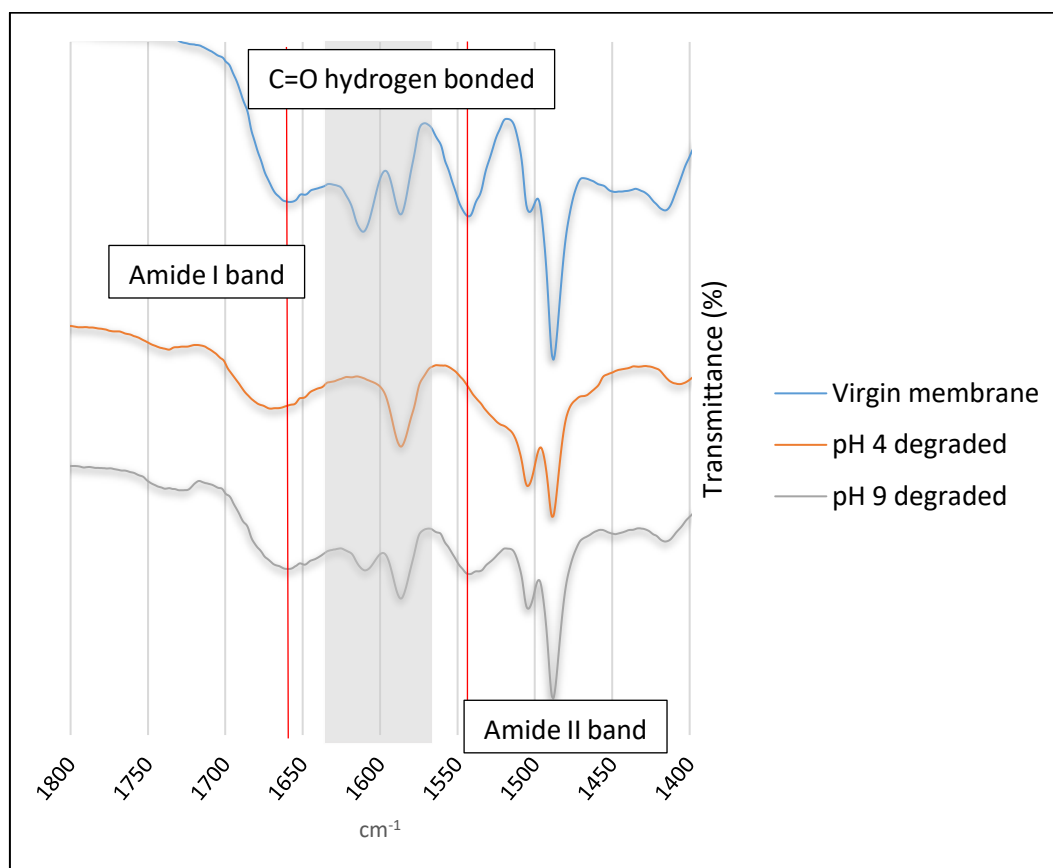
Figure 4.21. FTIR-ATR spectrum of membranes degraded at pH 4 and pH 9

The spectrum of degraded membrane with pH 9 and 2000 ppm·hr exposure where OCl$^-$ is the active specie is also given in Figure 4.21. The shift of the amide I band was not significant i.e., from 1665 to 1662 cm^{-1}. At elevated pH, the carboxylic group of end amine groups ionized to R─COO$^-$, therefore it may be concluded that N─H conversion to N─Cl is not favored as much as in pH 4 which is supported by doublet shape of C=O and slight shift of amide II band i.e., from 1544 to 1541 cm^{-}

[1]. It is possible to observe the decrease in the transmittance of N─H band around 3000 cm^{-1} however complete disappearance was not observed like in acidic conditions. The resulting spectrum can be found in Appendix G, Figure H. 2.

The C─Cl stretching vibration band of aromatic compounds does not show pure bands. Aromatic chloro compounds have a band at 760-395 cm^{-1} with medium to strong intensity. Even with harsh exposure conditions such as 2000 ppm·hr and pH 4, an expected peak around 790 or 810 cm^{-1} is not observed significantly. According to a study about the chlorination of crosslinked RO membranes, the reason behind this might be the surface coating of BW30 type membranes. Those coatings protect active regions; therefore, ring chlorination by orthon rearrangement is hard to observe. With their self-made crosslinked PA membranes, they observed the peak that indicated the Cl substituted aromatic group (Xu et al., 2013). The peak which represents aromatic chloro compounds observed very slightly for alkaline conditions for this experiment which can be found in Appendix G, Figure H. 3.

4.2.3   Rejuvenated membranes

The membrane which was exposed to 2000 ppm·hr NaOCl at pH 4 and pH 9, treated with Rejuvenating agent for 1 hour and scanned with FTIR-ATR is given in Figure 4.22. It was not possible to observe the tannic acid coating by investigating the spectrum of rejuvenated membrane after degradation with 2000 ppm·hr exposure at pH 4 and pH 9.

The difference function of FTIR-ATR software was used to investigate the presence of tannic acid. The spectra of degraded membrane at pH 9 subtracted from the spectra of rejuvenated membrane, the resulting spectra showed C=O stretching vibration at 1725 cm^{-1} which is due to aromatic esters and C─O at 1100-1300 cm^{-1} which is given in the Appendix G, Figure H. 5. (Hegab et al., 2016; Pantoja-Castro & González-Rodríguez, 2012).

The difference spectra of directly rejuvenated membrane and pre-treated membrane where slightly higher peak intensity observed around same wavelengths given in Appendix G, Figure H. 6. After degrading the rejuvenated membrane with 2000 ppm·hr NaOCl at pH 4, same rejuvenation treatment applied to investigate the re-rejuvenation option.
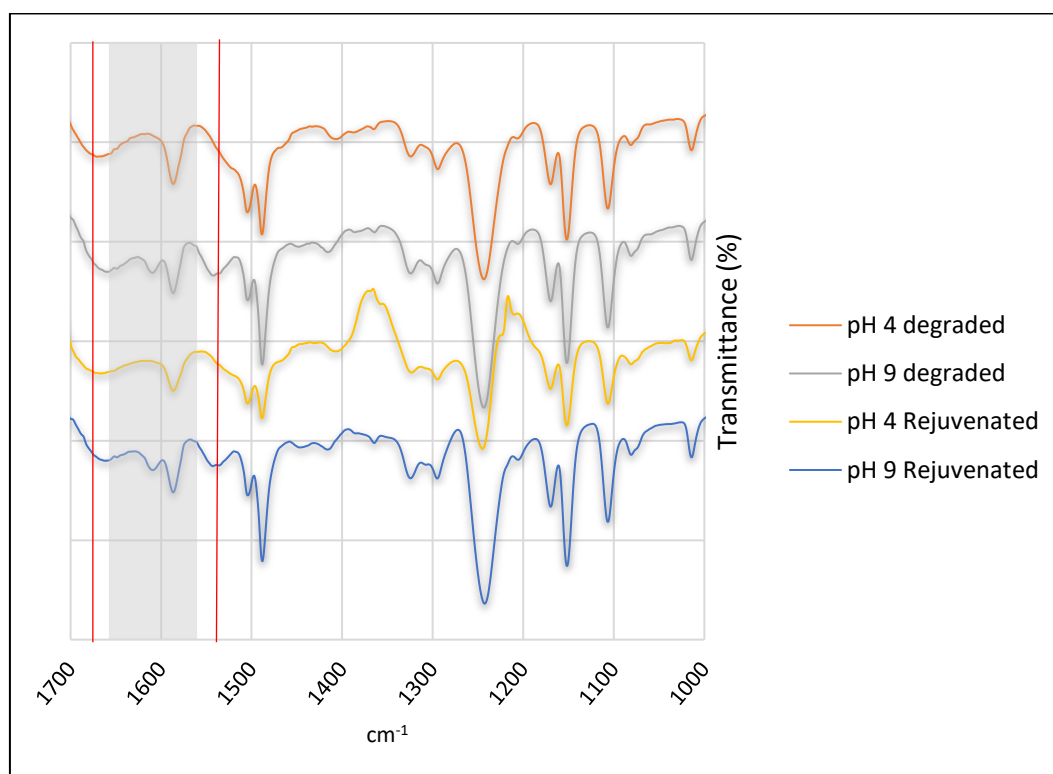
Figure 4.22. FTIR-ATR spectrum of membranes rejuvenated after degradation

4.3   Economic Analysis of Rejuvenation

The performance test results showed that rejuvenation process was able to recover salt rejection of degraded membranes both at pH 4 and pH 9. In order to have an idea on the real value the rejuvenation process might bring for cost reduction of membrane replacement, basic cost analysis was performed. It's known that one 8" BW30XFR element costs 780.0 $, assuming that useful life of membranes is approximately six years; replacement of one element will cost 130 $ yearly (Filterwater, 2021). It's known that for cleaning process each membrane

approximately requires 75 L of solution, assuming the same volume for rejuvenation treatment and 0.1 g/L rejuvenating agent use for the solution preparation, only 7.5 g of the product will be required. Considering that the product only costs 5.5 $/kg, it will add to variable cost only 4.1 cents. Compared to yearly cost of the membrane i.e., 130 USD, 4.1 cents, correspond to 3 h of additional operation of each membrane to offset the treatment costs.

CHAPTER 5

CONCLUSIONS & FUTURE WORKS

The focus of this thesis was the rejuvenation of mildly oxidized membranes with a tannic acid-based rejuvenating agent. The results of the performance tests, together with the FTIR-ATR analysis, have shown that rejuvenating agent successfully restored the salt rejection of mildly oxidized TFC PA RO membranes. The rejuvenating agent's effectiveness in increasing the salt rejection has been investigated for membranes degraded under different conditions. Regardless of membranes' condition, the rejuvenating agent was successful in increasing the salt rejection of membranes.

Mild oxidation was achieved through accelerated aging. Operational parameters and chlorine solutions concentrations have been optimized. 2000 ppm h was found to be suitable for this application: 250 ppm chlorine solution and 8 hour-contact time.

The average salt rejection of membranes degraded at pH 4 was recorded as 95.3 % from the performance tests with brackish water under 12 bar, and rejuvenation treatment increased the salt rejection of these membranes from 95.3 to 97.7 %. Additionally, rejuvenation was efficient in increasing the permeate flux which has been attributed to the increased hydrophilicity of membrane surface.

The performance test results at 12 bar showed that the salt rejection decreased from 97.7 % to 85.2% for membranes degraded at pH 9. After rejuvenation, the salt rejection of the degraded membranes increased from 85.2 % to 91.7 %. On the other hand, permeate flux decreased after the rejuvenation of these membranes, which is in agreement with the literature.

Even though hydrophilic characteristics of tannic acid might bring enhanced permeate flux to the membrane. This additional layer may increase the thickness of the membrane due to bulky groups of tannic acid. Thus, there is a competing positive

and negative effect of this treatment. It will be necessary to further analyze the surface hydrophilicity of the membranes by zeta potential and contact angle measurements.

The rejuvenation effectiveness depends on the condition of degraded membranes. Therefore, membrane degradation with chlorine solutions with different pH levels was also investigated. Even though researchers studied the effect of active chlorine agents on membrane degradation, i.e., HOCl and OCl$^-$, the comparison under active degradation conditions were not reported in the literature.

Rejuvenated membranes were further degraded with 2000 ppm·hr NaOCl at pH 4 to observe if rejuvenation protects membrane against chlorine and if re-rejuvenation is possible. The performance tests showed that after degradation salt rejection of the rejuvenated membranes decreased from 97.7 to 95.4 %. The re-rejuvenation after the second degradation again increased the salt rejection however at 12 bar salt rejection was observed to go down to 94.5% which is even lower than the salt rejection of the degraded membrane. However, at 4 bar salt rejection was around 97.9 % which means that re-rejuvenated membranes can be utilized for lower recovery or for the desalination of less saline water. This indicates that the membranes after second rejuvenation can only be employed under lower pressure levels. And further experiments are required to investigate the stability of the treatment. Additionally, scanning electron microscopy might be carried out to verify if there is a mechanical damage on membrane since salt rejection was increasing with pressure. FT-IR testing did not suggest any changes in membrane structure.

Direct rejuvenation of virgin membranes showed that application of rejuvenating agent directly on virgin membranes increased the salt rejection to 98.4 % at 12 bar. But it causes a significant decrease in permeate flux.

The changes in the chemical structure of the membrane were investigated via FTIR-ATR. The scans of virgin membranes showed that the peaks observed at 1667.5, 1615.0, 1546.6, and 1425.6 cm^{-1} are the characteristic bonds attributed to amide I, amide II bands. To investigate degradation by N-chlorination and orthon

rearrangement, the shifts in those bands and decrease in their intensity were the primary concerns.

In the analysis of membranes degraded at pH 4, the amide I band at 1667.5 cm^{-1} shifted to 1678.5 cm^{-1} because of the breakage of hydrogen bonding in the crosslink region. The peak representing hydrogen-bonded carbonyl group i.e., 1546.6 cm^{-1}, also shifted to lower frequency and band intensity decreased significantly. This indicates N-chlorinated species since newly formed N-Cl does not form hydrogen bonding with the neighboring C=O.

The scans of the degraded membrane at pH 9 showed that the shift in the amide I band was from 1667.5 cm^{-1} to 1662.5 cm^{-1}. As expected, the broad band around 3300 cm^{-1} which is due to N-H bond, was still observed around 3300 cm$^{-1,}$ and the shift of amide I and II band was lower than the one degraded at pH 4. These results indicate that the hydrogen bonding retardation was lower in pH 9 degradation experiments.

Additionally, to determine the presence of rejuvenating agent on the membrane surface, further analytical methods are needed. Because performance tests and FTIR-ATR results only verified the presence of a coating layer were just indicative of identifying the functional groups of TA.

A simple analysis proved that the cost of rejuvenation treatment is reasonably priced when compared to cost of membrane replacement.

The future works listed below will add on rejuvenation literature of the BW RO membranes and will be beneficial to understand this treatment more:

- In this thesis, the effectiveness of rejuvenation treatment on membranes degraded at pH 4 and pH 9 was investigated in detail. The degradation at pH 7 will be useful to understand the combined effects of HOCl and OCl$^-$ under active degradation conditions.
- Hypochlorite used as an oxidizing agent in this thesis by assuming that the reaction mechanism is same as monochloramines (MCA). However, MCA is known to be less aggressive towards the PA layer. Hence, a new experimental

procedure is required to investigate the effect of MCA. This will be useful to test rejuvenating agent's ability on membranes degraded with MCA.

- Metal ions coming from coagulation and flocculation shows a catalyst effect when combined with MCA. Therefore, investigation of this point will mimic the disinfection process better.

- Treatment on different RO membranes such as membranes used in seawater, and numerous brands or nanofiltration membranes.

- Investigation in pilot-scale experiments will be more realistic

- Pilot-scale experiments by evaluating the salt rejection increase with the drawback of permeate flux decrease; understanding the selectivity-permeability trade-off is vital to comment more on real value of rejuvenation treatment.

- The operational parameters for rejuvenation were selected following the rejuvenating agent supplier's recommendations and literature data. They may vary in the industry. Therefore, an optimization study according to industrial operating conditions will be beneficial. The experimental designs such as Taguchi or Response surface methods can be used for process optimization.

- The rejuvenating agent's concentration slightly affects the rejuvenation efficiency. Experiments with higher rejuvenating agent concentrations might give better salt rejection performance.

- Fujiwara tests can be undertaken to determine if the degraded membranes were damaged by the halogens

- Adsorption kinetics models can be evaluated for membrane rejuvenation process

REFERENCES

Alsawaftah, N., Abuwatfa, W., Darwish, N., & Husseini, G. (2021). A comprehensive review on membrane fouling: Mathematical modelling, prediction, diagnosis, and mitigation. *Water (Switzerland)*, *13*(9). https://doi.org/10.3390/w13091327

Ambrosi, A., & Tessaro, I. C. (2013). Study on Potassium Permanganate Chemical Treatment of Discarded Reverse Osmosis Membranes Aiming their Reuse. *Separation Science and Technology (Philadelphia)*, *48*(10), 1537–1543. https://doi.org/10.1080/01496395.2012.745876

Ambulkar, A. (2021). *Wastewater treatment*. Encyclopedia Britannica. https://www.britannica.com/technology/wastewater-treatment

Antony, A., & Leslie, G. (2011a). Degradation of polymeric membranes in water and wastewater treatment. *Advanced Membrane Science and Technology for Sustainable Energy and Environmental Applications*, 718–745. https://doi.org/10.1533/9780857093790.5.718

Antony, A., & Leslie, G. (2011b). Degradation of polymeric membranes in water and wastewater treatment. In *Advanced Membrane Science and Technology for Sustainable Energy and Environmental Applications*. https://doi.org/10.1533/9780857093790.5.718

Antony, Alice, Fudianto, R., Cox, S., & Leslie, G. (2010). Assessing the oxidative degradation of polyamide reverse osmosis membrane-Accelerated ageing with hypochlorite exposure. *Journal of Membrane Science*, *347*(1–2), 159–164. https://doi.org/10.1016/j.memsci.2009.10.018

Bartl, A. (2014). Moving from recycling to waste prevention: A review of barriers and enables. *Waste Management & Research*, *32*(9_suppl), 3–18.

https://doi.org/10.1177/0734242X14541986

Bruggen, B. Van Der, Vandecasteele, C., Gestel, T. Van, Doyenb, W., & Leysenb, R. (2003). *Review of Pressure-Driven Membrane Processes*. *1*.

Cadotte, J. E., Cobian, K. E., Forester, R. H., & Petersen, R. J. (1975). *Continued Evaluation of in situ-Formed Condensation Polymers for Reverse Osmosis Membranes*.

Cheng, Y. F., Pranantyo, D., Kasi, G., Lu, Z. S., Li, C. M., & Xu, L. Q. (2020). Amino-containing tannic acid derivative-mediated universal coatings for multifunctional surface modification. *Biomaterials Science*, *2120*(8), 2120–2028.

Collivignarelli, M. C., Abbà, A., Benigna, I., Sorlini, S., & Torretta, V. (2018). Overview of the main disinfection processes for wastewater and drinking water treatment plants. *Sustainability (Switzerland)*, *10*(1), 1–21. https://doi.org/10.3390/su10010086

Cran, M. J., Bigger, S. W., & Gray, S. R. (2011). Degradation of polyamide reverse osmosis membranes in the presence of chloramine. *Desalination*, *283*, 58–63. https://doi.org/10.1016/j.desal.2011.04.050

Da Silva, M. K., Ambrosi, A., Dos Ramos, G. M., & Tessaro, I. C. (2012). Rejuvenating polyamide reverse osmosis membranes by tannic acid treatment. *Separation and Purification Technology*, *100*(November 2017), 1–8. https://doi.org/10.1016/j.seppur.2012.07.027

da Silva, M. K., Tessaro, I. C., & Wada, K. (2006). Investigation of oxidative degradation of polyamide reverse osmosis membranes by monochloramine solutions. *Journal of Membrane Science*, *282*(1–2), 375–382. https://doi.org/10.1016/j.memsci.2006.05.043

Donose, B. C., Sukumar, S., Pidou, M., Poussade, Y., Keller, J., & Gernjak, W. (2013). Effect of pH on the ageing of reverse osmosis membranes upon

exposure to hypochlorite. *Desalination*, *309*, 97–105. https://doi.org/10.1016/j.desal.2012.09.027

Drewes, J. E., & Khan, S. J. (2015). Contemporary design, operation, and monitoring of potable reuse systems. *Journal of Water Reuse and Desalination*, *5*(1), 1–7. https://doi.org/10.2166/wrd.2014.148

El Gharras, H. (2009). Polyphenols: food sources, properties and applications – a review. *International Journal of Food Science \& Technology*, *44*(12), 2512–2518. https://doi.org/https://doi.org/10.1111/j.1365-2621.2009.02077.x

EPA. (2017). *Potable Reuse Compendium*.

Ettori, A., Gaudichet-Maurin, E., Schrotter, J.-C., Aimar, P., & Causserand, C. (2011). Permeability and chemical analysis of aromatic polyamide based membranes exposed to sodium hypochlorite. *Journal of Membrane Science*, *375*(1), 220–230. https://doi.org/https://doi.org/10.1016/j.memsci.2011.03.044

Fathizadeh, M., Aroujalian, A., & Raisi, A. (2012). Effect of lag time in interfacial polymerization on polyamide composite membrane with different hydrophilic sub layers. *Desalination*, *284*, 32–41. https://doi.org/10.1016/j.desal.2011.08.034

Filterwater. (2021). *DOW Filmtec BW30XFR-400-34 RO Membrane 11500 GPD*. https://www.filterwater.com/p-827-dow-filmtec-bw30xfr-400-34-ro-membrane-11500-gpd.aspx

Gabelich, C. J., Frankin, J. C., Gerringer, F. W., Ishida, K. P., & Suffet, I. H. (2005). Enhanced oxidation of polyamide membranes using monochloramine and ferrous iron. *Journal of Membrane Science*, *258*(1–2), 64–70. https://doi.org/10.1016/j.memsci.2005.02.034

García, L. A., & Díaz, M. (2011). Cleaning in Place. In *Comprehensive Biotechnology* (Second Edi, Vol. 1). Elsevier B.V. https://doi.org/10.1016/B978-0-08-088504-9.00447-5

Gauwbergen, D. Van, & Baeyens, J. (1998). *Modelling reverse osmosis by irreversible thermodynamics*. *13*, 117–128.

Gerrity, D., Pecson, B., Shane Trussell, R., & Rhodes Trussell, R. (2013). Potable reuse treatment trains throughout the world. *Journal of Water Supply: Research and Technology - AQUA*, *62*(6), 321–338. https://doi.org/10.2166/aqua.2013.041

Gohil, J. M., & Suresh, A. K. (2017). Chlorine attack on reverse osmosis membranes: Mechanisms and mitigation strategies. *Journal of Membrane Science*, *541*, 108–126. https://doi.org/10.1016/j.memsci.2017.06.092

Gombas, D., Luo, Y., Brennan, J., Shergill, G., Petran, R., Walsh, R., Hau, H., Khurana, K., Zomorodi, B., Rosen, J., Varley, R., & Deng, K. (2017). Guidelines to validate control of cross-contamination during washing of fresh-cut leafy vegetables. *Journal of Food Protection*, *80*(2), 312–330. https://doi.org/10.4315/0362-028X.JFP-16-258

Hegab, H. M., Elmekawy, A., Barclay, T. G., Michelmore, A., Zou, L., Saint, C. P., & Ginic-markovic, M. (2016). *Single-Step Assembly of Multifunctional Poly (tannic acid) − Graphene Oxide Coating To Reduce Biofouling of Forward Osmosis Membranes*. https://doi.org/10.1021/acsami.6b03719

Hung, D. C., Nguyen, N. C., Uan, D. K., & Son, L. T. (2017). *Membrane processes and their potential applications for fresh water provision in Vietnam Membrane processes and their potential applications for fresh water provision in Vietnam. January*. https://doi.org/10.15625/2525-2321.2017-00504

Hung, Y. C., Waters, B. W., Yemmireddy, V. K., & Huang, C. H. (2017). pH effect on the formation of THM and HAA disinfection byproducts and potential control strategies for food processing. *Journal of Integrative Agriculture*, *16*(12), 2914–2923. https://doi.org/10.1016/S2095-3119(17)61798-2

IWA. (2018). *Wastewater Report*.

Jang, E. S., Mickols, W., Sujanani, R., Helenic, A., Dilenschneider, T. J., Kamcev, J., Paul, D. R., & Freeman, B. D. (2019). Influence of concentration polarization and thermodynamic non-ideality on salt transport in reverse osmosis membranes. *Journal of Membrane Science*, *572*(August 2018), 668–675. https://doi.org/10.1016/j.memsci.2018.11.006

Jones, E. R., Van Vliet, M. T. H., Qadir, M., & Bierkens, M. F. P. (2021). Country-level and gridded estimates of wastewater production, collection, treatment and reuse. *Earth System Science Data*, *13*(2), 237–254. https://doi.org/10.5194/essd-13-237-2021

Joong, H., Choi, Y., Lim, M., Hwa, K., Kim, D., Kim, J., Kang, H., & Lee, J. (2016). Reverse osmosis nanocomposite membranes containing graphene oxides coated by tannic acid with chlorine-tolerant and antimicrobial properties. *Journal of Membrane Science*, *514*, 25–34. https://doi.org/10.1016/j.memsci.2016.04.026

Kang, G.-D., Gao, C.-J., Chen, W.-D., Jie, X.-M., Cao, Y.-M., & Yuan, Q. (2007). Study on hypochlorite degradation of aromatic polyamide reverse osmosis membrane. *Journal of Membrane Science*, *300*, 165–171. https://doi.org/10.1016/j.memsci.2007.05.025

Kawaguchi, T., & Tamura, H. (1984). Chlorine-resistant membrane for reverse osmosis. I. Correlation between chemical structures and chlorine resistance of polyamides. *Journal of Applied Polymer Science*, *29*(11), 3359–3367. https://doi.org/10.1002/app.1984.070291113

Kedem, O., & Katchalsky, A. (1958). Thermodynamic analysis of the permeability of biological membranes to non-electrolytes. *Biochimica et Biophysica Acta*, *27*(2), 229–246. https://doi.org/10.1016/0006-3002(58)90330-5

Khan, S. J., & Anderson, R. (2018). Potable reuse: Experiences in Australia. In *Current Opinion in Environmental Science and Health* (Vol. 2, pp. 55–60). Elsevier B.V. https://doi.org/10.1016/j.coesh.2018.02.002

Kobylinski, E. A., & Bhandari, A. (2010). Disinfection of Wastewater. *White's*

Handbook of Chlorination and Alternative Disinfectants: Fifth Edition, 363–403. https://doi.org/10.1002/9780470561331.ch6

Kucera, J. (2010). *Reverse Osmosis: Design, Process, and Applications for Engineers*. Wiley.

Kwon, Y. N., & Leckie, J. O. (2006a). Hypochlorite degradation of crosslinked polyamide membranes. I. Changes in chemical/morphological properties. *Journal of Membrane Science*, *283*(1–2), 21–26. https://doi.org/10.1016/j.memsci.2006.06.008

Kwon, Y. N., & Leckie, J. O. (2006b). Hypochlorite degradation of crosslinked polyamide membranes. II. Changes in hydrogen bonding behavior and performance. *Journal of Membrane Science*, *282*(1–2), 456–464. https://doi.org/10.1016/j.memsci.2006.06.004

Landaburu-Aguirre, J., García-Pacheco, R., Molina, S., Rodríguez-Sáez, L., Rabadán, J., & García-Calvo, E. (2016). Fouling prevention, preparing for reuse and membrane recycling. Towards circular economy in RO desalination. *Desalination*, *393*, 16–30. https://doi.org/10.1016/j.desal.2016.04.002

Lau, W. J. (2016). Polyamide (PA). In E. Drioli & L. Giorno (Eds.), *Encyclopedia of Membranes* (pp. 1586–1588). Springer Berlin Heidelberg. https://doi.org/10.1007/978-3-662-44324-8_1725

Lau, W. J., Ismail, A. F., Misdan, N., & Kassim, M. A. (2012). A recent progress in thin film composite membrane: A review. *Desalination*, *287*, 190–199. https://doi.org/10.1016/j.desal.2011.04.004

Lautze, J., Stander, E., Drechsel, P., da Silva, A. K., & Keraita, B. (2014). Global experiences in water reuse. In *Global experiences in water reuse*. https://doi.org/10.5337/2014.209

Lawler, W., Antony, A., Cran, M., Duke, M., Leslie, G., & Le-Clech, P. (2013). Production and characterisation of UF membranes by chemical conversion of

used RO membranes. *Journal of Membrane Science*, *447*, 203–211. https://doi.org/10.1016/j.memsci.2013.07.015

Lawler, W., Bradford-Hartke, Z., Cran, M. J., Duke, M., Leslie, G., Ladewig, B. P., & Le-Clech, P. (2012). Towards new opportunities for reuse, recycling and disposal of used reverse osmosis membranes. *Desalination*, *299*, 103–112. https://doi.org/10.1016/j.desal.2012.05.030

Lenntech. (n.d.-a). *Water Conductivity*. Retrieved September 13, 2021, from https://www.lenntech.com/applications/ultrapure/conductivity/water-conductivity.htm

Lenntech. (n.d.-b). *What is water disinfection?* Retrieved August 30, 2021, from https://www.lenntech.com/processes/disinfection/what-is-water-disinfection.htm

Leverenz, H. L., Tchobanoglous, G., & Asano, T. (2011). Direct potable reuse: A future imperative. *Journal of Water Reuse and Desalination*, *1*(1), 2–10. https://doi.org/10.2166/wrd.2011.000

Li, D., Yan, Y., & Wang, H. (2016). Progress in Polymer Science Recent advances in polymer and polymer composite membranes for reverse and forward osmosis processes. *Progress in Polymer Science*, *61*, 104–155. https://doi.org/10.1016/j.progpolymsci.2016.03.003

Lin, S., & Lee, C. (2007). *Water and Wastewater Calculations Manual, 2nd Ed.* McGraw-Hill Professional. https://doi.org/doi:10.1036/9780071542661

Liu, F., Wang, L., Li, D., & Liu, Q. (2019). *RSC Advances A review : the e ff ect of the microporous support during interfacial polymerization on the morphology and performances of a thin fi lm composite membrane for liquid puri fi cation*. 35417–35428. https://doi.org/10.1039/c9ra07114h

López-ruiz, S., Moya-fernández, P. J., García-rubio, M. A., González-gómez, F., Moya-fernández, P. J., & García-rubio, M. A. (2020). Acceptance of direct

potable water reuse for domestic purposes : evidence from southern Spain. *International Journal of Water Resources Development*, *00*(00), 1–21. https://doi.org/10.1080/07900627.2020.1799762

Lui J, Dorjderem A, Fu J, Lei X, Lui H, Macer D, Qiao Q, Sun A, Tachiyama K, Yu L, Z. Y. (2011). *Water Ethics and Water Resource Management*.

McMurry, J. E. (2012). *Organic Chemistry* (8th ed.). Brooks/Cole.

Metcalf, & Eddy. (2003). *Wastewater engineering : treatment and reuse* (H. D. S. George Tchobanoglous, Franklin L. Burton (Ed.); 5th ed.). McGraw-Hill. https://search.library.wisc.edu/catalog/999935704402121

Metcalf, & Eddy. (2007). *Water Reuse:Issues,Technologies and Applications*. McGraw Hill.

Mitrouli, S. T., Karabelas, A. J., Isaias, N. P., Sioutopoulos, D. C., & Al Rammah, A. S. (2010). Reverse Osmosis Membrane Treatment Improves Salt-Rejection Performance. *IDA Journal of Desalination and Water Reuse*, *2*(2), 22–34. https://doi.org/10.1179/ida.2010.2.2.22

Mohan, G. R., Speth, T. F., Murray, D., & Garland, J. L. (2014). Municipal wastewater: A rediscovered resource for sustainable water reuse. *Handbook of Environmental Chemistry*, *30*, 153–179. https://doi.org/10.1007/978-3-319-06563-2_6

Morgan, P. W. (2011). Interfacial Polymerization. In *Encyclopedia of Polymer Science and Technology*. John Wiley & Sons, Inc. https://doi.org/10.5059/yukigoseikyokaishi.18.206

Mulder, M. (2003). Membrane Processes. In *Basic Principles of Membrane Technology* (2nd ed., pp. 280–412). Kluwer Academic Publishers.

Nas, B., Aygun, A., Dogan, S., & Dolu, T. (2020). Wastewater reuse in Turkey : from present status to future potential. *Water Supply*, *20*(1), 73–82. https://doi.org/10.2166/ws.2019.136

Nguyen, T., Roddick, F. A., & Fan, L. (2012). Biofouling of water treatment membranes: a review of the underlying causes, monitoring techniques and control measures. *Membranes*, *2*(4), 804–840. https://doi.org/10.3390/membranes2040804

Ould Mohamedou, E., Penate Suarez, D. B., Vince, F., Jaouen, P., & Pontie, M. (2010). New lives for old reverse osmosis (RO) membranes. *Desalination*, *253*(1–3), 62–70. https://doi.org/10.1016/j.desal.2009.11.032

Pantoja-Castro, M., & González-Rodríguez, H. (2012). Study by infrared spectroscopy and thermogravimetric analysis of Tannins and Tannic acid. *Revista Latinoamericana de Química*, *3*(39), 107–112.

Paula, E. C. De, Célia, J., Gomes, L., Cristina, M., & Amaral, S. (2017). *Recycling of end-of-life reverse osmosis membranes by oxidative treatment: a technical evaluation*. *ii*, 1–18. https://doi.org/10.2166/wst.2017.238

Qasim, M., Badrelzaman, M., Darwish, N. N., Darwish, N. A., & Hilal, N. (2019). Reverse osmosis desalination: A state-of-the-art review. *Desalination*, *459*(February), 59–104. https://doi.org/10.1016/j.desal.2019.02.008

Raaijmakers, M. J. T., & Benes, N. E. (2016). Current trends in interfacial polymerization chemistry. *Progress in Polymer Science*, *63*, 86–142. https://doi.org/10.1016/j.progpolymsci.2016.06.004

Roccaro, P. (2018). Treatment processes for municipal wastewater reclamation: The challenges of emerging contaminants and direct potable reuse. *Current Opinion in Environmental Science and Health*, *2*, 46–54. https://doi.org/10.1016/j.coesh.2018.02.003

Rodríguez, J. J., Jiménez, V., Trujillo, O., & Veza, J. (2002). Reuse of reverse osmosis membranes in advanced wastewater treatment. *Desalination*, *150*(3), 219–225. https://doi.org/10.1016/S0011-9164(02)00977-3

Salgot, M., & Folch, M. (2018). Wastewater treatment and water reuse. *Current*

Opinion in Environmental Science and Health, *2*, 64–74. https://doi.org/10.1016/j.coesh.2018.03.005

Scott, K. (1995). Introduction to Membrane Separations. In K. Scott (Ed.), *Handbook of Industrial Membranes* (pp. 3–185). Elsevier Science. https://doi.org/https://doi.org/10.1016/B978-185617233-2/50004-0

Senán-Salinas, J., García-Pacheco, R., Landaburu-Aguirre, J., & García-Calvo, E. (2019). Recycling of end-of-life reverse osmosis membranes: Comparative LCA and cost-effectiveness analysis at pilot scale. *Resources, Conservation and Recycling*, *150*(July), 104423. https://doi.org/10.1016/j.resconrec.2019.104423

Shmeis, R. M. A. (2018). Water Chemistry and Microbiology. In *Fundamentals of Quorum Sensing, Analytical Methods and Applications in Membrane Bioreactors* (1st ed., Vol. 81). Elsevier B.V. https://doi.org/10.1016/bs.coac.2018.02.001

Siddiqui, M. U., Arif, A. F. M., & Bashmal, S. (2016). Permeability-selectivity analysis of microfiltration and ultrafiltration membranes: Effect of pore size and shape distribution and membrane stretching. *Membranes*, *6*(3), 1–14. https://doi.org/10.3390/membranes6030040

Socrates, G. (2001). *Infraredand Raman Characteristic Group Frequencies*. John Wiley & Sons, Ltd.

Soice, N. P., Maladono, A. C., Takigawa, D. Y., Norman, A. D., Krantz, W. B., & Greenberg, A. R. (2003). Oxidative degradation of polyamide reverse osmosis membranes: Studies of molecular model compounds and selected membranes. *Journal of Applied Polymer Science*, *90*(5), 1173–1184. https://doi.org/10.1002/app.12774

Song, Y., Fan, J. B., & Wang, S. (2017). Recent progress in interfacial polymerization. *Materials Chemistry Frontiers*, *1*(6), 1028–1040. https://doi.org/10.1039/c6qm00325g

Sterlitech. (2017a). *Crossflow filtration handbook*.

Sterlitech. (2017b). *Sepa CF Cell: Assembly & Operational Manual*.

Su, Y. (2019). Chapter 1 Current State-of-the-art Membrane Based Filtration and Separation Technologies. In *Graphene-based Membranes for Mass Transport Applications* (pp. 1–13). The Royal Society of Chemistry. https://doi.org/10.1039/9781788013017-00001

Tessaro, I. C., da Silva, J. B. A., & Wada, K. (2005). Investigation of some aspects related to the degradation of polyamide membranes: Aqueous chlorine oxidation catalyzed by aluminum and sodium laurel sulfate oxidation during cleaning. *Desalination*, *181*(1–3), 275–282. https://doi.org/10.1016/j.desal.2005.04.008

U.S. EPA. (2000). Wastewater Technology Fact Sheet Package Plants. *United States Environmental Protection Agency*, 1–7. http://www3.epa.gov/npdes/pubs/final_sgrit_removal.pdf

UN. (2019). *The Sustainable Development Goals Report*.

Veatch, & Black. (2009a). Chlorination of Potable Water. In *White's Handbook of Chlorination and Alternative Disinfectants* (pp. 230–325). John Wiley & Sons, Ltd. https://doi.org/https://doi.org/10.1002/9780470561331.ch4

Veatch, & Black. (2009b). Determination of Chlorine Residuals in Water and Wastewater Treatment. In *White's Handbook of Chlorination and Alternative Disinfectants* (pp. 174–229). John Wiley & Sons, Ltd. https://doi.org/https://doi.org/10.1002/9780470561331.ch3

Verbeke, R., Gómez, V., & Vankelecom, I. F. J. (2017). Chlorine-resistance of reverse osmosis (RO) polyamide membranes. *Progress in Polymer Science*, *72*, 1–15. https://doi.org/10.1016/j.progpolymsci.2017.05.003

von Sperling, M. (2007). *Wastewater Characteristics, Treatment and Disposal* (Vol. 1). IWA Publishing.

Wang, J., Dlamini, D. S., Mishra, A. K., Theresa, M., Pendergast, M., Wong, M. C. Y., Mamba, B. B., Freger, V., Verliefde, A. R. D., & Hoek, E. M. V. (2014). A critical review of transport through osmotic membranes. *Journal of Membrane Science*, *454*, 516–537. https://doi.org/10.1016/j.memsci.2013.12.034

Warsinger, D. M., Chakraborty, S., Tow, E. W., Plumlee, M. H., Bellona, C., Loutatidou, S., Karimi, L., Mikelonis, A. M., Achilli, A., Ghassemi, A., Padhye, L. P., Snyder, S. A., Curcio, S., Vecitis, C. D., Arafat, H. A., & V, J. H. L. (2018). Progress in Polymer Science A review of polymeric membranes and processes for potable water reuse. *Progress in Polymer Science*, *81*, 209–237. https://doi.org/10.1016/j.progpolymsci.2018.01.004

Wijmans, J. G., & Baker, R. W. (1995). The solution-diffusion model: a review. *Journal of Membrane Science*, *107*(1–2), 1–21. https://doi.org/10.1016/S0166-4115(08)60038-2

Wilf, M. (2010). *The Guidebook to Membrane Technology for Wastewater Reclamation: Wastewater Treatment, Pollutants, Membrane Filtration, Membrane Bioreactors, Reverse Osmosis, Fouling, UV Oxidation, Process Control, Implementation, Economics, Commercial Plants Design*. Balaban Desalination Publications. https://books.google.com.cy/books?id=yVHgSAAACAAJ

Wilf, Mark, & Glueckstern, P. (1985). Restoration of Commercial Reverse Osmosis Membranes Under Field Conditions. *Desalination*, *54*, 343–350.

Wong, K. C., Goh, P. S., & Ismail, A. F. (2016). Thin film nanocomposite: The next generation selective membrane for CO2 removal. *Journal of Materials Chemistry A*, *4*(41), 15726–15748. https://doi.org/10.1039/c6ta05145f

Xu, J., Wang, Z., Wei, X., Yang, S., Wang, J., & Wang, S. (2013). The chlorination process of crosslinked aromatic polyamide reverse osmosis membrane : New insights from the study of self-made membrane. *DES*, *313*, 145–155. https://doi.org/10.1016/j.desal.2012.12.020

Yan, W., Shi, M., Dong, C., Liu, L., & Gao, C. (2020). Applications of tannic acid in membrane technologies : A review. *Advances in Colloid and Interface Science*, *284*(229), 102267. https://doi.org/10.1016/j.cis.2020.102267

Yang, J., Monnot, M., Ercolei, L., & Moulin, P. (2020). *Membrane-Based Processes Used in Municipal Wastewater Treatment for Water Reuse : State-Of-The-Art and Performance Analysis*. 1–55.

Yang, Z., Zhou, Y., Feng, Z., Rui, X., Zhang, T., & Zhang, Z. (2019). *A Review on Reverse Osmosis and Nanofiltration Membranes for Water Purification*. 1–22.

Yip, N. Y., & Elimelech, M. (2011). Performance limiting effects in power generation from salinity gradients by pressure retarded osmosis. *Environmental Science and Technology*, *45*(23), 10273–10282. https://doi.org/10.1021/es203197e

Zhang, Y., Ruan, H., Guo, C., Liao, J., Shen, J., & Gao, C. (2020). Thin-film nanocomposite reverse osmosis membranes with enhanced antibacterial resistance by incorporating p-aminophenol-modified graphene oxide. *Separation and Purification Technology*, *234*(April 2019), 1–9. https://doi.org/10.1016/j.seppur.2019.116017

Zhang, Z., Qin, Y., Kang, G., Yu, H., Jin, Y., & Cao, Y. (2020). Tailoring the internal void structure of polyamide films to achieve highly permeable reverse osmosis membranes for water desalination. *Journal of Membrane Science*, *595*(July 2019). https://doi.org/10.1016/j.memsci.2019.117518

Zhou, W., & Song, L. (2005). Experimental study of water and salt fluxes through reverse osmosis membranes. *Environmental Science & Technology*, *39*(9), 3382–3387. https://doi.org/10.1021/es0403561

APPENDICES

A. E1: Virgin membrane performance tests results

Table A. 1. Virgin membrane DI performance test results

Pressure (bar)	SET1 (LMH)	SET2 (LMH)	SET3 (LMH)	SET4 (LMH)	Avg. (LMH)	Max. error	Min. error
4	16.4	15.8	14.1	11.9	14.6	1.9	2.7
8	27.6	29.8	26.5	29.7	28.4	1.4	1.9
12	51.5	44.7	44.2	46.4	46.7	4.8	2.5
16	66.4	62.2	54.5	64.6	61.9	4.4	7.4

Table A. 2. Virgin membrane BW performance test results

Pressure (bar)	SET1 (LMH)	SET2 (LMH)	SET3 (LMH)	SET4 (LMH)	SET5 (LMH)	Avg. (LMH)	Max. error	Min. error
4	11.9	12.1	7.7	9.3	7.1	9.8	12.5	10.0
8	23.5	23.9	20.4	22.7	20.6	19.9	25.4	22.3
12	38.5	37.8	34.0	36.8	37.1	30.6	42.0	36.7
16	50.9	54.9	48.0	45.3	51.0	47.3	51.0	49.8

Table A. 3. Virgin membrane salt rejection (%)

Pressure (bar)	SET1 (LMH)	SET2 (LMH)	SET3 (LMH)	SET4 (LMH)	SET5 (LMH)	Avg. (LMH)	Max. error	Min. error
4	96.5	95.7	93.0	95.3	95.9	95.3	1.2	2.3
8	97.8	97.5	96.7	96.8	97.5	97.3	0.5	0.5
12	98.1	97.9	97.4	97.1	97.9	97.7	0.4	0.5
16	98.4	98.0	97.7	97.5	97.8	97.9	0.5	0.3

B. E2-D2000-(pH 9): Degraded membrane performance test results

Table B. 1. Degraded membrane DI performance test results (pH 9)

Pressure (bar)	SET1 (LMH)	SET2 (LMH)	SET3 (LMH)	SET4 (LMH)	Avg. (LMH)	Max. error	Min. error
4	12.9	11.6	12.1	12.4	12.3	0.7	0.7
8	24.9	21.4	31.1	28.1	25.9	5.3	4.5
12	38.1	44.3	50.6	35.4	43.5	7.1	8.1
16	48.6	59.2	68.2	58.8	60.5	7.7	11.9

Table B. 2. Degraded membrane BW performance test results (pH 9)

Pressure (bar)	SET1 (LMH)	SET2 (LMH)	SET3 (LMH)	SET4 (LMH)	Avg. (LMH)	Max. error	Min. error
4	7.7	6.0	7.7	4.0	6.3	1.4	2.4
8	19.9	19.2	25.1	12.7	19.2	5.9	6.5
12	43.8	34.4	42.7	19.8	35.2	8.7	15.4
16	59.7	45.8	61.2	30.4	49.3	12.0	18.9

Table B. 3. Degraded membrane salt rejection (%) (pH 9)

Pressure (bar)	SET1 (LMH)	SET2 (LMH)	SET3 (LMH)	SET4 (LMH)	Avg. (LMH)	Max. error	Min. error
4	91.0	92.5	96.1	92.2	93.2	2.9	2.2
8	91.9	90.4	85.4	92.0	89.2	2.6	3.8
12	90.0	87.1	78.4	88.7	85.2	4.8	6.8
16	90.3	85.2	76.3	86.7	84.0	6.4	7.7

C. E2-R2000-(pH 4): Degraded membrane performance test results

Table C. 1. Degraded membrane DI performance test results (pH 4

Pressure (bar)	SET1 (LMH)	SET2 (LMH)	SET3 (LMH)	Average (LMH)	Max. error	Min. error
4	4.9	6.5	5.1	5.5	1.0	0.6
8	8.6	14.2	8.4	10.4	3.8	2.0
12	12.6	22.4	12.7	15.9	6.5	3.3
16	18.2		17.4	17.8	0.4	0.4

Table C. 2. Degraded membrane BW performance test results (pH 4)

Pressure (bar)	SET1 (LMH)	SET2 (LMH)	SET3 (LMH)	Average (LMH)	Max. error	Min. error
4	6.7	5.5	3.7	5.3	1.4	1.6
8	14.5	11.8	8.3	11.5	2.9	3.2
12	21.8	19.0	14.0	18.3	3.5	4.3
16	33.5	28.7	18.2	26.8	6.7	8.6

Table C. 3. Degraded membrane salt rejection

Pressure (bar)	SET1 (LMH)	SET2 (LMH)	SET3 (LMH)	Average (LMH)	Max. error	Min. error
4	95.1	95.4	93.5	94.7	0.7	1.1
8	96.5	96.0	94.9	95.8	0.7	0.9
12	96.3	94.3	95.4	95.3	1.0	1.1
16	94.6	88.2	97.0	93.3	3.7	5.1

D. E3-R2000: Rejuvenated membranes performance tests

Table D. 1. Rejuvenated membrane DI performance test results (pH 4)

Pressure (bar)	SET1 (LMH)	SET2 (LMH)	SET3 (LMH)	Average (LMH)	Max. error	Min. error
4	6.2	8.8	6.5	7.2	1.6	1.0
8	12.2	15.7	11.9	13.3	2.4	1.3
12	17.6	26.1	18.5	20.7	5.4	3.2
16		32.9	29.6	31.2	1.6	1.6

Table D. 2. Rejuvenated membrane BW performance test results (pH 4)

Pressure (bar)	SET1 (LMH)	SET2 (LMH)	SET3 (LMH)	Average (LMH)	Max. error	Min. error
4	5.7	7.2	5.4	6.1	1.1	0.7
8	10.7	12.9	10.4	11.4	1.6	0.9
12	16.1	20.7	16.6	17.8	2.9	1.7
16		28.8	22.4	25.6	3.2	3.2

Table D. 3. Rejuvenated membrane salt rejection (%)

Pressure (bar)	SET1 (LMH)	SET2 (LMH)	SET3 (LMH)	Average (LMH)	Max. error	Min. error
4	93.7	98.6	98.1	96.8	1.8	3.1
8	96.7	98.9	98.5	98.1	0.8	1.3
12	96.9	97.7	98.4	97.7	0.7	0.8
16		95.9	98.1	97.0	1.1	1.1

E. E4-R2000: Rejuvenated membranes performance tests

Table E. 1. Rejuvenated membrane DI performance test results (pH 9)

Pressure (bar)	SET1 (LMH)	SET2 (LMH)	SET3 (LMH)	Average (LMH)	Max. error	Min. error
4	10.3	8.3	7.4	8.7	1.7	1.3
8	21.8	22.8	19.7	21.4	1.4	1.7
12	32.9	36.2	30.9	33.3	2.9	2.4
16	48.4	51.3	42.4	47.4	4.0	5.0

Table E. 2. Rejuvenated membrane BW performance test results (pH 9)

Pressure (bar)	SET1 (LMH)	SET2 (LMH)	SET3 (LMH)	Average (LMH)	Max. error	Min. error
4	5.5	8.3	6.3	6.7	1.6	1.2
8	16.2	22.8	15.4	18.1	4.7	2.7
12	28.1	36.2	24.1	29.5	6.7	5.4
16	44.1	51.3	39.4	45.0	6.4	5.5

Table E. 3. Rejuvenated membrane salt rejection (%) (pH 9)

Pressure (bar)	SET1 (LMH)	SET2 (LMH)	SET3 (LMH)	Average (LMH)	Max. error	Min. error
4	95.2	96.5	95.8	95.8	0.7	0.6
8	94.9	91.6	95.8	94.1	1.7	2.5
12	93.2	87.4	94.5	91.7	2.8	4.3
16	92.7	85.1	94.2	90.7	3.5	5.6

F. E4-RR2000: Re-rejuvenated membranes performance tests results

Table F. 1. Degraded membrane DI performance test results (pH 4, after rejuvenation)

Pressure (bar)	SET1 (LMH)	SET2 (LMH)	Average (LMH)	Max. error	Min. error
4	7.4	6.2	6.8	0.6	0.6
8	14.2	15.5	14.8	0.6	0.6
12	23.1	16.3	19.7	3.4	3.4
16	29.4	20.5	24.9	4.4	4.4

Table F. 2. Degraded membrane BW performance test results (pH 4, after rejuvenation)

Pressure (bar)	SET1 (LMH)	SET2 (LMH)	Average (LMH)	Max. error	Min. error
4	6.6	4.8	5.7	0.9	0.9
8	12.8	10.6	11.7	1.1	1.1
12	22.5	18.6	20.6	1.9	1.9
16	30.9	24.9	27.9	3.0	3.0

Table F. 3. Degraded membrane salt rejection (%) (after rejuvenation

Pressure (bar)	SET1 (LMH)	SET2 (LMH)	Average (LMH)	Max. error	Min. error
4	96.9	95.7	96.3	0.6	0.6
8	96.4	96.6	96.5	0.1	0.1
12	94.5	96.3	95.4	0.9	0.9
16	93.0	95.6	94.3	1.3	1.3

Table F. 4. Re-rejuvenated membrane DI performance test results

Pressure (bar)	SET1 (LMH)	SET2 (LMH)	Average (LMH)	Max. error	Min. error
4	11.4	7.9	9.6	1.7	1.7
8	16.8	15.2	16.0	0.8	0.8
12	27.1	23.7	25.4	1.7	1.7
16	35.7	33.7	34.7	1.0	1.0

Table F. 5. Re-rejuvenated membrane BW performance test results

Pressure (bar)	SET1 (LMH)	SET2 (LMH)	Average (LMH)	Max. error	Min. error
4	7.7	5.9	6.8	0.9	0.9
8	14.8	13.8	14.3	0.5	0.5
12	25.4	22.4	23.9	1.5	1.5
16	33.7	29.8	31.7	1.9	1.9

Table F. 6. Re-rejuvenated membrane salt rejection (%)

Pressure (bar)	SET1 (LMH)	SET2 (LMH)	Average (LMH)	Max. error	Min. error
4	98.1	97.7	97.9	0.2	0.2
8	97.8	95.0	96.4	1.4	1.4
12	96.6	91.6	94.1	2.5	2.5
16	95.5	90.2	92.9	2.7	2.7

G. E5-DR: Direct Rejuvenation

Table G. 1 Directly rejuvenated membrane DI performance test results

Pressure (bar)	SET1 (LMH)	SET2 (LMH)	Average (LMH)	Max. error	Min. error
4	6.8	8.1	7.4	0.6	0.6
8	15.8	16.6	16.2	0.4	0.4
12	24.2	24.7	24.5	0.2	0.2
16	34.3	33.3	33.8	0.5	0.5

Table G. 2. Directly rejuvenated membrane BW performance test results

Pressure (bar)	SET1 (LMH)	SET2 (LMH)	Average (LMH)	Max. error	Min. error
4	4.0	4.6	4.3	0.3	0.3
8	11.9	11.3	11.6	0.3	0.3
12	19.0	18.5	18.7	0.2	0.2
16	27.1	27.1	27.1	0.0	0.0

Table G. 3. Directly rejuvenated membrane salt rejection (%)

Pressure (bar)	SET1 (LMH)	SET2 (LMH)	Average (LMH)	Max. error	Min. error
4	97.6	96.5	97.0	0.5	0.5
8	98.6	97.8	98.2	0.4	0.4
12	98.6	98.1	98.3	0.2	0.2
16	98.7	98.2	98.4	0.2	0.2

H. FTIR-ATR Spectrum of membranes
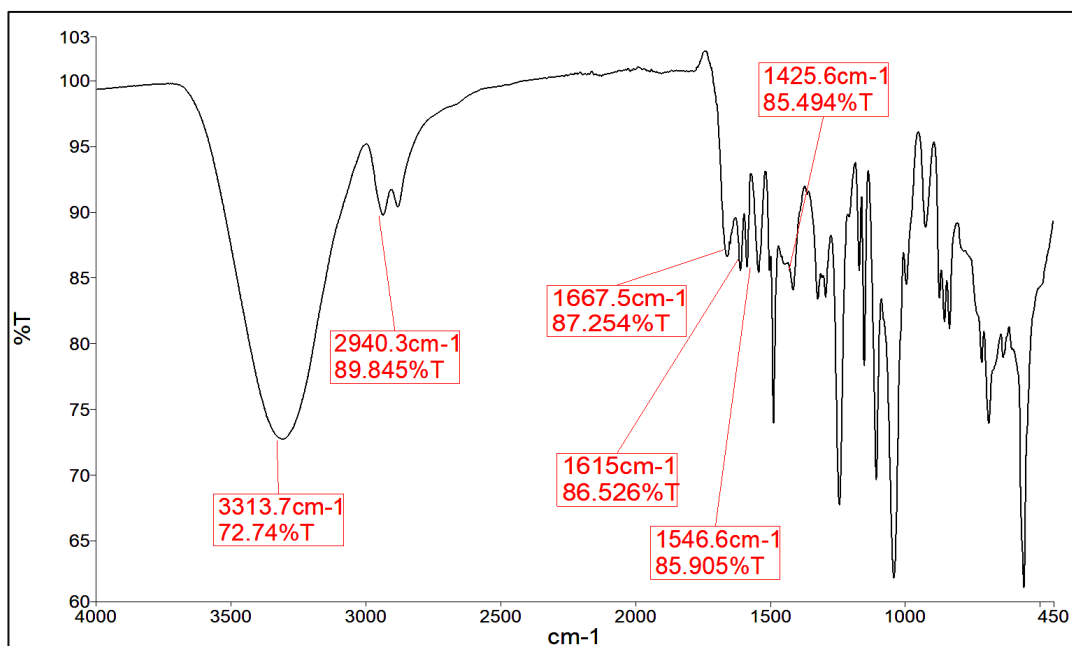
Figure H. 1. FTIR-ATR spectra of virgin membrane

Figure H. 2. FTIR-ATR spectra of degraded membrane (2000 ppm·hr , pH 4)
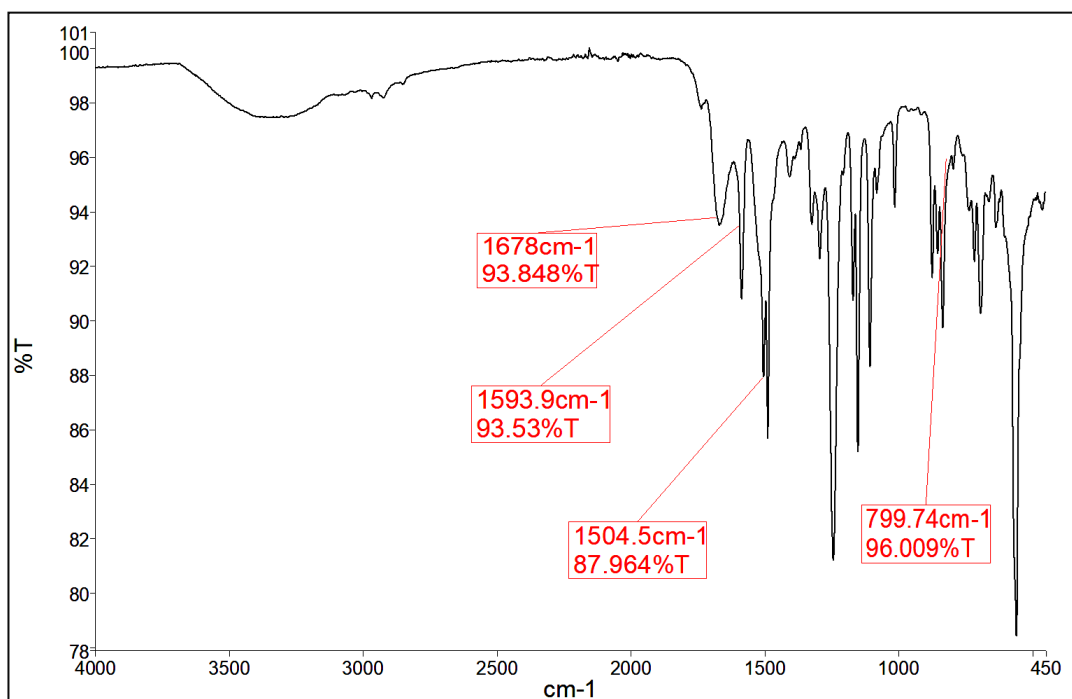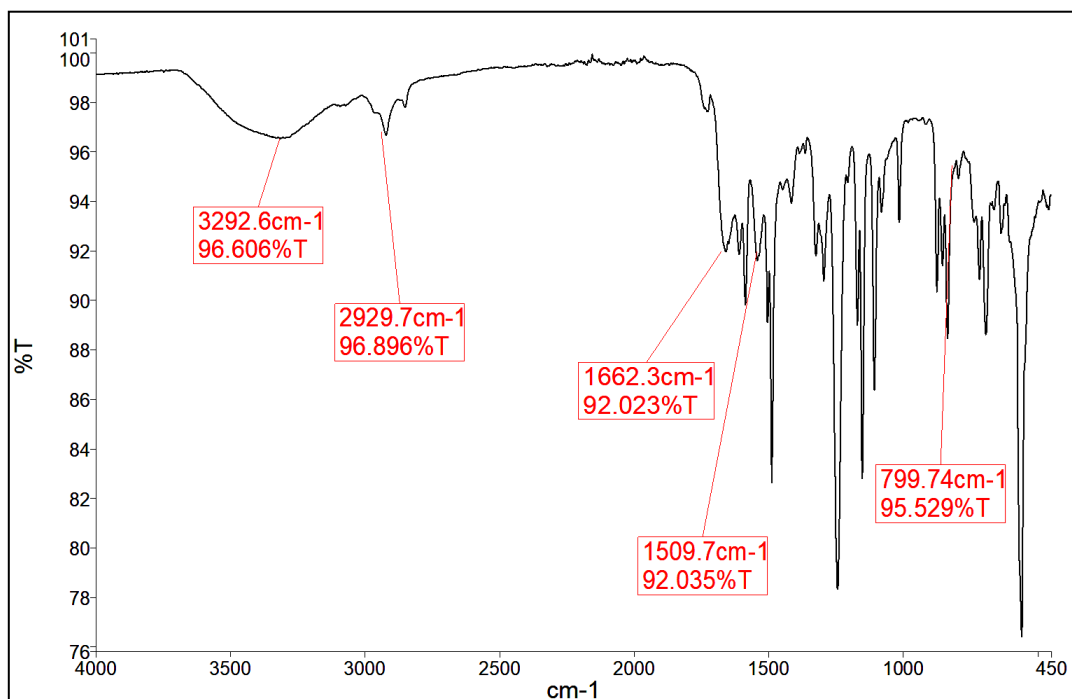
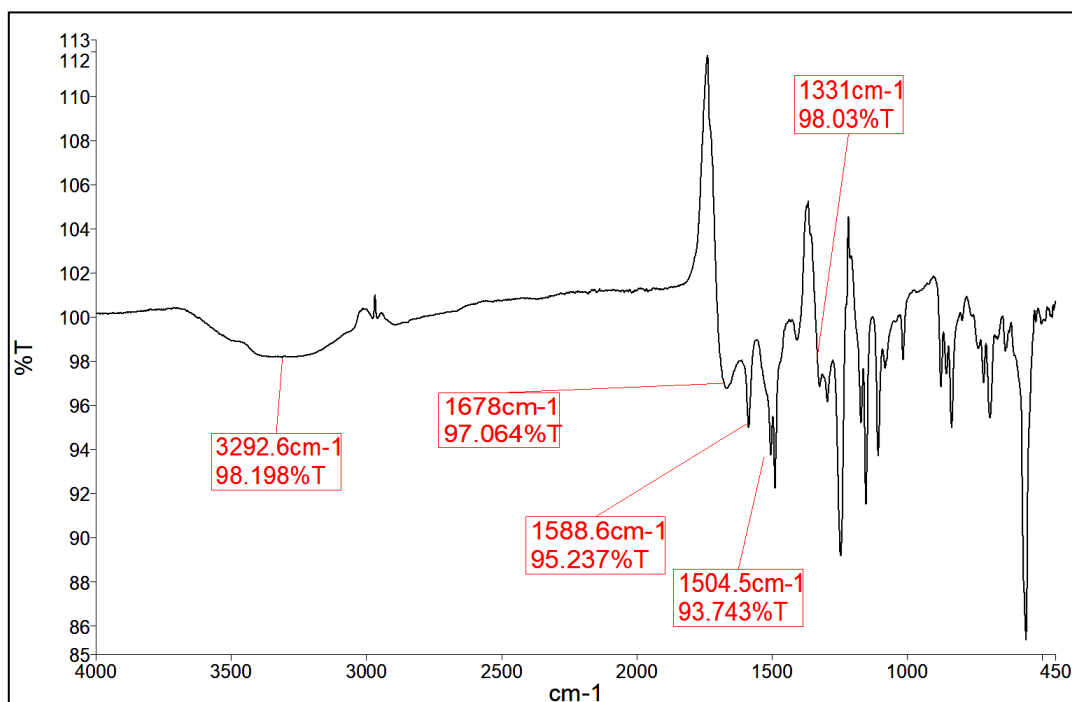Figure H. 3. FTIR-ATR spectra of the degraded membrane (2000 ppm. hr, pH 9)

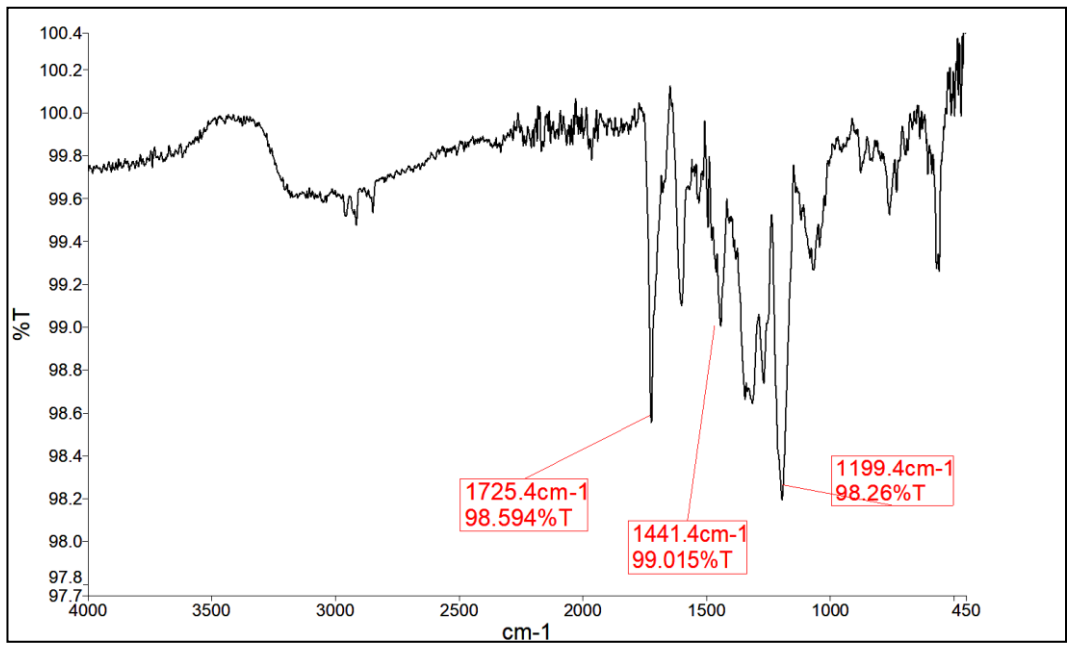Figure H. 4. FTIR-ATR spectra of the rejuvenated membrane (2000 ppm. hr, pH 4)

101

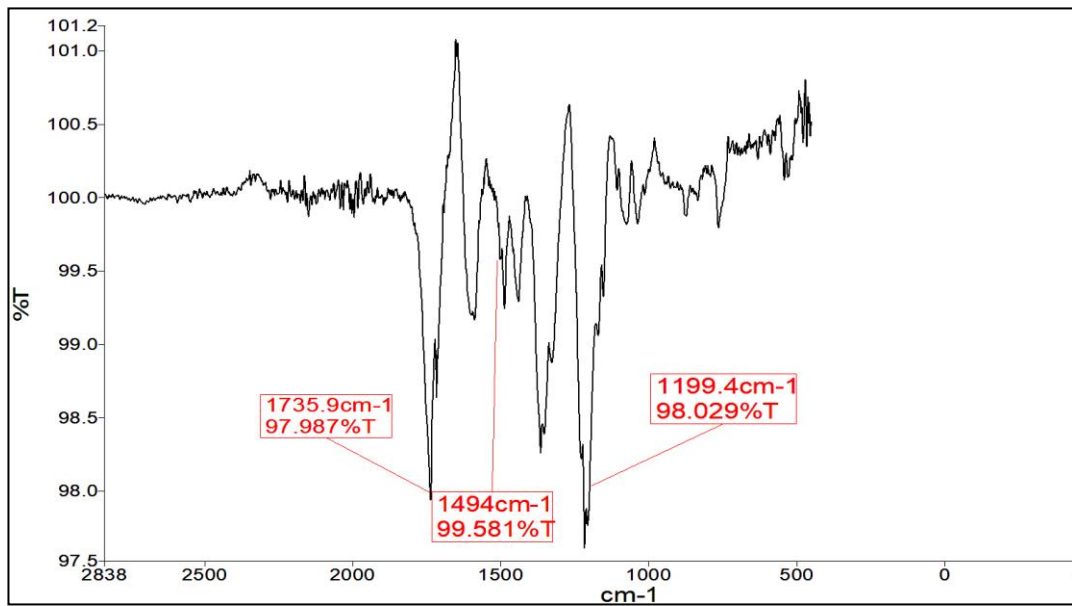Figure H. 5. Difference results of the rejuvenated membrane (2000 ppm·hr , pH 9)

Figure H. 6. Difference results of directly rejuvenated membrane
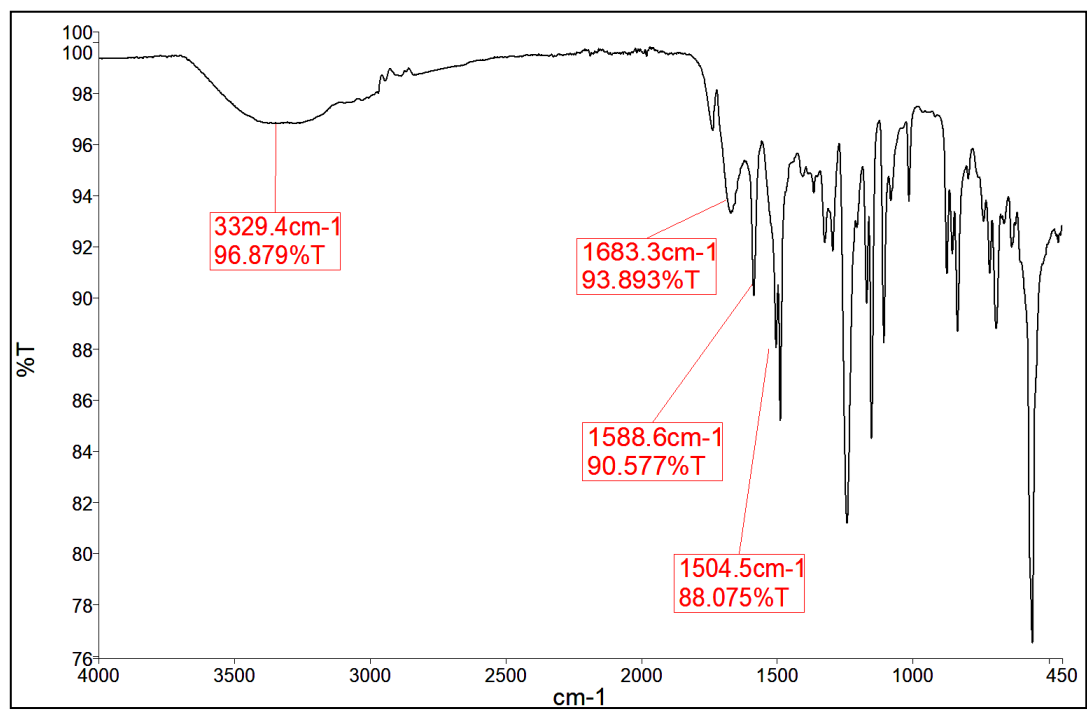
Figure H. 7. FTIR-ATR spectra of the re-rejuvenated membrane (2000 ppm·hr , pH 4)

I. Rejuvenating agent SDS

Section 1. PRODUCT NAME AND COMPANY IDENTIFICATION	

Product name	Renomate 2000
Other means of identification	Not applicable
Recommended use	Membrane rejuvenation
Restriction on use	Refer to available product literature or ask your local sales representative on use and dose limits
Company	Ochemate Advanced Material Technologies Ltd No. 688 Xifeng Road Huzhou China 12603 Southwest Freeway suite 210, Stafford TX 77477 USA. www.ochemate.com
Emergency telephone number	Phone +86 572 265 6888 Phone +1 281 491 9505
Issuing date	09/05/2018

Section 2. HAZARDS IDENTIFICATION	
GHS Classification	Category 1 - Skin irritation, eye irritation,ingestion, inhalation Potential chronic health effects: Carcinogenic effects: 3 (not classifiable forhuman) by IARC. Mutagenic effects: Not available. Teratogenic effects: Not available Developmental toxicity: Classified reproductive system/toxin/female [Possible].The substance may be toxic to kidneys, liver. Repeated or prolonged exposure to thesubstance can produce target organs damage.
Precautionary Statements	**Prevention:** Wash exposed skin thoroughly afterhandling. **Response:** Specific measures: consult SDS section 4. **Storage:** Store in accordance with local regulations.

Section 3. COMPOSITION/INFORMATION ON INGREDIENTS

Name	CAS number	Concentration
Organic acid	1401-55-4	> 90%

Section 4. FIRST AID MEASUREMENTS

In case of eye contact	Check for and remove any contact lenses. Rinse with water immediately. Continue to rinse for at least 15 minutes. Get medical attention.
In case of skin contact	Immediately remove contaminated clothing. Rinse immediately with plenty of water. Continueto rinse for at least 15 minutes. Get medical attention.
If swallowed	NEVER MAKE AN UNCONSCIOUS PERSONVOMIT OR DRINK FLUIDS! DO NOT INDUCE VOMITING! Rinse mouth thoroughly. Get medical attention.
If inhaled	Provide fresh air, warmth and rest, preferable in a comfortable upright sitting position. Remove tofresh air. If not breathing, give artificial respiration. If breathing is difficult, give oxygen. Get medical attention.
Protection of first aiders	In event of emergency assess the danger beforetaking action. Do not put yourself at risk of injury.If in doubt, contact emergency responders. Use personal protective equipment as required.

See Toxicological Information (section 11)

Section 5. FIREFIGHTING MEASURES

Suitable extinguishing media	Use extinguishing measures that are appropriate to local circumstances and the surrounding environment: dry chemical powder, water spray, fog or

	foam
Unsuitable extinguishing media	Do not use water jet.
Specific hazards during firefighting	Thermal decomposition can lead to release of irritating gases and vapors.
Suitable extinguishing media	Use extinguishing measures that are appropriate to local circumstances and the surrounding environment: dry chemical powder, water spray, fog or foam
Unsuitable extinguishing media	Do not use water jet.
Specific hazards during firefighting	Thermal decomposition can lead to release of irritating gases and vapors of in accordance with local regulations..

Section 6. ACCIDENTAL RELEASE MEASURES

Personal precautions, protective equipment and emergency procedures	Refer to protective measures listed in sections 7 and 8.
Environmental precautions	Avoid discharge into drains. The product should not be dumped in nature but collected and delivered according to agreement with local authorities.
Methods and materials for containment and cleaning up	Stop leak if safe to do so. Contain spillage. Neutralize the residue with a dilute solution of sodium carbonate. Finish cleaning by spreading water on the contaminated surface. Dispose of according to local/national regulations (see section 13). For large spills, dike spilled material or otherwise contain material to ensure runoff does not reach a waterway.

Section 7. HANDLING AND STORAGES

Advice on safe handling	For personal protection see section 8. Wash hands after handling.
Conditions for safe storage	Keep in a cool, well ventilated place. Keep away from heat, sources of

	ignition. Keep out of reach of children. Keep container tightly closed. Store in suitable labeled containers.
Packaging material	Suitable material. Keep in properly labeled containers. Sensitive to light. Store in light-resistant containers.

Section 8. EXPOSURE CONTROLS/ PERDONAL PROTECTION

No allocable occupational exposure limits	
Engineering measures	Use process enclosures, local exhaust ventilation, or other engineering controls to keep airbornelevels below recommended exposurelimits. If user operations generate dust, fume, or mist, use ventilation to keep exposure to airborne contaminants below the exposure limit. Ensure adequate ventilation.

Personal protective equipment	
Eye protection	Chemical goggles. Use face shield in case of splash risk.
Hand protection	Wear chemical resistant protectivegloves. Gloves should be discarded and replaced if there is any indication ofdegradation or chemical breakthrough.
Skin protection	Wear suitable protective clothing. Wash contaminated clothing and drythoroughly before use.
Respiratory protection	Personal respiratory protection in case of dust/powder release.
Hygiene measures	Wash hands before breaks andimmediately after handling the product.
Other	Do not eat, drink or smoke duringuse.

Section 9. PHYSICAL AND CHEMICAL PROPERTIES

Appearance	Powder
Color	Light amber to light brown
pH (1% solution)	3.0 – 4.0
Water solubility	Completely soluble
Melting point	200 °C
Flash point (closed cup)	199 °C

Section 10. STABILITY AND REACTIVITY

Chemical stability	Stable under normal conditions
Possibility of hazardous reactions	No dangerous reaction known under conditions of normal use.
Conditions to avoid	Excess heat, incompatible materials, light, moisture.
Incompatible materials	Reactive with oxidizing agents, alkalis
Hazardous decomposition products (formed under fire conditions)	Carbon oxides (CO, CO2)

Section 11. TOXICOLOGICAL INFORMATION

Routes of exposure:

Primary routes are inhalation and ingestion

Potential Health Effects	
Eyes	Health injuries are not known orexpected under normal use.
Skin	Health injuries are not known orexpected under normal use.
Ingestion	Health injuries are not known orexpected under normal use.
Inhalation	Health injuries are not known orexpected under normal use.
Chronic exposure	Carcinogenic effects: 3 (not classifiable for human) by

	IARC Developmental toxicity: classified reproductive system/toxin/female [Possible]. May cause damage to kidneys, liver.
Special remarks on chronic effect onhumans	May affect genetic material (mutagenic. May cause adversereproductive effects. May cause cancer based on animal test data.
Product	
LD50 (rat)	2260 mg/kg

Section 12. ECOLOGICAL INFORMATION

LC50, 96 hrs, gambusia affinis(mosquito fish), mg/l	37
Toxicity	
This product and its products of degradation are not toxic.	
Other adverse effects	
An environmental hazard cannot be excluded in the event of unprofessionalhandling or disposal. Harmful to aquatic life.	

Section 13. DISPOSAL CONSIDERATIONS

Disposal methods	Dispose of in compliance with local regulations. Dispose of wastes in an approved waste disposal facility.
Disposal considerations	Dispose of as unused product. Empty containers should be taken to an approved waste handling site for recycling or disposal. Do not re-use empty containers.

Section 14. TRANSPORT INFORMATION

The shipper/consignor/sender is responsible to ensure that the packaging, labeling and markings are in compliance with the selected mode of transport.

Land transport (DOT) Proper shippingname	Not a DOT controlled material

TDG Shipping Name	Not regulated
DOT hazard class	Not dangerous goods
Identification number	Not regulated
Sea Transport (IMDG/IMO) class	Not dangerous goods
IMDG Packing Group	Not regulated
UN No. Air	Not regulated
Air class	Not dangerous goods
Air Packing Group	Not regulated
TDG Packing Group	Not regulated

Section 15. REGULATORY INFORMATION

Labelling	
Symbols	 Harmful to aquatic life
EPCRA – Emergency Planning and Community Right-to-Know-Act	

CERCLA Reportable Quantity This material does not contain any components with a CERCLA RQ.	
SARA 311/312 Hazards	Chronic: yes
SARA 313	This material does not contain any chemical components with known CAS numbers that exceed the threshold (De Minimis) reporting level established by SARA title III, Section313.

International Chemical Control Laws:

Toxic Substances Control Act (TSCA) The substance(s) in this preparation are included in or exempted from the TSCA 8(b) Inventory (40 CFR 710)
Canadian Environmental Protection Act (CEPA) The substance(s) in this preparation are included in or exempted from the domestic Substance List (DSL).

Australia
All substance(s) in this product comply with the National Industrial ChemicalsNotification & Assessment Scheme (NICNAS).
China
All substance(s) in this product comply with the Provisions on the Environmental Administration of New Chemical Substances and are listed onor exempt from the Inventory of Existing Chemical Substances China (IECSC).
Europe
The substance(s) in this preparation are included or exempted from the EINECS or ELINCS inventories.
Korea
All substance(s) in this product comply with the Toxic Chemical Control Law(TCCL) and are listed on the Existing Chemicals List (ECL).
New Zealand
All substances in this product comply with the Hazardous Substances and New Organisms (HSNO) Act 1996 and are listed on or are exempt from the New Zealand Inventory of Chemicals.
Philippines
All substances in this product comply with the Republic Act 6969 (RA 6969) and are listed on the Philippines Inventory of Chemicals & ChemicalSubstances (PICCS).

Section 16. OTHER INFORMATION

NFPA

Health	0
Flammability	1
Instability	0
Special Hazard	

HMIS III

Health	2
Flammability	1
Physical Hazard	0

0 = not significant, 1 = Slight,2 = Moderate, 3 = High,
4 = Extreme, * = Chronic

General information

Renomate 2000 is used to restore the rejection of mild oxidized thin film

composite reverse osmosis and nanofiltration membranes.

Revision date	09/05/2018
Version number	1.0
Prepared by	Ochemate Advanced Material Technologies Co Ltd

The information provided in this Safety Data Sheet is correct to the best of ourknowledge, information and belief at the date of its publication. The information given is designed only as guidance for safe handling, use, processing, storage, transportation, disposal and release and is not to be considered a warranty or quality specification. The information relates only tothe specific material designated and may not be valid for such material used in combination with any other materials or in any process, unless specified in the text.

TEZ İZİN FORMU / THESIS PERMISSION FORM

PROGRAM / PROGRAM

Sürdürülebilir Çevre ve Enerji Sistemleri / Sustainable Environment and Energy Systems ☐

Siyaset Bilimi ve Uluslararası İlişkiler / Political Science and International Relations ☐

İngilizce Öğretmenliği / English Language Teaching ☐

Elektrik Elektronik Mühendisliği / Electrical and Electronics Engineering ☐

Bilgisayar Mühendisliği / Computer Engineering ☐

Makina Mühendisliği / Mechanical Engineering ☐

YAZARIN / AUTHOR

Soyadı / Surname　　　: ....

Adı / Name　　　　　　: ....

Programı / Program　　: ....

TEZİN ADI / TITLE OF THE THESIS (**İngilizce** / English) : ....
....
....
....

　TEZİN TÜRÜ / DEGREE**:**　　　**Yüksek Lisans** / Master　☐　　**Doktora** / PhD　☐

　1. **Tezin tamamı dünya çapında erişime açılacaktır. /** Release the entire work immediately for access worldwide. ☐

2. **Tez iki yıl süreyle erişime kapalı olacaktır.** / Secure the entire work for patent and/or proprietary purposes for a period of **two years. *** ☐

3. **Tez altı ay süreyle erişime kapalı olacaktır.** / Secure the entire work for period of **six months**. *** ☐

Yazarın imzası / Author Signature .... **Tarih** / Date ....

Tez Danışmanı / Thesis Advisor Full Name: ……………………………….

Tez Danışmanı İmzası / Thesis Advisor Signature: ……………………..

Eş Danışmanı / Co-Advisor Full Name: ……………………………….

Eş Danışmanı İmzası / Co-Advisor Signature: ……………………..

Program Koordinatörü / Program Coordinator Full Name: ……………………………

Program Koordinatörü İmzası / Program Coordinator Signature: …………………..